UNCLASSIFIED

AD NUMBER
AD848311

LIMITATION CHANGES

TO:

Approved for public release; distribution is unlimited.

FROM:

Distribution authorized to U.S. Gov't. agencies and their contractors; Administrative/Operational Use; FEB 1969. Other requests shall be referred to Air Force Flight Dynamics Lab., Wright-Patterson AFB, OH 45433.

AUTHORITY

AFFDL ltr 8 Jun 1973

THIS PAGE IS UNCLASSIFIED

AEDC-TR-68-278

(AD ⸱⸱⸱⸱⸱⸱

Jones

FORCE TESTS ON A
SEPARABLE-NOSE CREW ESCAPE CAPSULE
IN PROXIMITY TO THE PARENT FUSELAGE
WITH COLD FLOW ROCKET PLUME SIMULATION
AT MACH NUMBERS 2 THROUGH 5

Jerry H. Jones and L. J. Pfaff

ARO, Inc.

February 1969

VON KÁRMÁN GAS DYNAMICS FACILITY
ARNOLD ENGINEERING DEVELOPMENT CENTER
AIR FORCE SYSTEMS COMMAND
ARNOLD AIR FORCE STATION, TENNESSEE

NOTICES

FORCE TESTS ON A
SEPARABLE-NOSE CREW ESCAPE CAPSULE
IN PROXIMITY TO THE PARENT FUSELAGE
WITH COLD FLOW ROCKET PLUME SIMULATION
AT MACH NUMBERS 2 THROUGH 5

Jerry H. Jones and L. J. Pfaff

ARO, Inc.

FOREWORD

The work reported herein was done at the request of the Air Force Flight Dynamics Laboratory (AFFDL), Air Force Systems Command (AFSC). under program element 64706F, Project 421A.

The results of tests presented were obtained by ARO, Inc. (a subsidiary of Sverdrup & Parcel and Associates, Inc.), contract operator of the Arnold Engineering Development Center (AEDC), AFSC, Arnold Air Force Station, Tennessee, under Contract F40600-69-C-0001. The tests were conducted, intermittently, from October 30, 1967, to September 18, 1968, under ARO Project No. VA0508. The manuscript was submitted for publication on November 14, 1968.

Information in this report is embargoed under the Department of State International Traffic in Arms Regulations. This report may be released to foreign governments by departments or agencies of the U. S. Government subject to approval of the Air Force Flight Dynamics Laboratory (FDFR), or higher authority within the Department of the Air Force. Private individuals or firms require a Department of State export license.

This technical report has been reviewed and is approved.

Eugene C. Fletcher
Lt Colonel, USAF
AF Representative, VKF
Directorate of Test

Roy R. Croy, Jr.
Colonel, USAF
Director of Test

ABSTRACT

Static force tests were conducted on a separable-nose crew escape capsule in the presence of the forward section of the airplane fuselage. The capsule escape rocket jet plume was simulated with air heated to a total temperature of approximately 100°F. Data were obtained at Mach numbers from 2 through 5 at capsule angles of attack from -15 to 25 deg and angles of sideslip from 0 to 15 deg for various positions of the capsule relative to the fuselage section. All testing was conducted at a fuselage angle of attack and angle of sideslip of zero. Reynolds number, based on a model length of 18.1 in., ranged from 5.7×10^6 to 12.3×10^6. Results are presented showing the effects of the fuselage section on the aerodynamic characteristics of the capsule, with and without simulation of the escape rocket exhaust plume.

CONTENTS

APPENDIXES

I. ILLUSTRATIONS

NOMENCLATURE

A	Reference area (cross-sectional area at separation bulkhead), 22.608 in.^{2}
C_D	Drag coefficient, drag/$q_\infty A$
C_ℓ	Rolling-moment coefficient, rolling moment/$q_\infty A\ell$
C_L	Lift coefficient, lift/$q_\infty A$
C_m	Pitching-moment coefficient, pitching moment/$q_\infty A\ell$
C_n	Yawing-moment coefficient, yawing moment/$q_\infty A\ell$
C_Y	Side-force coefficient, side force/$q_\infty A$
ℓ	Reference length (distance from nose to separation bulkhead), 16.5 in.
M_∞	Free-stream Mach number
p_c	Jet chamber pressure, psia
p_o	Tunnel stilling chamber pressure, psia
p_∞	Free-stream static pressure, psia
q_∞	Free-stream dynamic pressure, psia
Re_∞	Free-stream unit Reynolds number, in.$^{-1}$
T_o	Tunnel stilling chamber temperature, °R
x	Longitudinal separation distance between the capsule and fuselage, in the wind axis, and measured from the capsule moment reference point before separation to the capsule moment reference point after separation, in.
y	Lateral separation distance between the capsule and fuselage, perpendicular to the x-z plane, and measured as noted for x, in.

z   Vertical separation distance between the capsule and fuselage, perpendicular to the wind axis, and measured as noted for x, in.

α_c Capsule angle of attack, deg

β_c Capsule angle of sideslip, deg

Note: Force and moment coefficients are in the stability axis system.

SECTION I
INTRODUCTION

These tests constitute the second part of Phase II of a wind tunnel test program requested by the Flight Recovery Group (FDFR), AFFDL, to provide data for investigating crew escape systems for high-speed flight vehicles. In Phase I (Ref. 1), the static stability and drag characteristics of the F-104 aircraft separable-nose crew escape capsule were obtained for angles of attack from -30 to 30 deg with cold flow simulation of the exhaust plume from the escape rocket at various altitudes. In the first part of the Phase II tests (Ref. 2), static longitudinal stability and drag data were obtained on the capsule in proximity to the forward section of the airplane fuselage where the fuselage section was fixed at six positions with respect to the capsule.

In the present Phase II tests, static stability and drag data were obtained on the capsule using a remotely controlled support system that positioned the fuselage with respect to the capsule and also provided pitch and yaw of the capsule. The fuselage section position relative to the capsule was varied from 12 in. aft to 18 in. forward of the capsule, and from 0 to 14 in. below the capsule. Laterally, the fuselage was aligned with the capsule and was also positioned 5 in. to the side of the capsule.

Static force data were obtained at Mach numbers from 2 through 5 at capsule angles of attack from -15 to 25 deg and capsule angles of sideslip from 0 to 15 deg. The fuselage angle of attack and angle of sideslip was zero. Reynolds number, based on a model length of 18.1 in. ranged from 5.7×10^6 to 12.3×10^6. The escape rocket jet plume was simulated with air heated to approximately 100°F.

SECTION II
APPARATUS

2.1 WIND TUNNEL

The 40-in. supersonic tunnel (Gas Dynamic Wind Tunnel, Supersonic (A)) is a continuous, closed-circuit, variable density wind tunnel with an automatically driven, flexible-plate-type nozzle and a 40- by 40-in. test section. The tunnel can be operated at Mach numbers from 1.5 to 6 at maximum stagnation pressures from 29 to 200 psia, respectively, and stagnation temperatures up to 300°F ($M_\infty = 6$). Minimum operating pressures range from about one-tenth to one-twentieth of the

maximum at each Mach number. A description of the tunnel and airflow calibration information may be found in Ref. 3.

2.2 MODELS AND SUPPORT SYSTEM

The separable-nose crew escape capsule model and the fuselage section model (Figs. 1 through 3, Appendix I) were 1/10-scale models of the F-104 aircraft and were provided by AFFDL. The capsule had three wedge-shaped stabilizing booms extending to the rear. These booms (Fig. 1c) were positioned 120 deg apart, and the upper boom was fitted with a trim tab (Figs. 1a and b). The escape rocket nozzle was positioned in a cutout on the lower aft portion of the model (Fig. 1e) and was attached to the sting such that the model was isolated from the jet reaction force.

Details of the nozzle are given in Fig. 1d, and the procedures used to calculate the nozzle dimensions and chamber pressures for simulation of the full-scale jet plume shape at various altitudes over the Mach number range are given in Ref. 1.

The fuselage section details are given in Fig. 1f. As shown in this figure, a section of the fuselage front face formed a door. The door could be closed with a gas operated cylinder and was spring loaded so that it would open when the cylinder pressure was released. The purpose of this was to provide clearance for the capsule sting support when the capsule and fuselage were in proximity. The two longitudinal slots in the fuselage and the cutout in the top of the door simulate the storage locations of the stabilizer booms while the aircraft is in normal flight. The cutout on the bottom of the fuselage is a relief for the escape rocket exhaust during initial firing.

The fuselage and capsule were mounted on a support system (Fig. 3) that allowed remote control of capsule angle of attack and capsule-to-fuselage position in three directions. Capsule pitch and vertical separation were accomplished with two pitch mechanisms (fore and aft, see Fig. 3a) which gave capsule angles of attack from -15 to 25 deg at vertical separations from 0 to 14 in. Longitudinal separation was accomplished by a drive mechanism which could traverse the fuselage 14 in. aft and 40 in. forward of the capsule. Lateral separation was produced by a drive mechanism which could traverse the capsule 10 in. to the left and 2 in. to the right of the fuselage (looking upstream). For capsule sideslip data both models were rolled 90 deg on the support system in order to use the pitch mechanisms to yaw the capsule (see Fig. 3b).

2

2.3 INSTRUMENTATION AND PROCEDURES

Capsule force measurements were made with a six-component, moment-type, strain-gage balance supplied and calibrated by the von Kármán Gas Dynamics Facility. Before the test, loadings in a single plane and combined static loadings were applied to the balance which simulated the range of model loadings anticipated for the test. The ranges of uncertainties listed below correspond to the differences between the applied loads and the values calculated with the balance equations used in the final data reduction. The minimum uncertainties given are for loads up to about 10 percent of the maximum applied and are for loadings on the particular component only (no combined loading interaction effects). The maximum uncertainties are for combined loadings.

Balance Component	Design Load	Range of Static Loadings	Range of Uncertainties
Normal Force, lb	500	±25 to ±500	±0.30 to ±1.50
Pitching Moment, in.-lb	2000	0 to ±400	±2.00 to ±3.00
Side Force, lb	250	±25 to ±200	±0.40 to ±1.00
Yawing Moment, in.-lb	1000	0 to ±160	±1.60 to ±3.00
Rolling Moment, in.-lb	400	0 to ±385	±0.80 to ±1.40
Axial Force, lb	300	25 to 300	±0.40 to ±0.70

The jet chamber pressure was measured with a 1000-psid transducer and is considered accurate to within 1 percent of capacity.

The base pressure was measured with a transducer calibrated for full-scale ranges of 15, 5, and 1 psid, referenced to a near vacuum, and is considered accurate to within 0.3 percent of full scale. A base drag correction was made for the balance cavity area only.

The model attitude and position were measured with potentiometers, recorded on digital voltmeters, and the accuracies of each are listed in the following table:

Drive System	Range	Uncertainty
α_c, β_c, deg	-15 to 25	±0.05
x, in.	-14 to 40	±0.10
y, in.	- 2 to 10	±0.05
z, in.	0 to 14	±0.08

3

Each data group was obtained by setting α_c or β_c, y, and z and vary-
ing z. In order to obtain data more rapidly, x was varied continuously
as the data were being taken; consequently, the x values obtained were
not in even increments. A curve fit program was later used to calcu-
late all test parameters for any desired value of x. Given the values
of x, y, and z, this program would pick the six data points closest to
the given x, fit a fifth-degree equation to the data, and retabulate the
data for varying α_c or β_c. Plotted data in this form were also supplied
to FDFR to aid in their analysis of the results. For the purpose of a
timely documentation of the test results, however, the data presented
herein are in the original form as a function of x.

All data were taken with the door on the fuselage front face closed
except when clearance was necessary for the capsule sting.

SECTION III
RESULTS AND DISCUSSION

No attempt will be made herein to discuss these results in relation
to the concept of this escape capsule as a practical system since this
work is only a portion of the overall effort and the final analysis will be
done by FDFR. A summary of the test conditions is presented in
Table I (Appendix II), and Table II presents a summary of the model
attitudes tested.

The effects of the presence of the fuselage section on the lift, drag,
and pitching-moment characteristics of the escape capsule, jet off, are
presented in Figs. 4 through 11 for Mach numbers 2, 3, 4, and 5. Of
primary interest here are the pitching-moment data. For the condition
of zero lateral separation (y = 0), the abrupt decrease in pitching moment,
which occurs as the fuselage moves forward (increasing x) at all Mach
numbers and angles of attack, is directly the result of the fuselage bow
shock impinging on the lower trailing booms. Then as the fuselage moves
farther forward, a reversal in pitching-moment slope occurs when the
fuselage bow shock and resulting high pressure region move toward and
beyond the moment reference point. It may also be noted that a gradual
increase in lift coefficient was obtained as the fuselage bow shock moved
onto the capsule. These and other flow conditions to be noted can be seen
in the schlieren photographs presented for each Mach number. The solid
symbols in the data figures indicate that a schlieren photograph is pre-
sented for these conditions.

Laterally moving the capsule to y = 5 in. (see Figs. 4e, 6e, 8e, and
10e) generally reduced the magnitude of the fuselage effects as noted for

y = 0. This reduction results from the lower left trailing boom being moved away from the fuselage bow shock. It should be noted that the magnitude of these fuselage interference effects generally decreased with increasing Mach number and vertical separation distance (z).

Another interference effect of consequence was the large regions of flow separation over the bottom surface of the capsule at negative angles of attack with the fuselage in proximity to the capsule (note photographs of Figs. 5c, 7a, 9c, and 11c). This condition, which occurred at all Mach numbers, caused a rather abrupt rise in pitching moment.

For the models in the sideslip attitude (see Fig. 3b), Figs 12 through 15 present the effects of the presence of the fuselage section on the capsule side-force, yawing-moment, and rolling-moment characteristics, jet off, for Mach numbers 2, 3, 4, and 5. For these data, the most significant variations were obtained in the rolling moment. For the condition ($-8 \leqq x \leqq -4$) where the fuselage bow shock was standing on the trailing booms, and as the angle of sideslip increased, the lower left trailing boom moved into the shock region and the lower right trailing boom moved out of the shock region, resulting in a large increase in rolling moment which these data show. As the fuselage moved farther forward ($-4 \leqq x \leqq 4$), a decrease in rolling moment was obtained as a result of the fuselage bow shock once again moving over the lower right trailing boom. With the capsule displaced laterally to y = -5 in., the decrease in rolling moment noted previously for y = 0 was not as abrupt because the lower right trailing boom was further removed from the influence of the fuselage bow shock. The magnitude of these effects increased somewhat with increasing Mach number. Only small variations were obtained in side force and yawing moment for the range of fuselage travel investigated.

Similar results, as shown previously for the capsule in pitch and sideslip, are presented in Figs. 16 through 27 with flow simulation of the escape rocket exhaust plume. The trends of the interference effects for these data were very similar to those for jet off. However, the following additional observation is made. The interference effects, jet on as compared to jet off, are of greater magnitude when the capsule is in proximity to the fuselage. This is largely because of the jet impingment on the forward portion of the fuselage section causing flow separation on the capsule earlier than obtained with the jet off. Of the schlieren photographs presented showing this flow separation, two particularly good examples (Figs. 5d and 17d) show for identical model conditions that the jet-on separation (Fig. 17d) occurs much farther forward on the capsule than the jet-off separation (Fig. 5d).

REFERENCES

1. Jenke, Leroy M., Jones, Jerry H., and Myers, A. W. "Force Tests on a Separable-Nose Crew Escape Capsule with Cold Flow Rocket Jet Simulation at Mach Numbers 1.5 through 6." AEDC-TR-66-74 (AD481301), April 1966.

2. Jones, Jerry H. "Force Tests on a Separable-Nose Crew Escape Capsule in Proximity to the Parent Fuselage at Mach Numbers 1.5 through 4.5." AEDC-TR-66-140 (AD487406), August 1966.

3. Test Facilities Handbook (Seventh Edition). "von Kármán Gas Dynamics Facility, Vol. 4." Arnold Engineering Development Center, July 1968.

APPENDIXES

I. ILLUSTRATION

II. TABLES

Section D-D

0.564

0.755R

Section C-C

0.334

1.751R

Fuselage
Reference
Line

Section B-B

0.325
1.385
1.350R
1.859R
2.085R
2.444R
1.780
1.297
0.456
0.280
0.078
0.257
1.885R
2.408R
0.298

Section A-A

0.150
1.605R
1.850R
2.205R
3.269R
1.667
1.376
0.657
0.280
1.777R
0.418
3.001
0.276
0.587
0.892

All Dimensions in Inches

Moment Reference

Trim Tab

30° (Typ)

120° (Typ)

Balance ₵

0.30

A

B

C

2°13'

D

Fuselage Reference Line

1.400

3.500

D

9.400

C

12.900

B

13.475

25°

A

13°

13.880

2.120

ℓ = 16.500

18.100

Separation Bulkhead
Location

a. Capsule Details
Fig. 1 Model Details

9

AEDC-TR-68-278

All Dimensions in Inches

1.125 R

1.500

1.200

1.425

1.000

0.700

0.110

1.700

2.870

0.518

1.577

60 deg (Typ.)

0.590   0.700

0.110

b. Trim Tab Details

1.200

9.450

9.060

8.520

0.900

1.030

30 deg

0.600

0.850
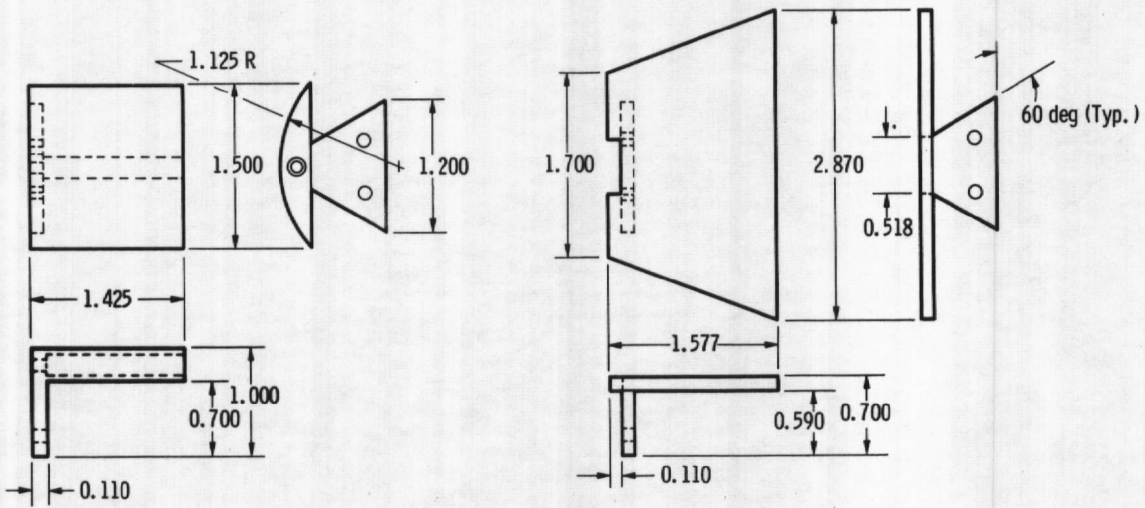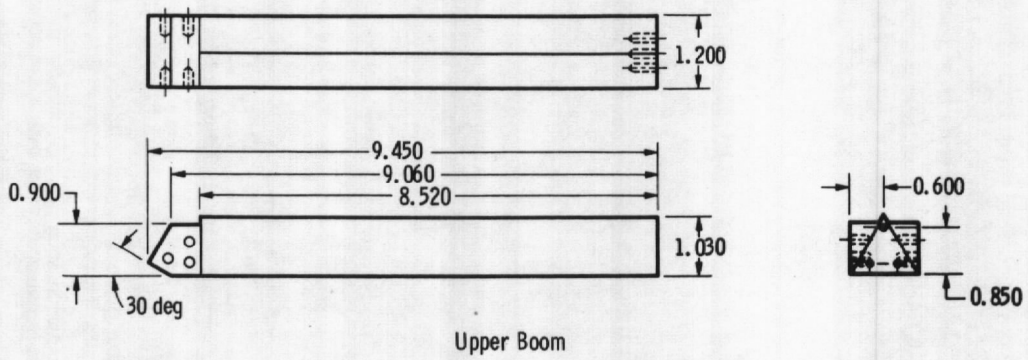
Upper Boom

All Dimensions in Inches

0.720

0.500

30 deg

0.620

1.220

1.030   5.650

1.030

11.250

1.200
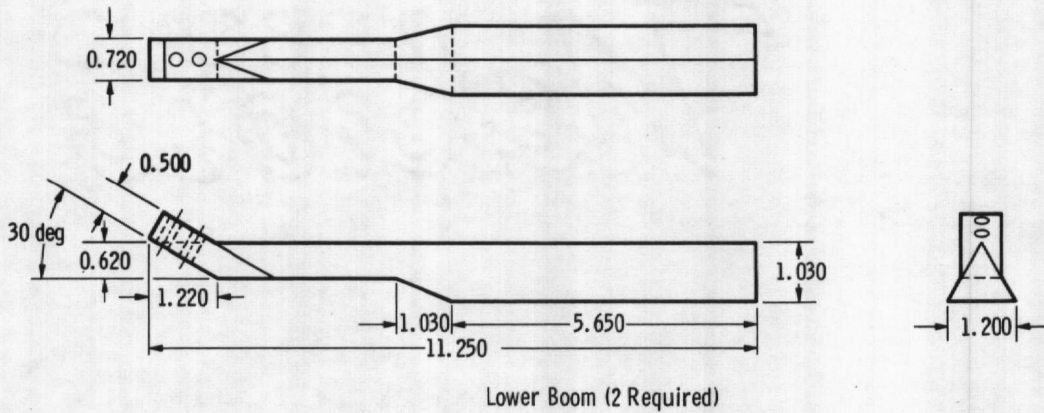
Lower Boom (2 Required)

c. Trailing Boom Details

Fig. 1 Continued

All Dimensions in Inches
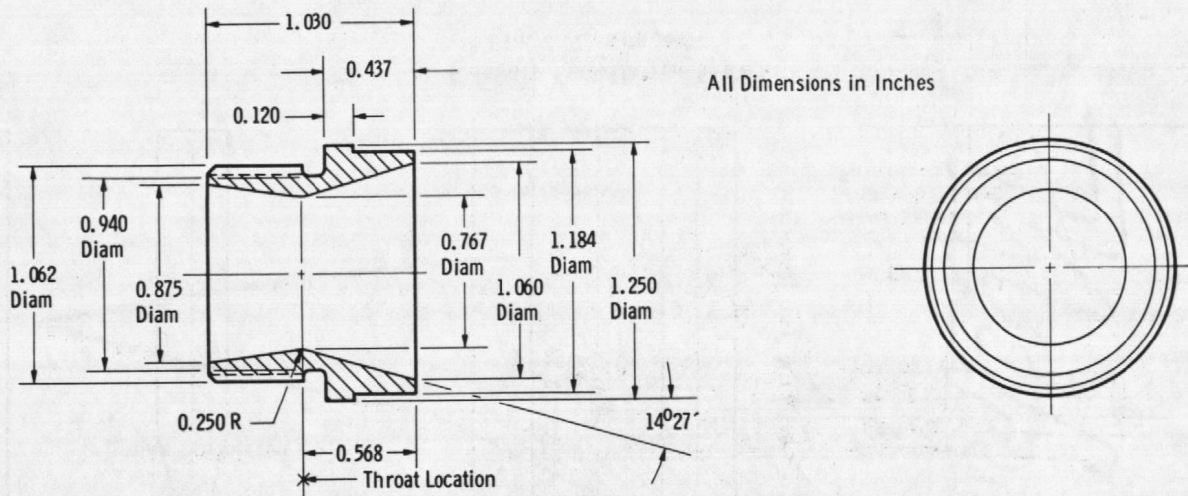
d. Nozzle Details
Fig. 1 Continued

Balance Shroud

Moment
Reference
Point

Balance

Balance Cable
Shroud

Sting

Fuselage Reference Line

Nozzle Air Supply Duct

Nozzle

Nozzle Thrust Axis
(Angle with Fuselage
Reference Line = 35 deg)

Nozzle Stilling Chamber

Flow Straightener
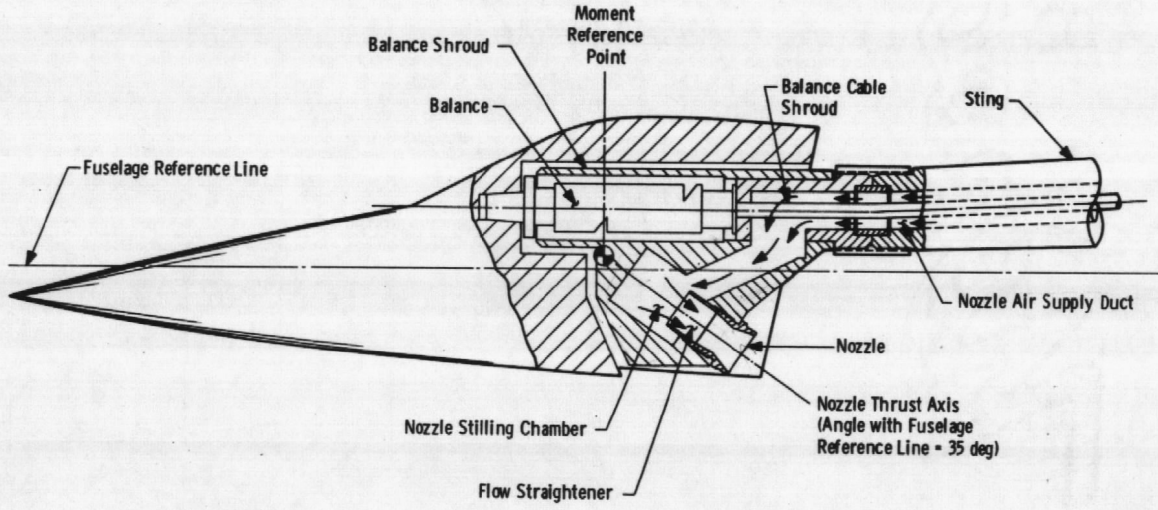
e. Capsule Installation Sketch
Fig. 1 Continued
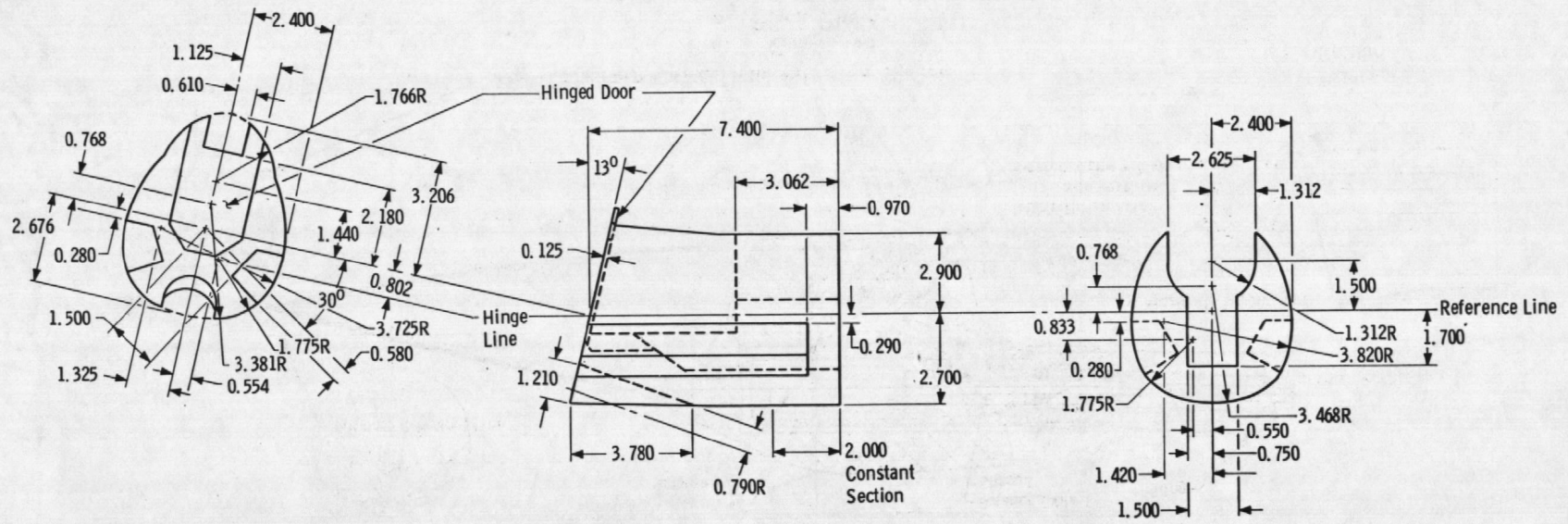
f. Fuselage Details
Fig. 1 Concluded
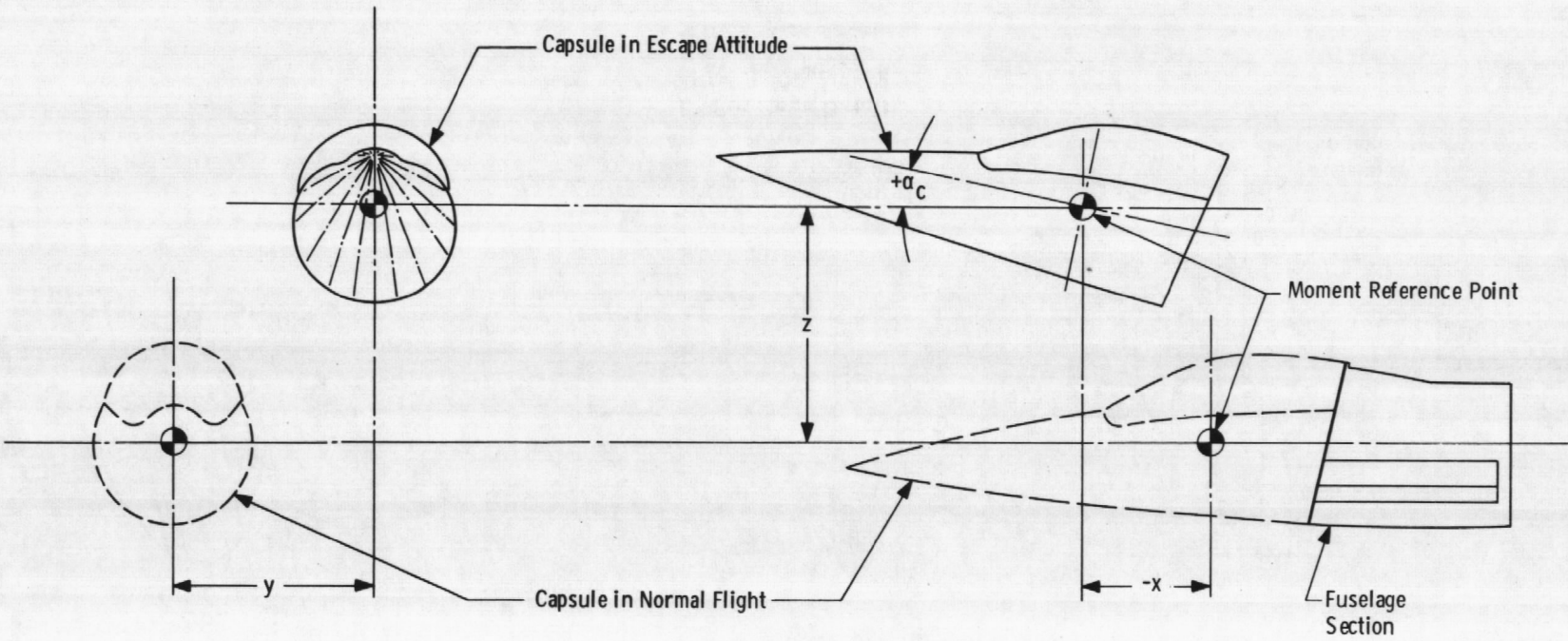
a. Pitch Plane
Fig. 2 Capsule and Fuselage Proximity Details

Capsule in Escape Attitude

$+\beta_c$

$-y$

Moment Reference Point

Capsule in Normal Flight

Fuselage Section

z

$-x$
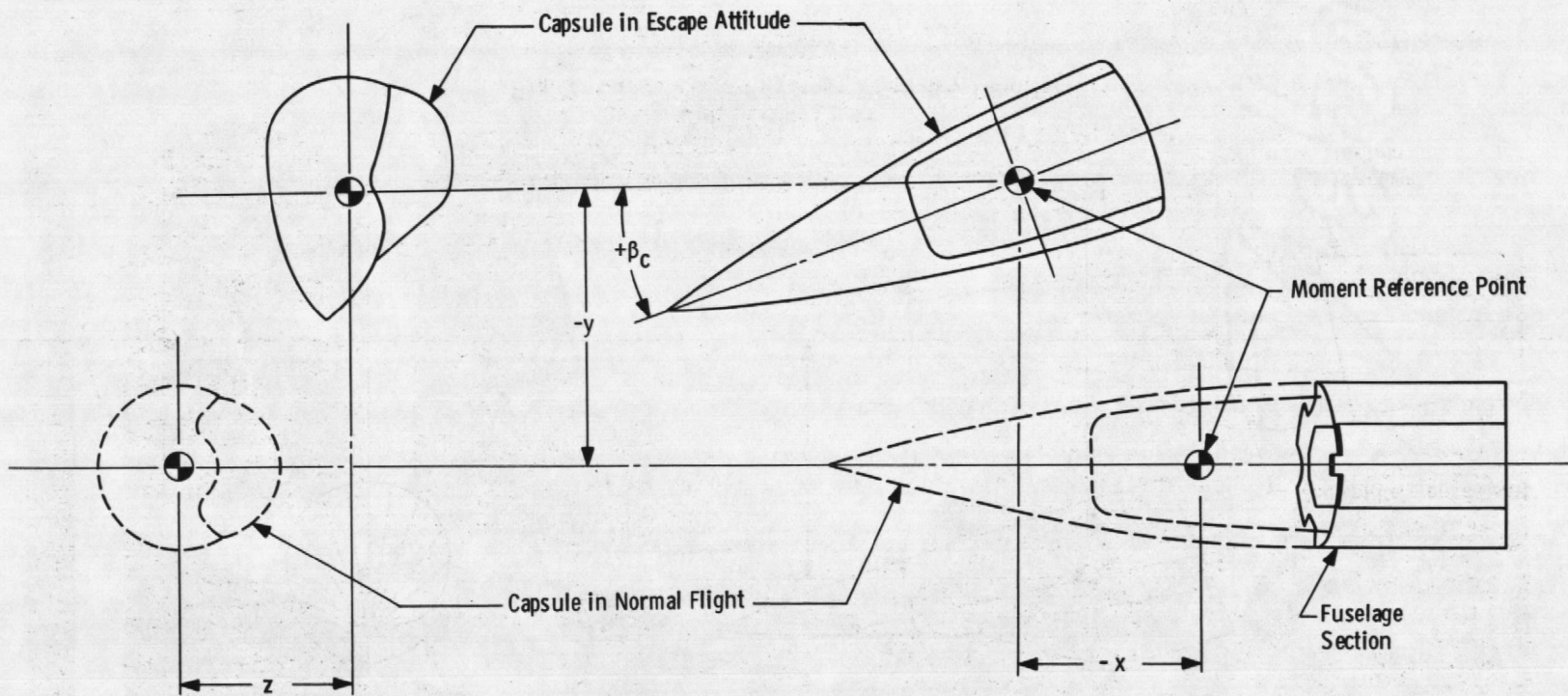
b. Yaw Plane
Fig. 2 Concluded.
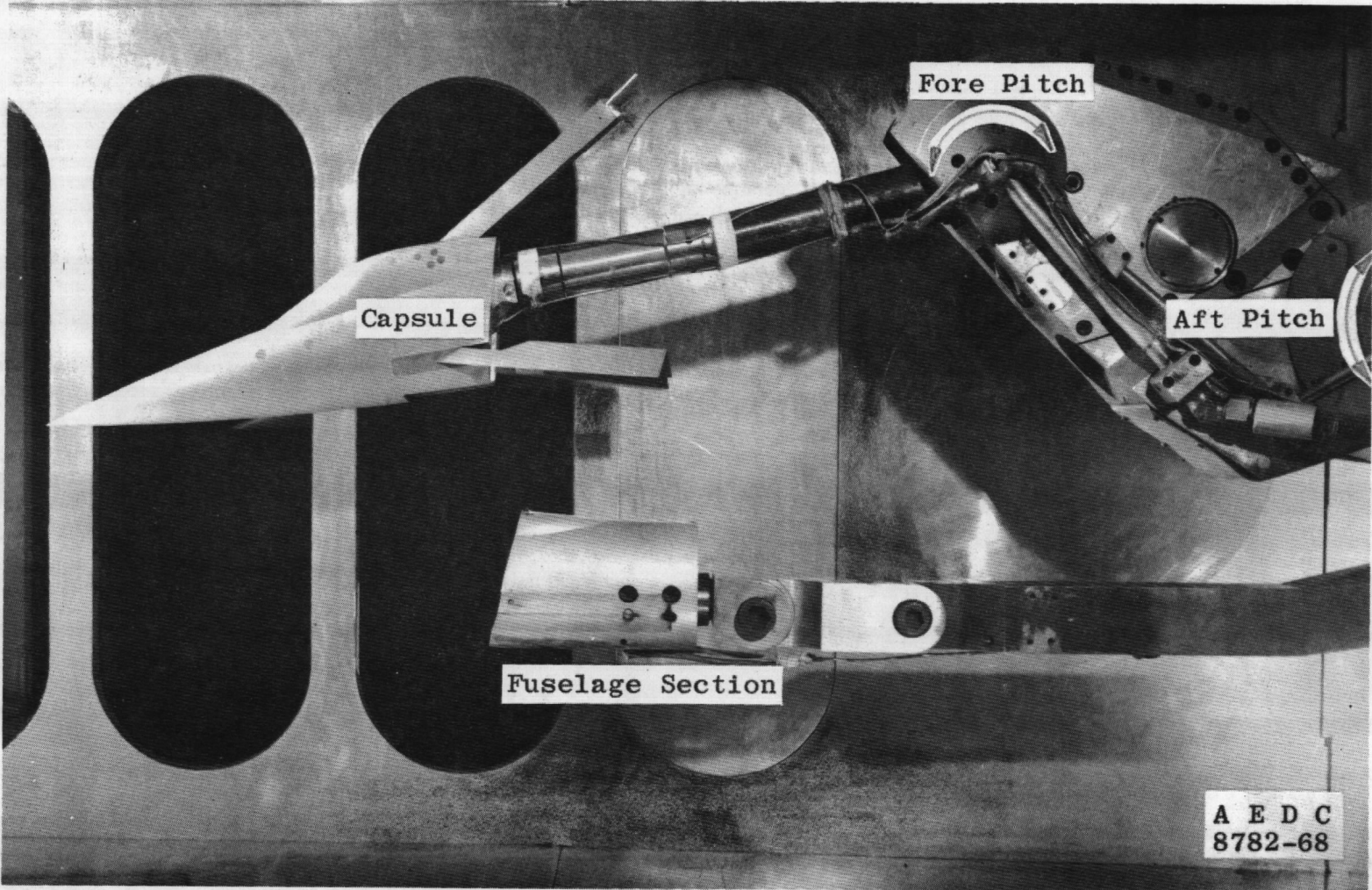
a. Capsule Pitch Installation
Fig. 3 Installation Photographs

Capsule

Fuselage Section

AEDC
8780-68
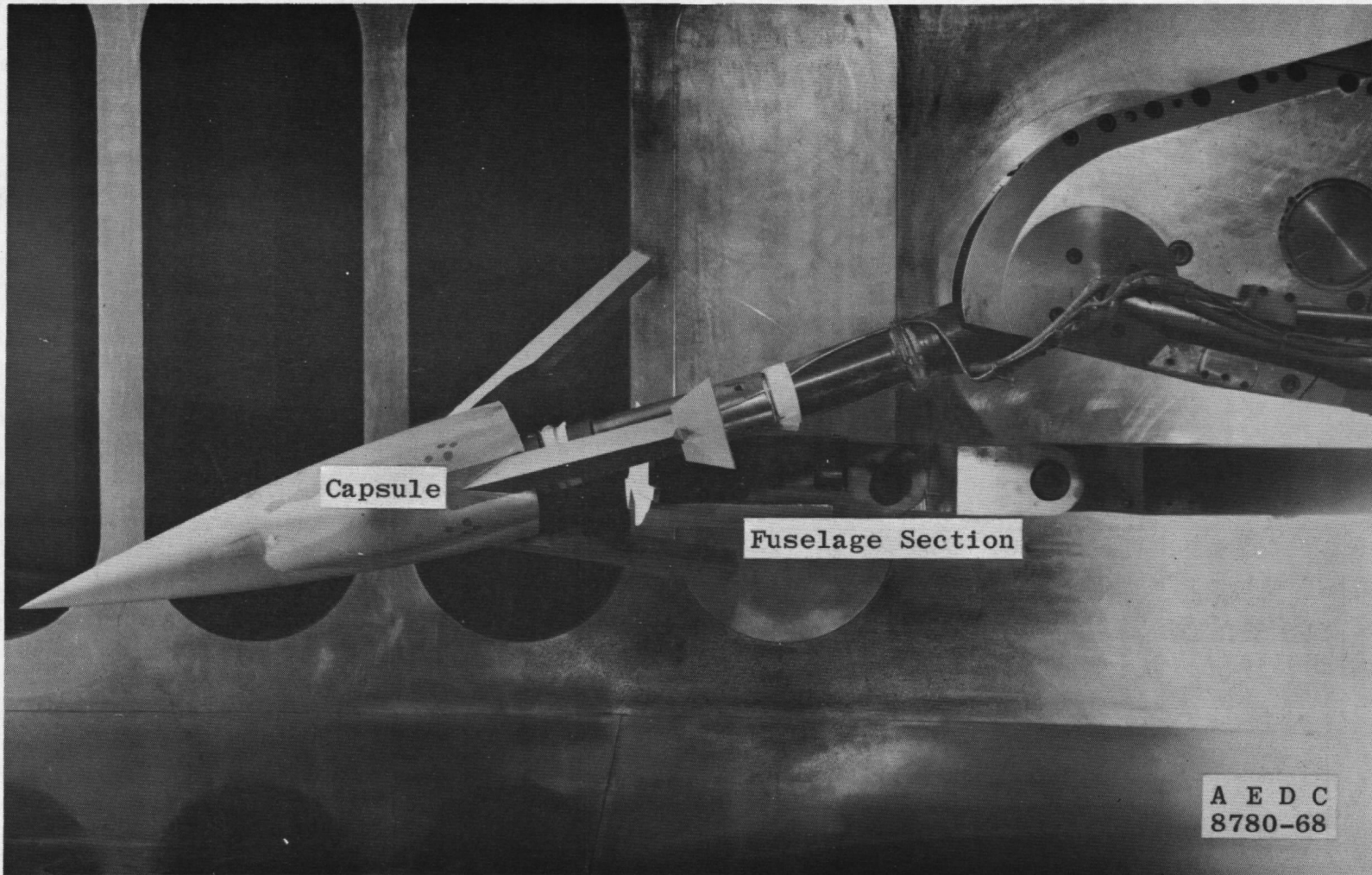
b. Capsule Yaw Installation
Fig. 3 Concluded
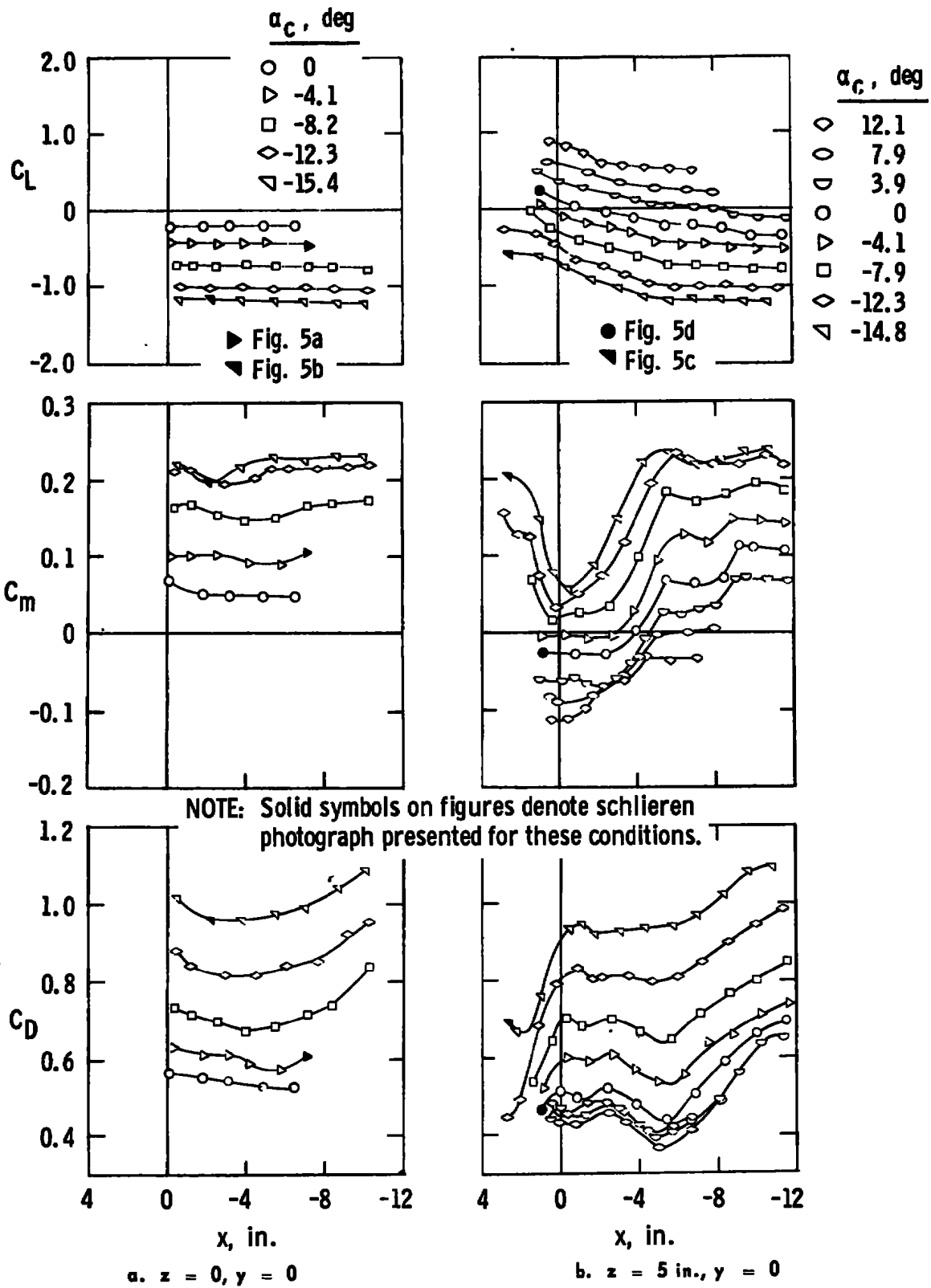
Fig. 4 Lift, Drag, and Pitching-Moment Characteristics of the Capsule, Jet Off, M_∞ = 2

18
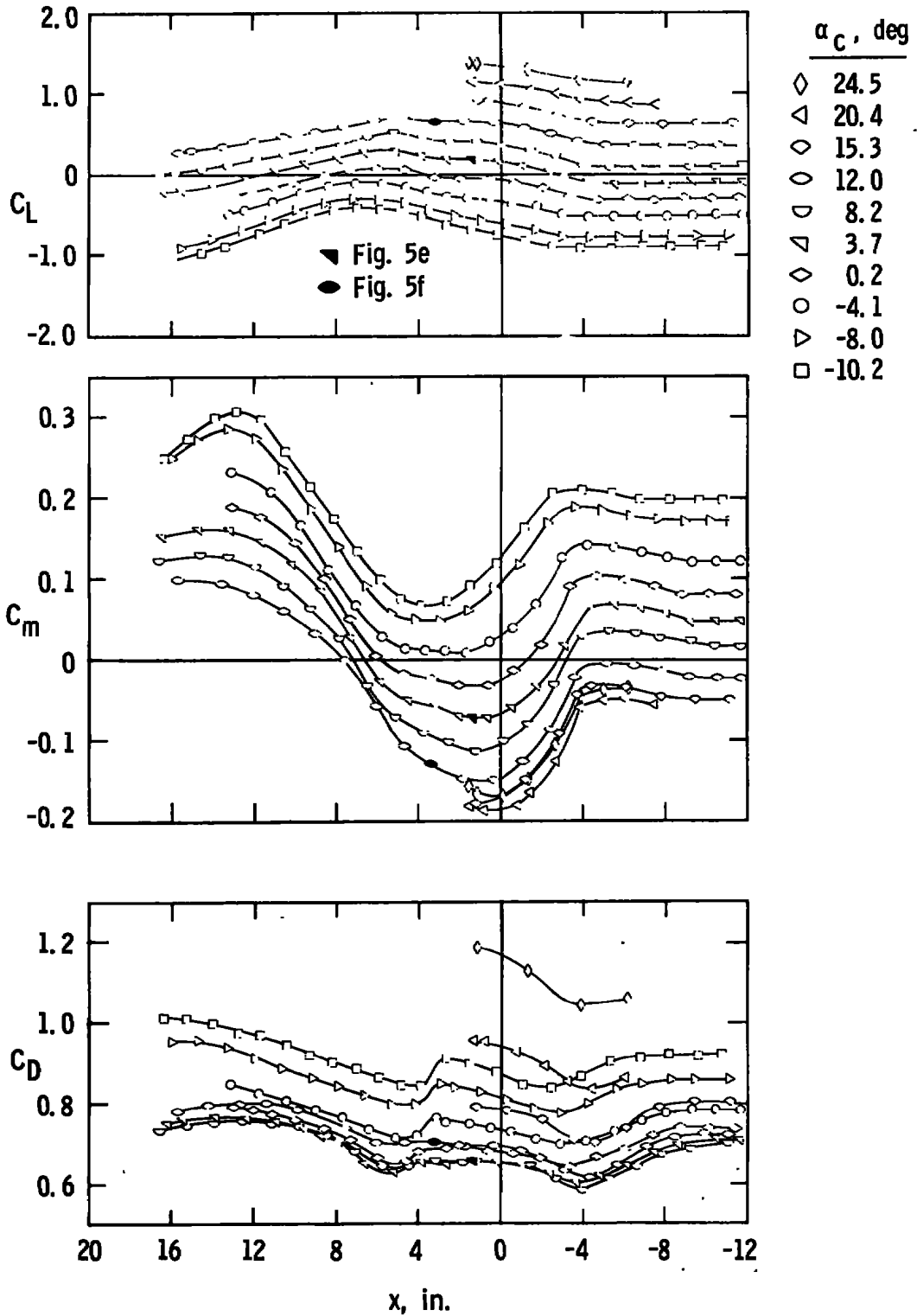
c. z = 10 in., y = 0
Fig. 4 Continued
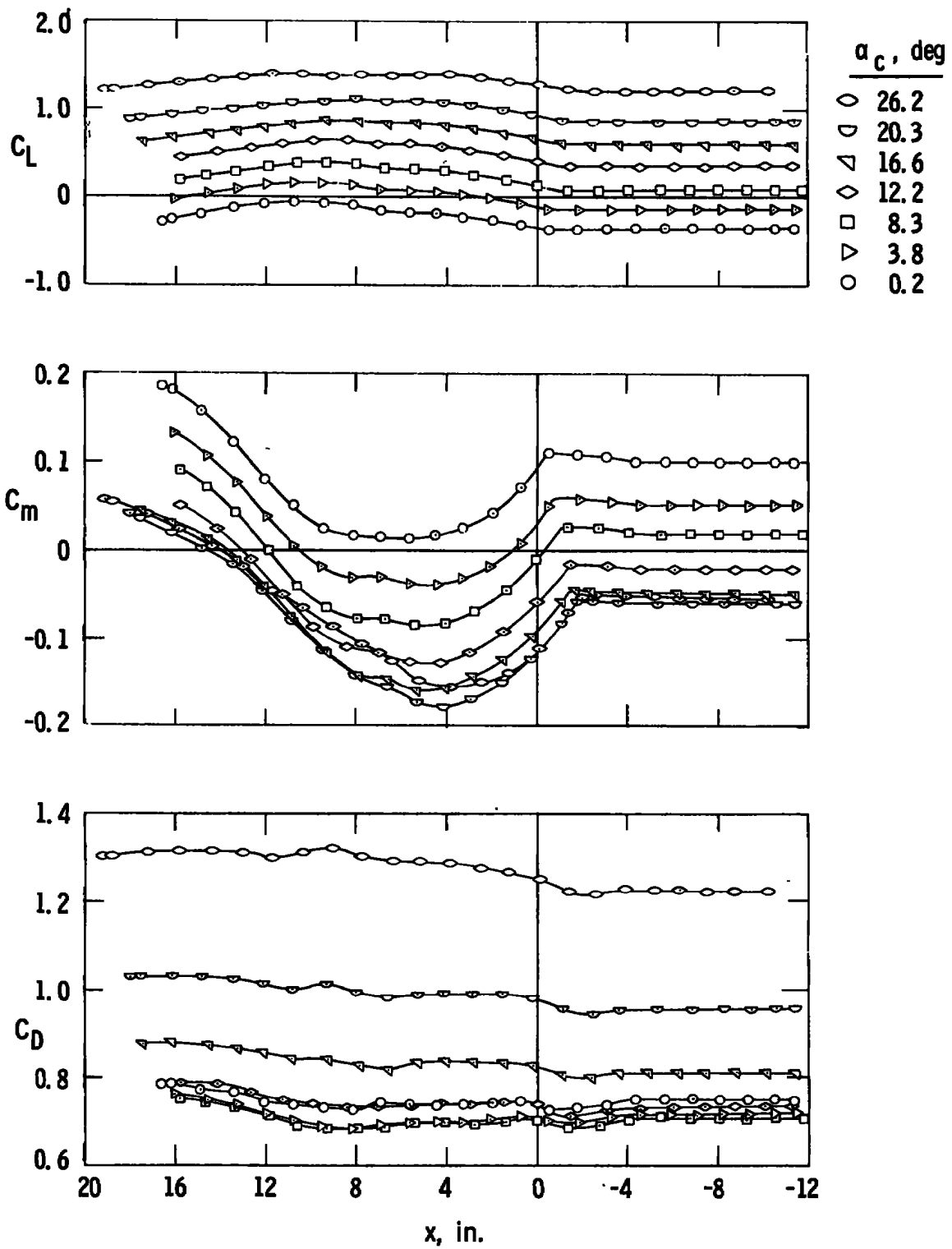
d. z = 14 in., y = 0
Fig. 4 Continued
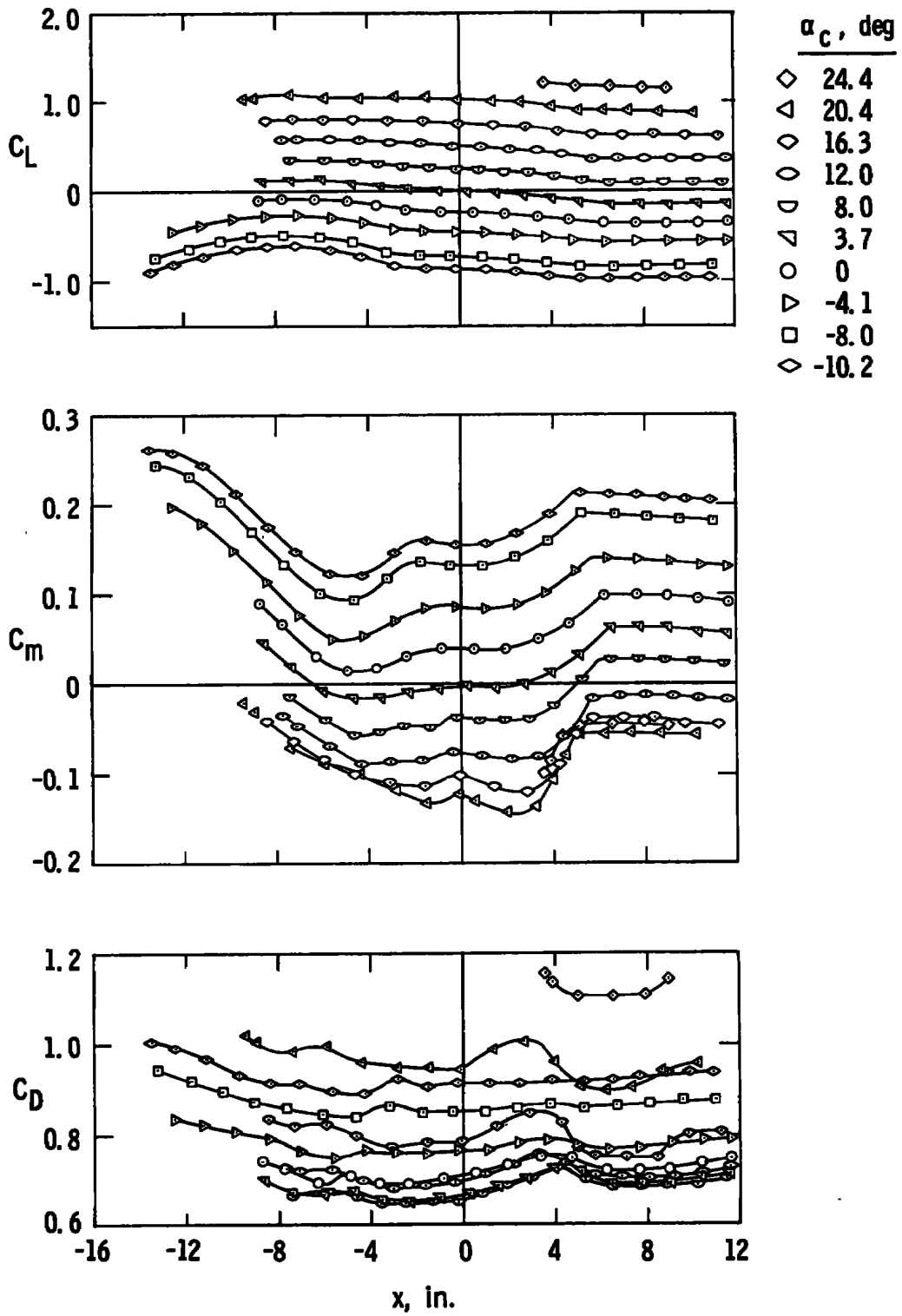
e. z = 10 in., y = 5 in.
Fig. 4 Concluded
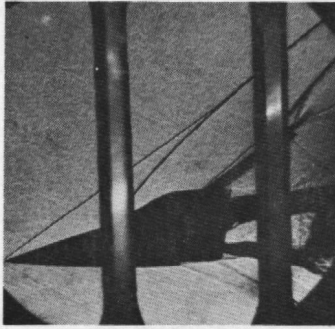
a. α_c = –4.1 deg, y = 0
z = 0, x = –7.0 in.
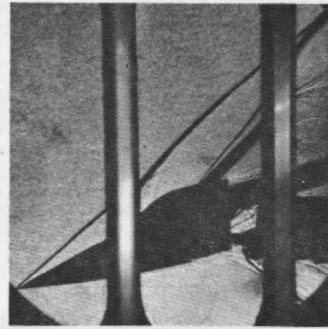
b. α_c = –15.4 deg, y = 0
z = 0, x = –2.0 in.
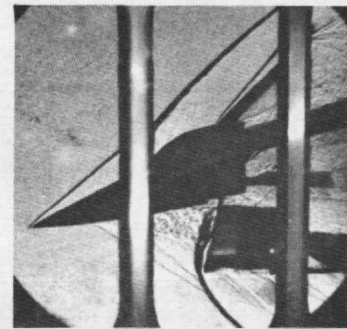
c. α_c = –14.8 deg, y = 0
z = 5 in., x = 2.5 in.

d. α_c = 0, y = 0
z = 5 in., x = 1.0 in.
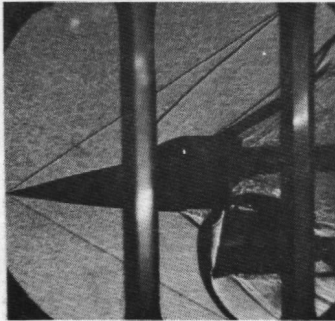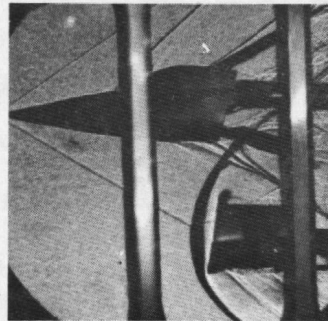
e. α_c = 3.7 deg, y = 0
z = 10 in., x = 1.5 in.
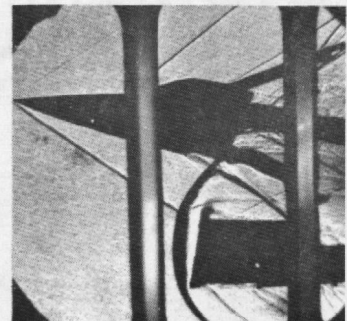
f. α_c = 12.0 deg, y = 0
z = 10 in., x = 3.75 in.

Fig. 5 Schlieren Photographs, Jet Off, M_∞ = 2
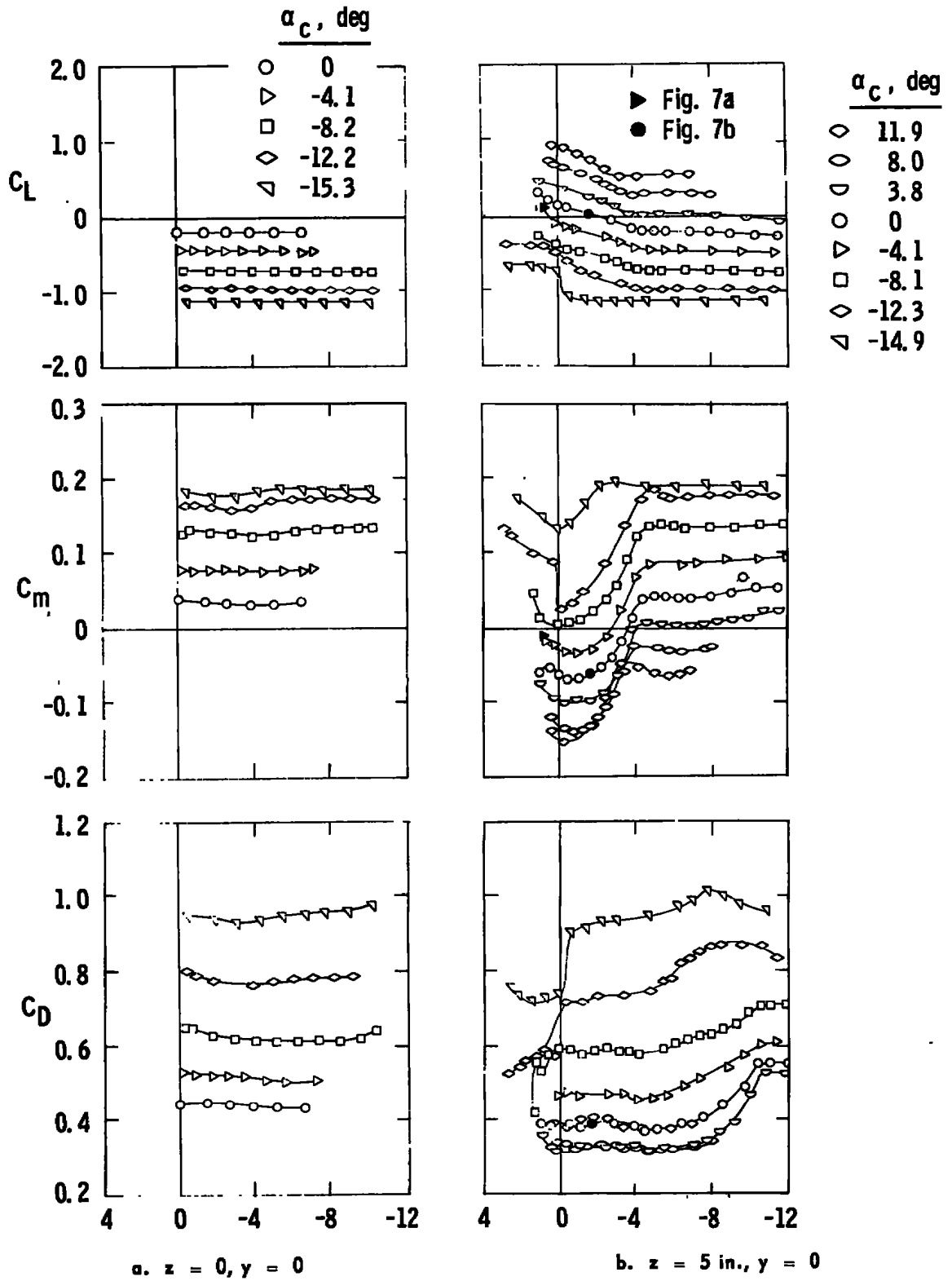
Fig. 6 Lift, Drag, and Pitching-Moment Characteristics of the Capsule, Jet Off, $M_\infty = 3$

a. $z = 0, y = 0$

b. $z = 5$ in., $y = 0$

23
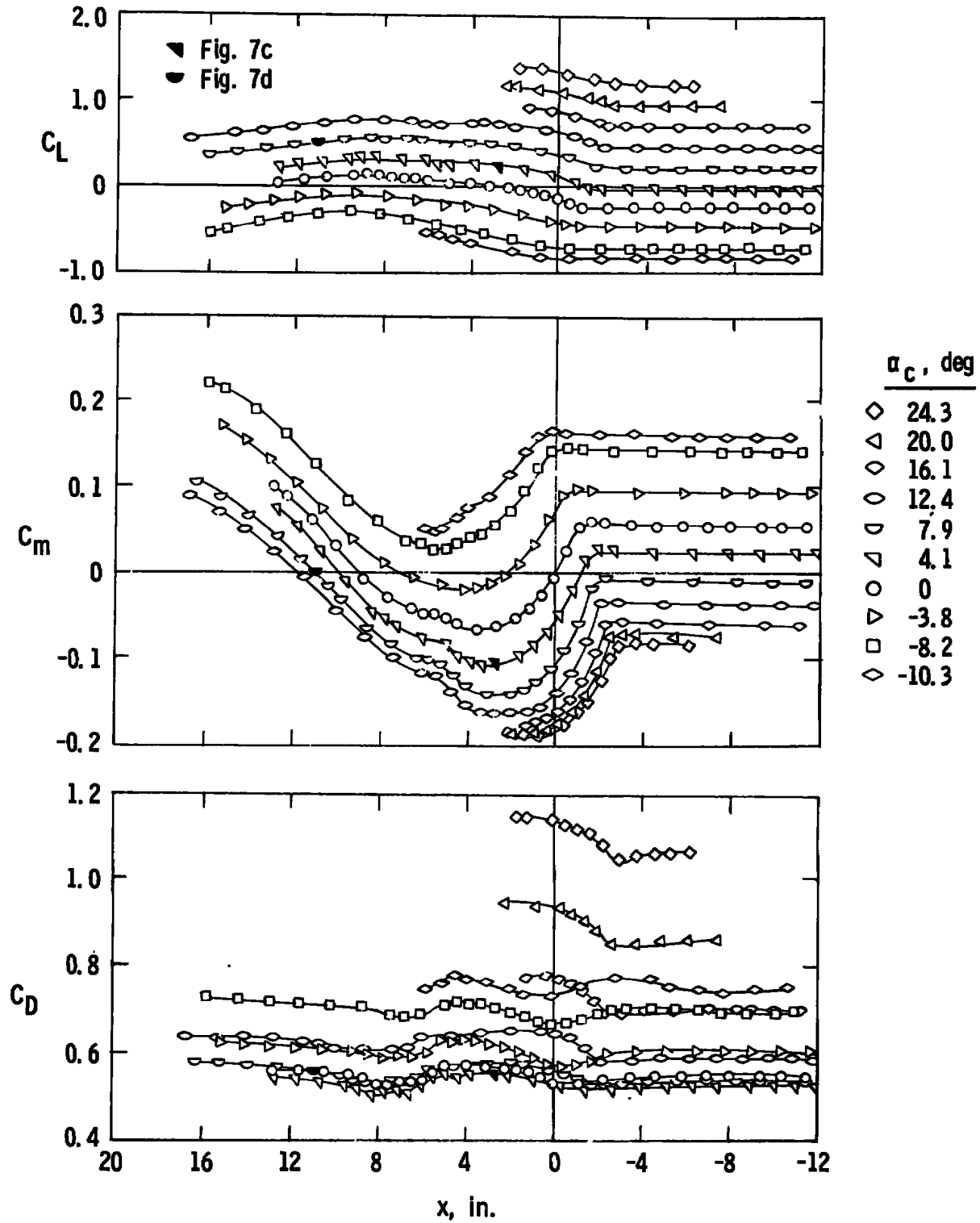
c. z = 10 in., y = 0
Fig. 6 Continued
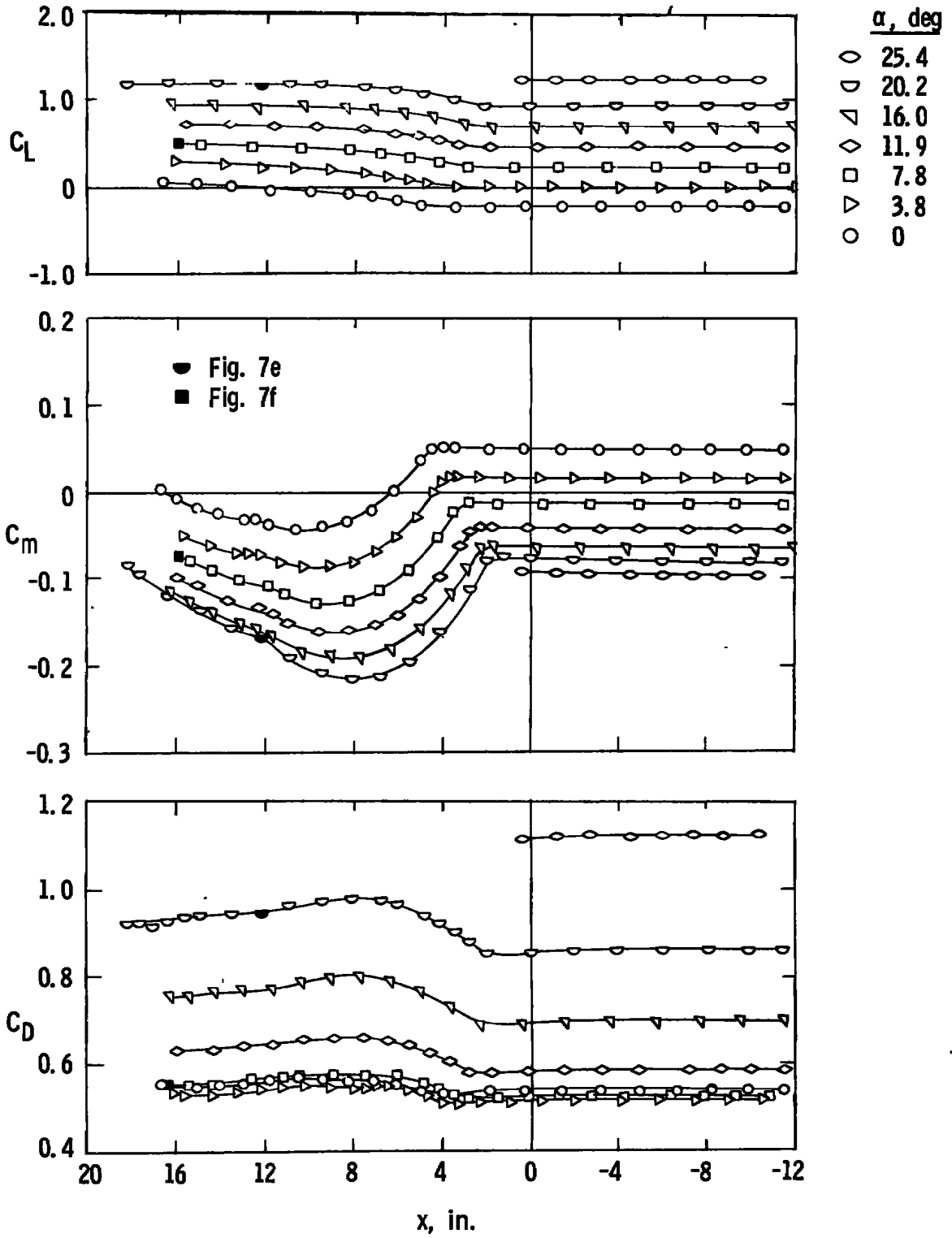
d. $z = 14$ in., $y = 0$
Fig. 6 Continued
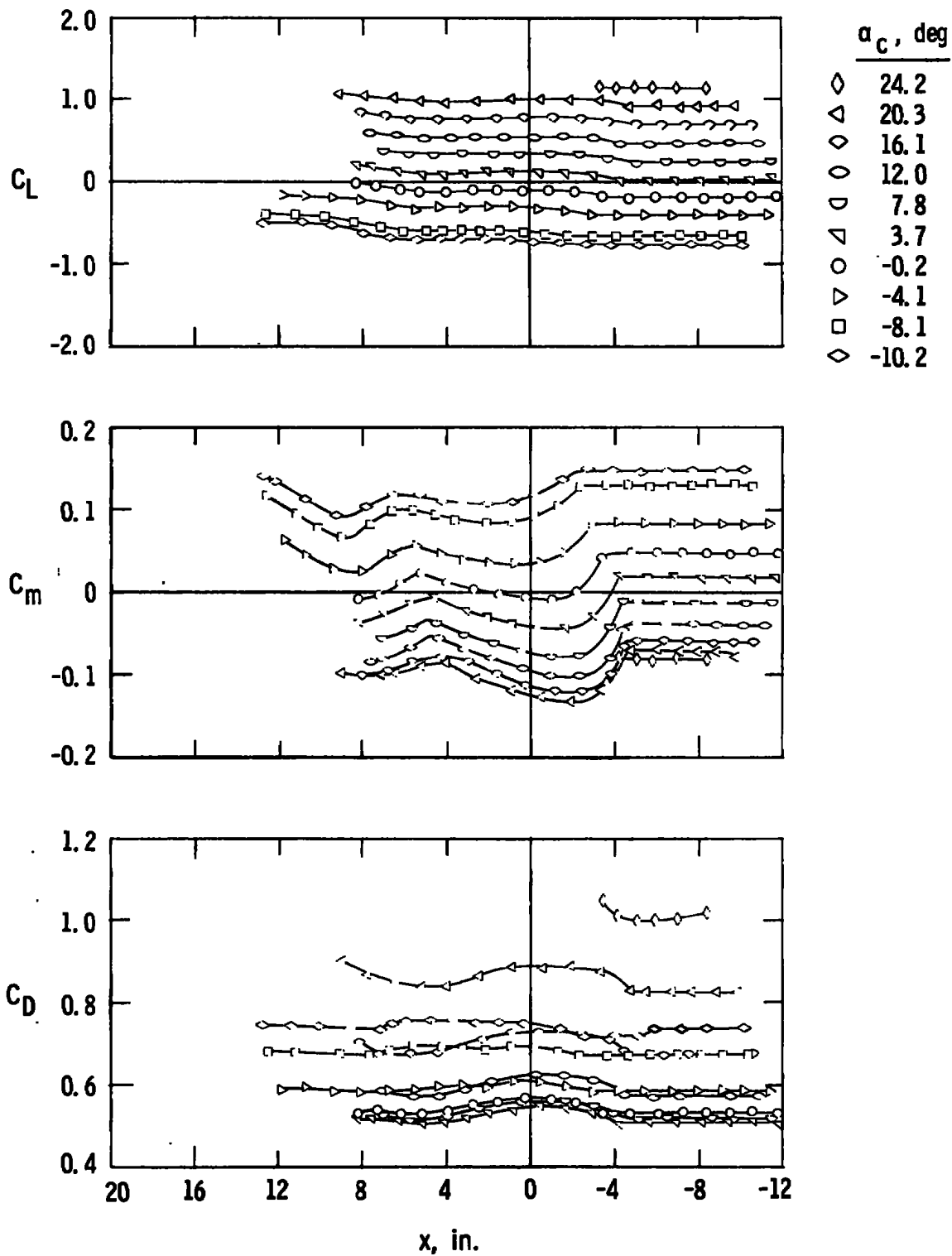
e. z = 10 in., y = 5 in.
Fig. 6 Concluded
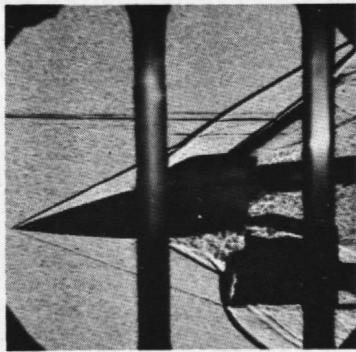
a. $\alpha_c = -4.1$ deg, $y = 0$
   $z = 5$ in., $x = 1.0$ in.
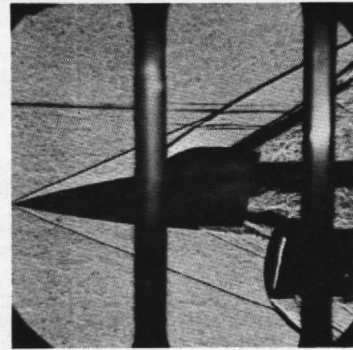
b. $\alpha_c = 0$, $y = 0$
   $z = 5$ in., $x = -2.2$ in.
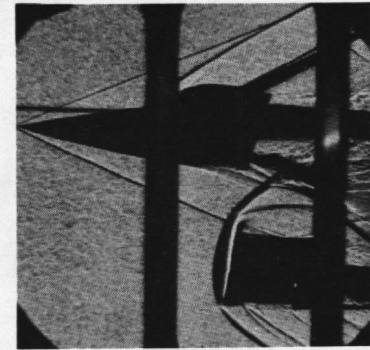
c. $\alpha_c = 4.1$ deg, $y = 0$
   $z = 10$ in., $x = 2.2$ in.
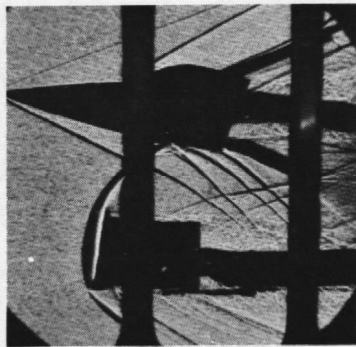
d. $\alpha_c = 7.9$ deg, $y = 0$
   $z = 10$ in., $x = 10.6$ in.
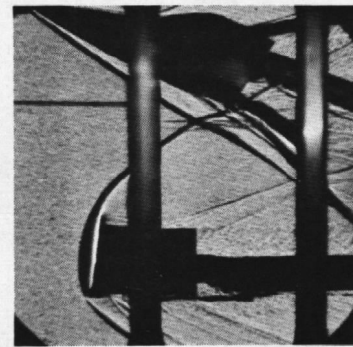
e. $\alpha_c = 20.2$ deg, $y = 0$
   $z = 14$ in., $x = 12.5$ in.
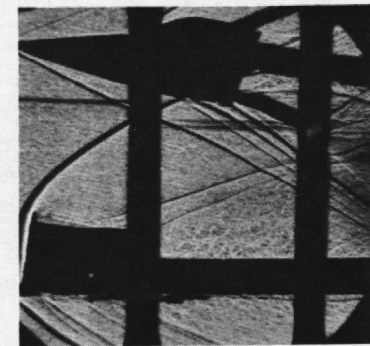
f. $\alpha_c = 7.8$ deg, $y = 0$
   $z = 14$ in., $x = 16.5$ in.

Fig. 7 Schlieren Photographs, Jet Off, $M_\infty = 3$
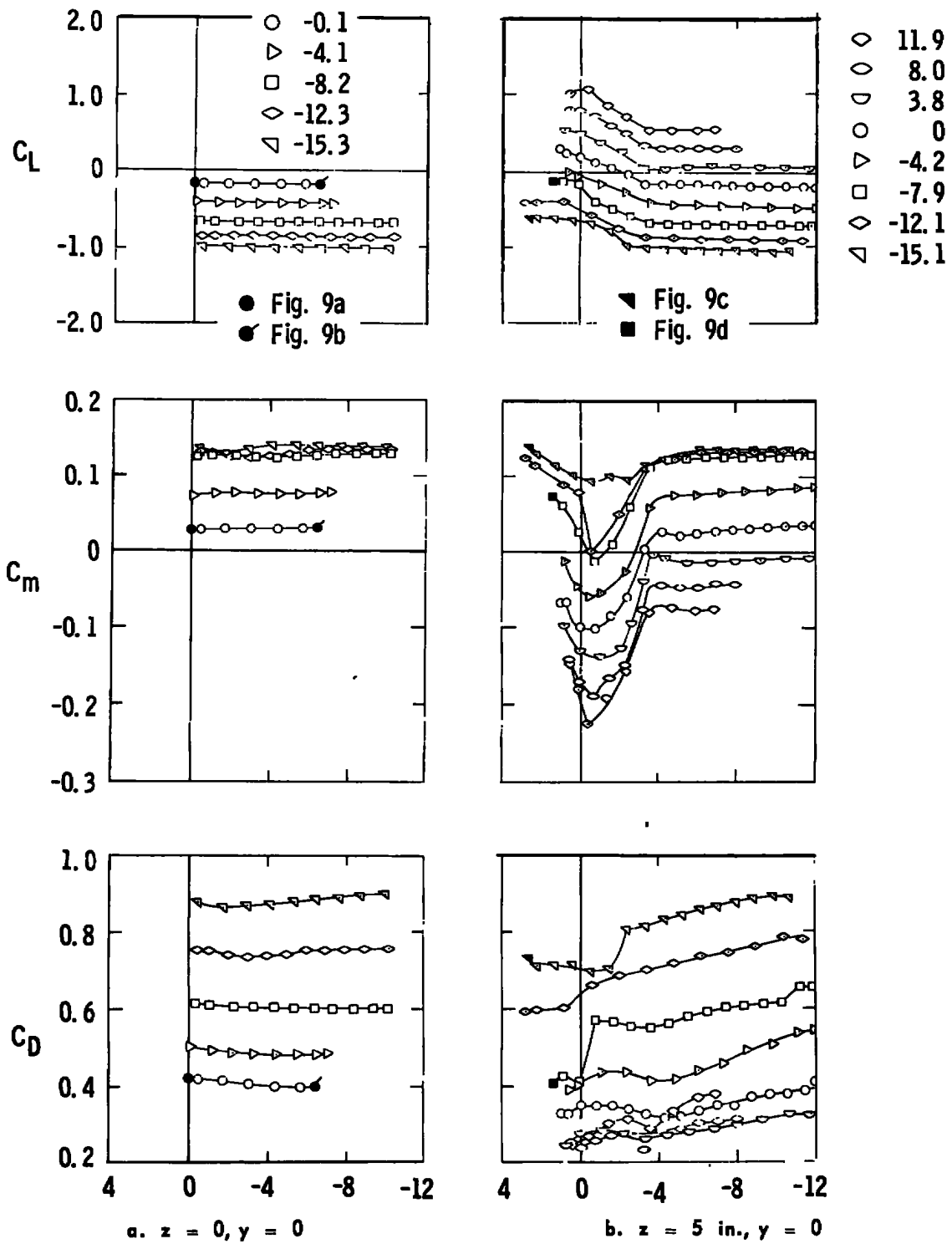
a. z = 0, y = 0 b. z = 5 in., y = 0

Fig. 8 Lift, Drag, and Pitching-Moment Characteristics of the Capsule, Jet Off, M_∞ = 4

c. z = 10 in., y = 0
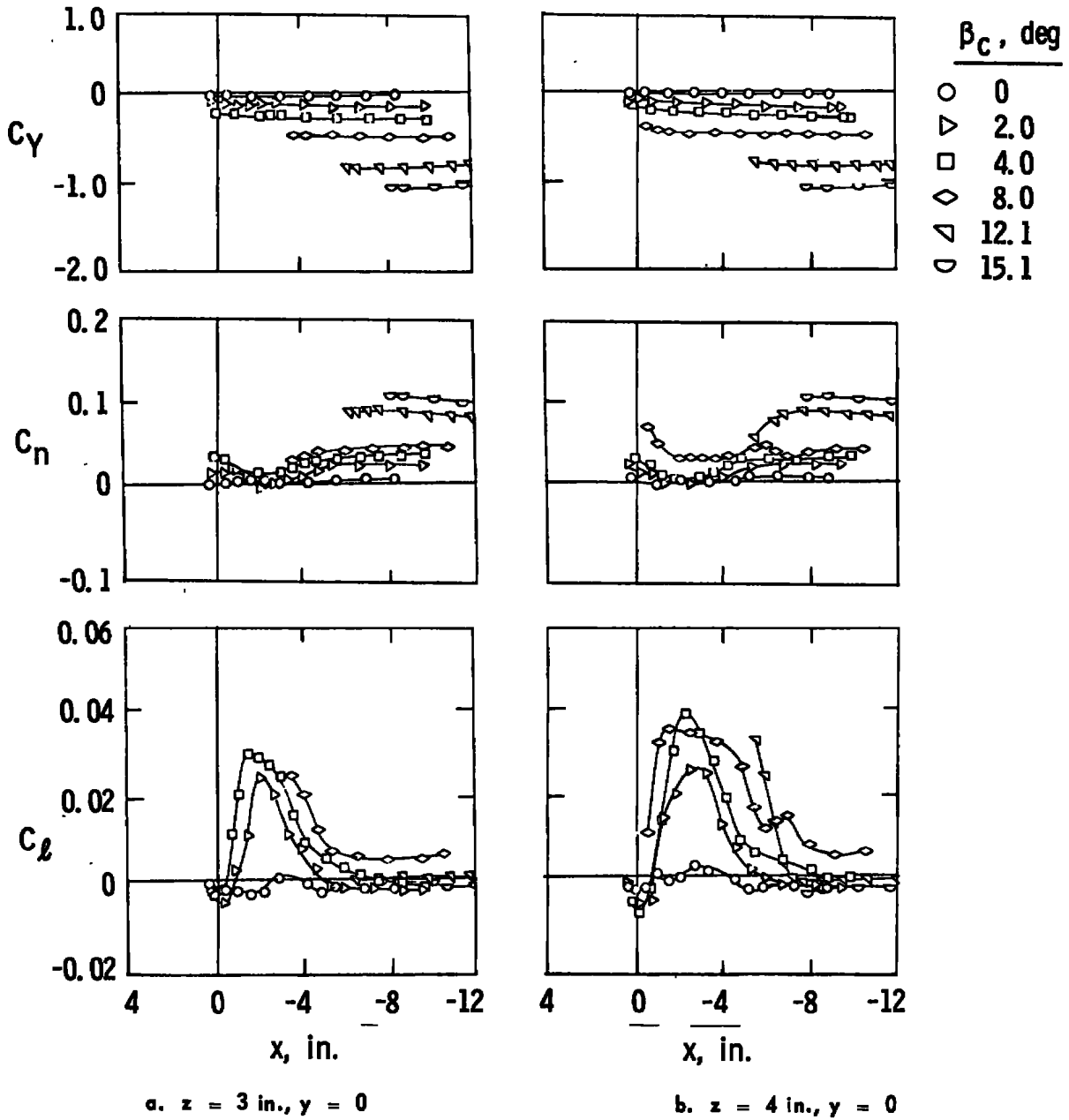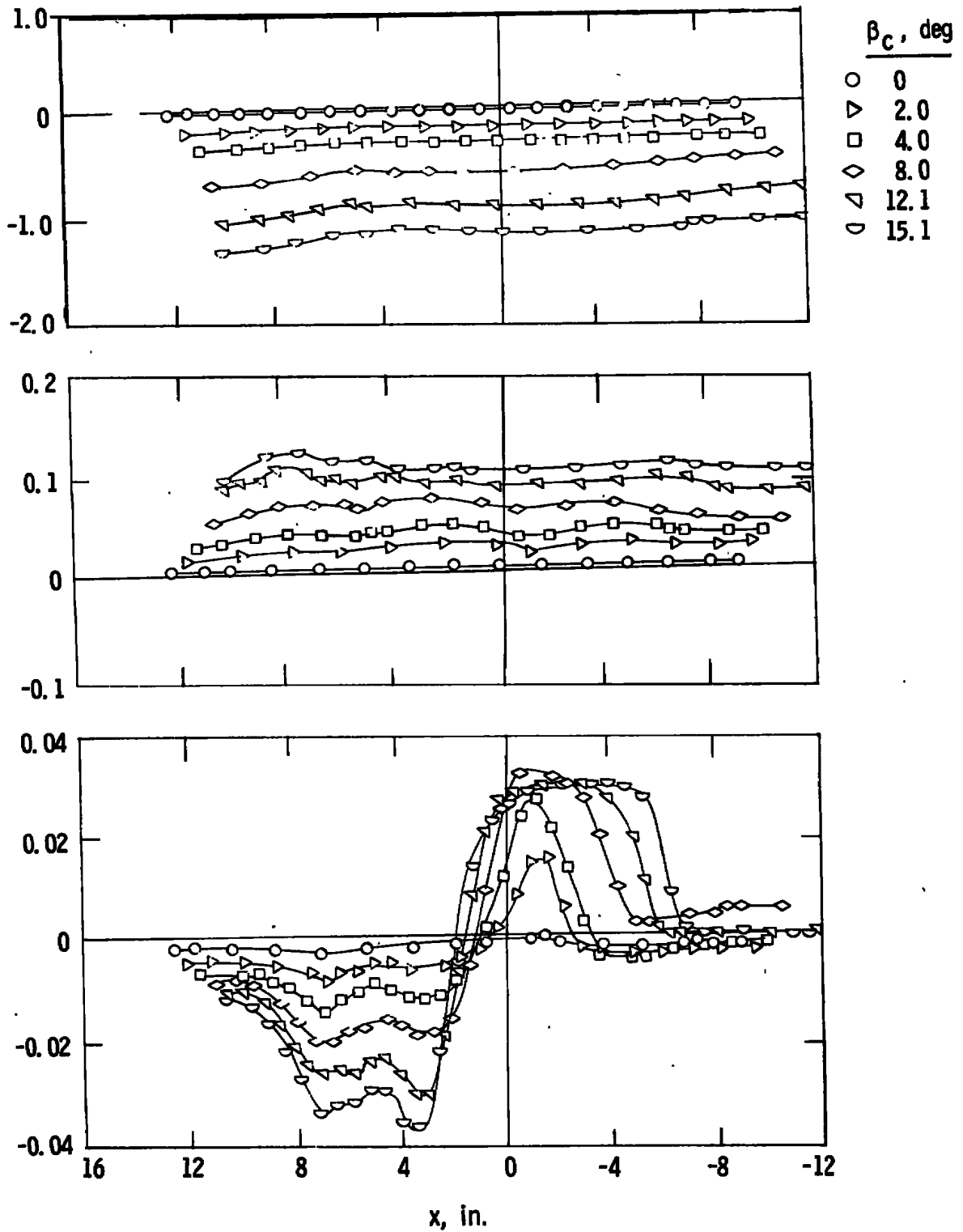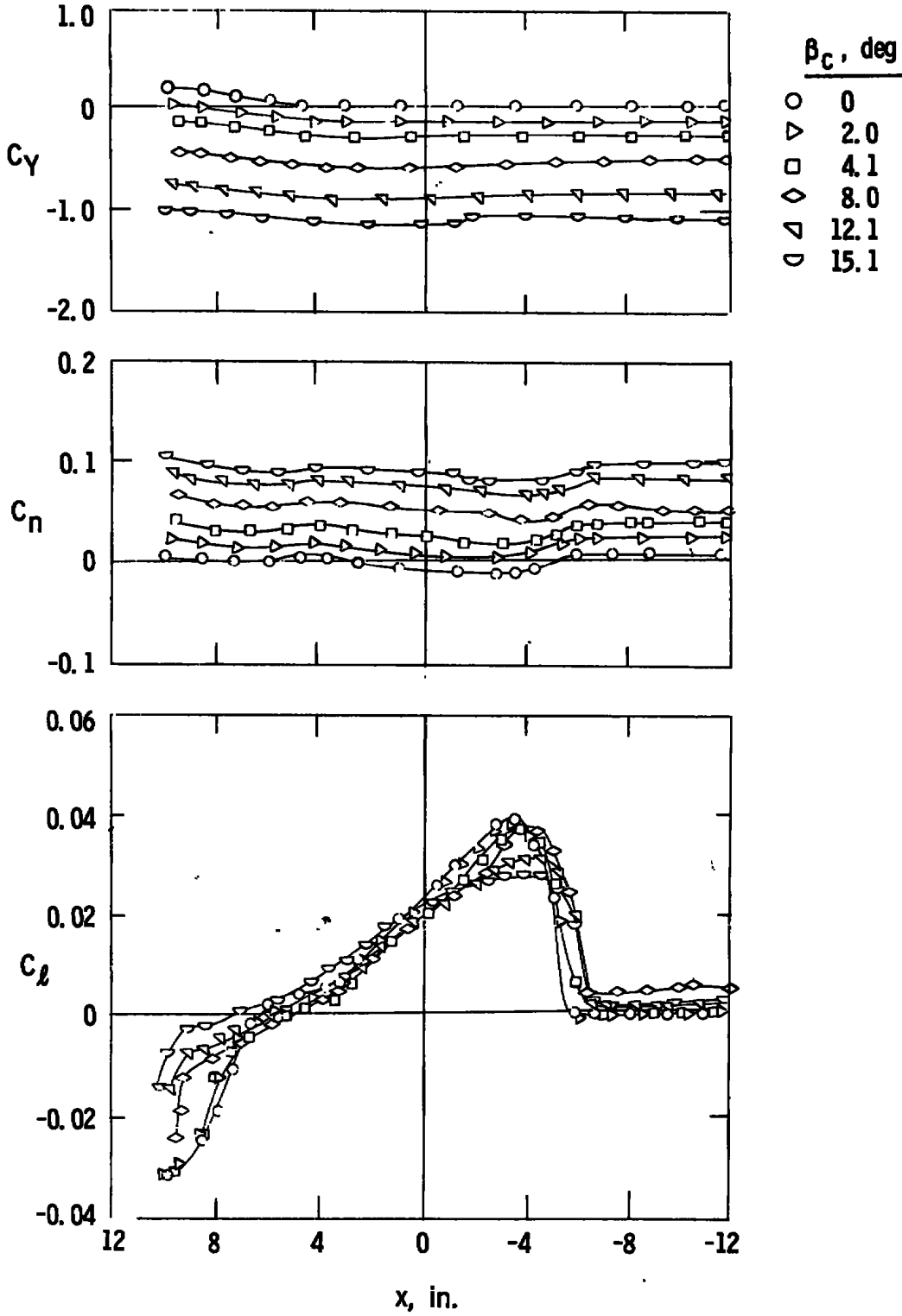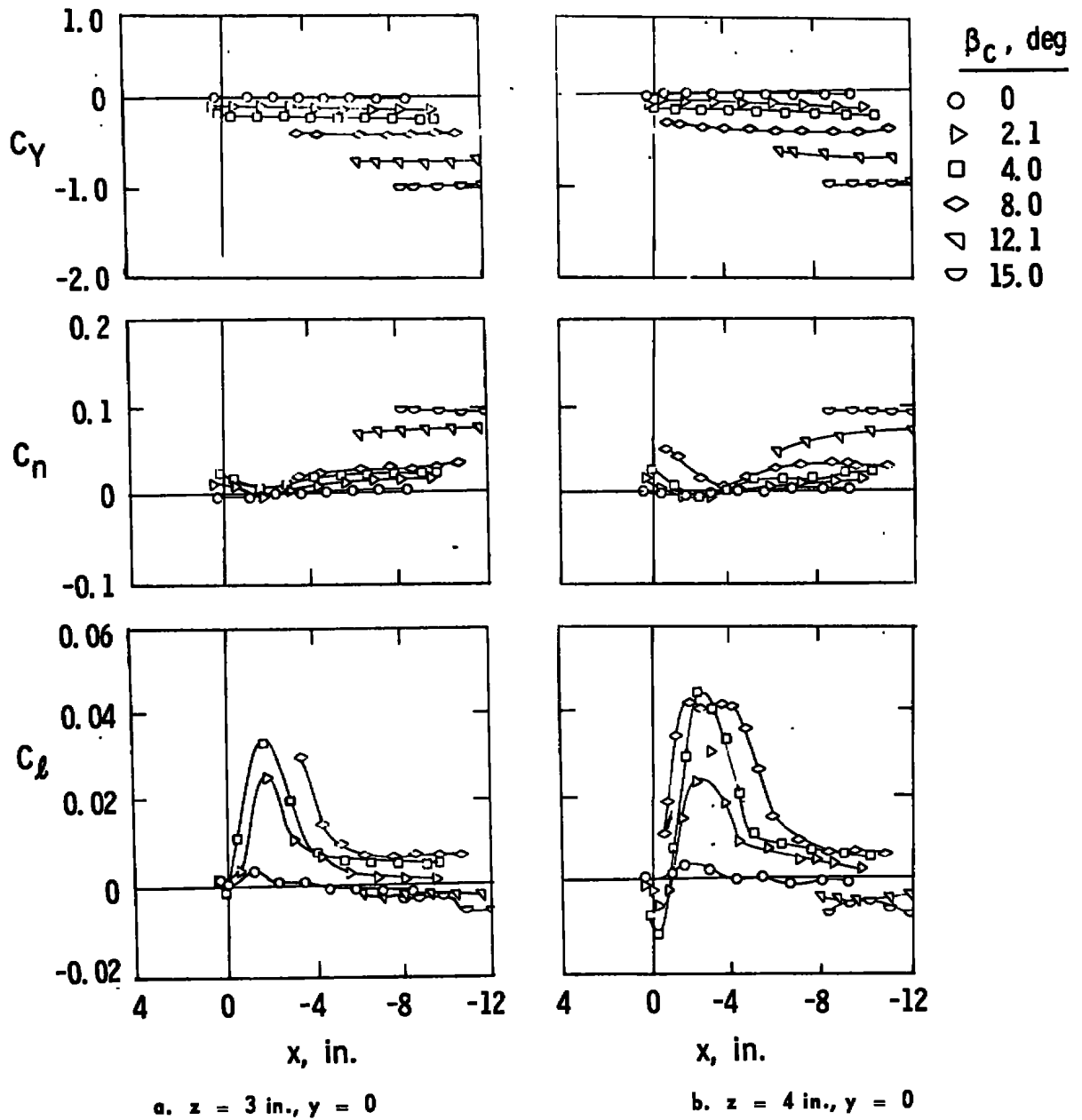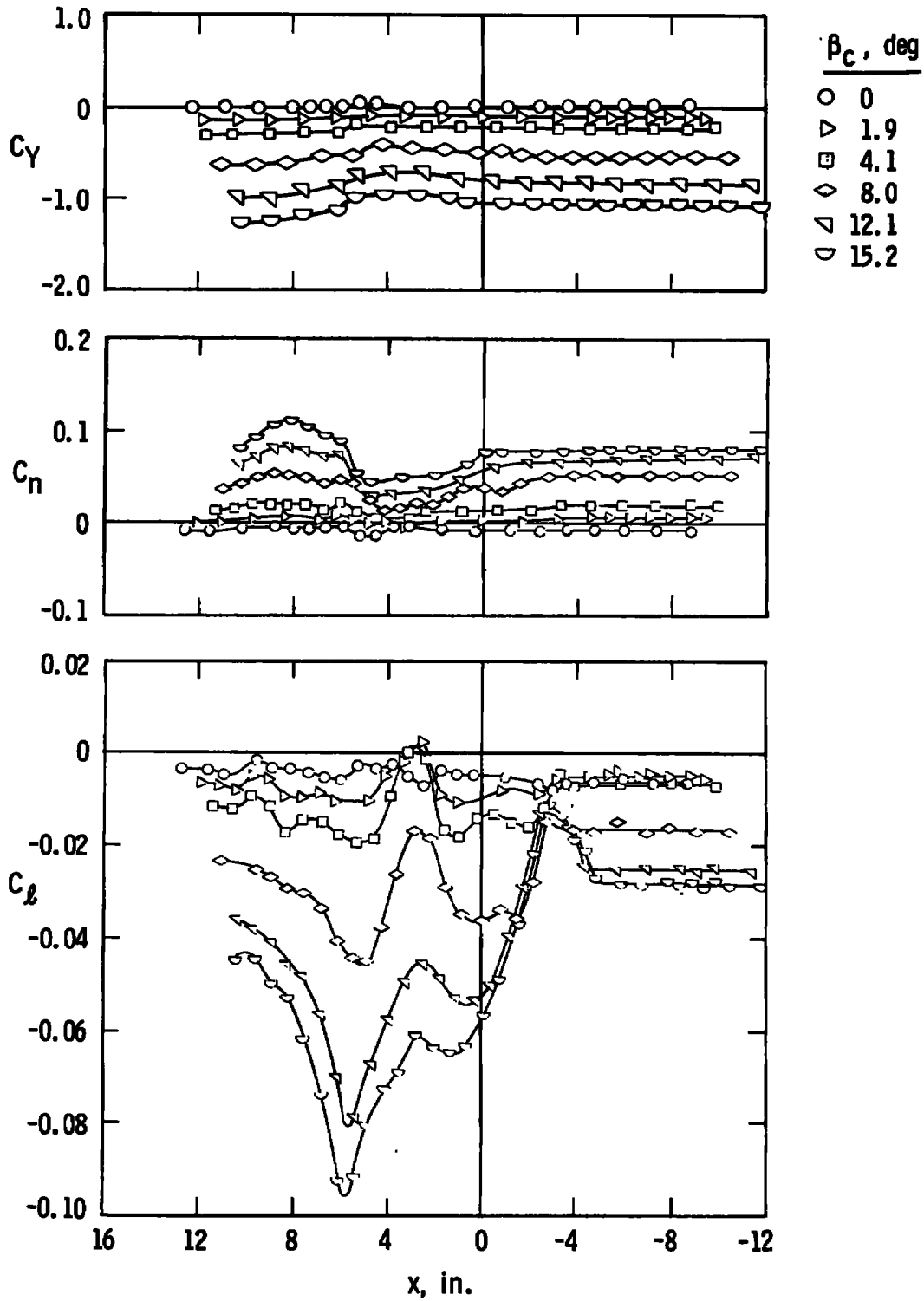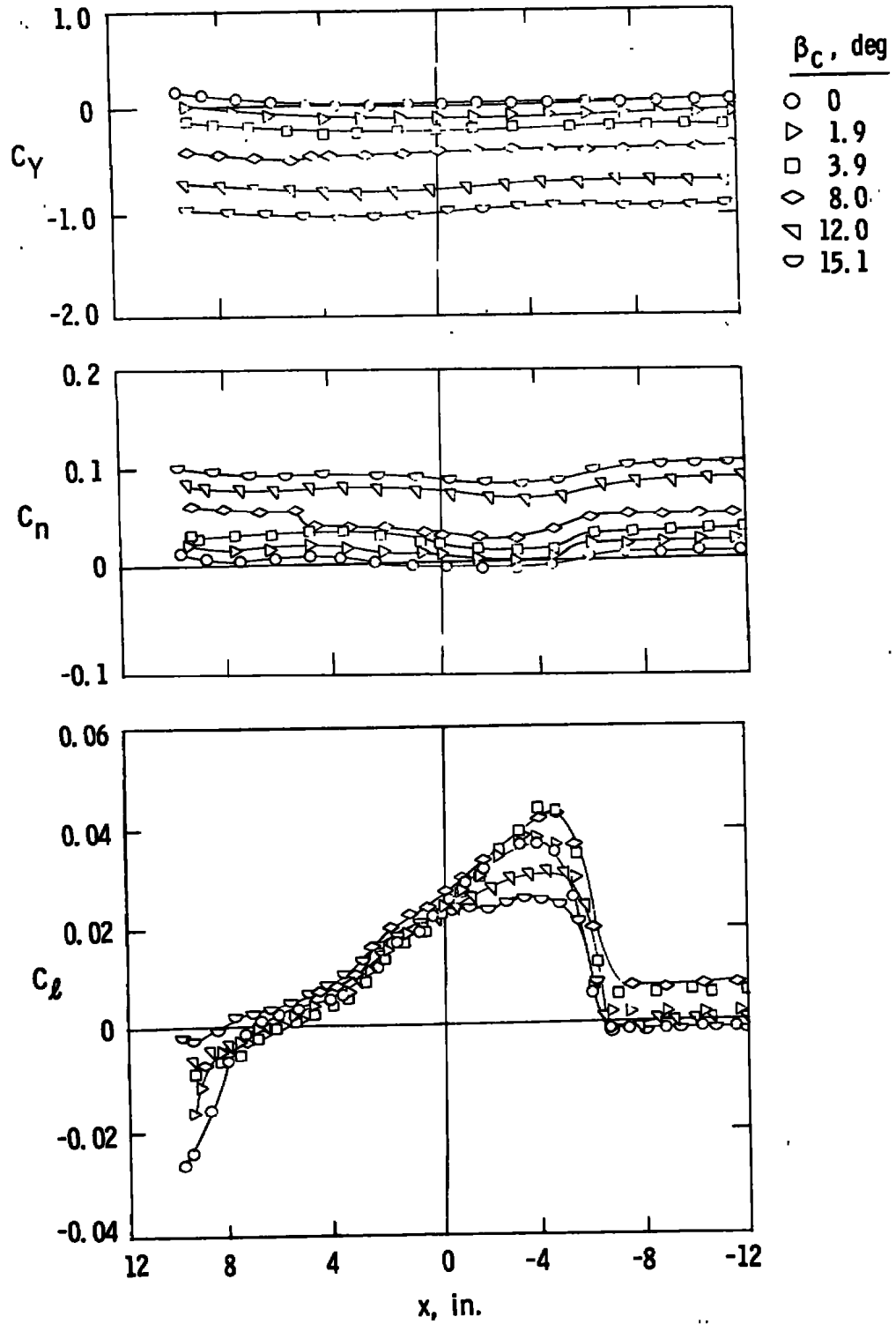Fig. 8 Continued
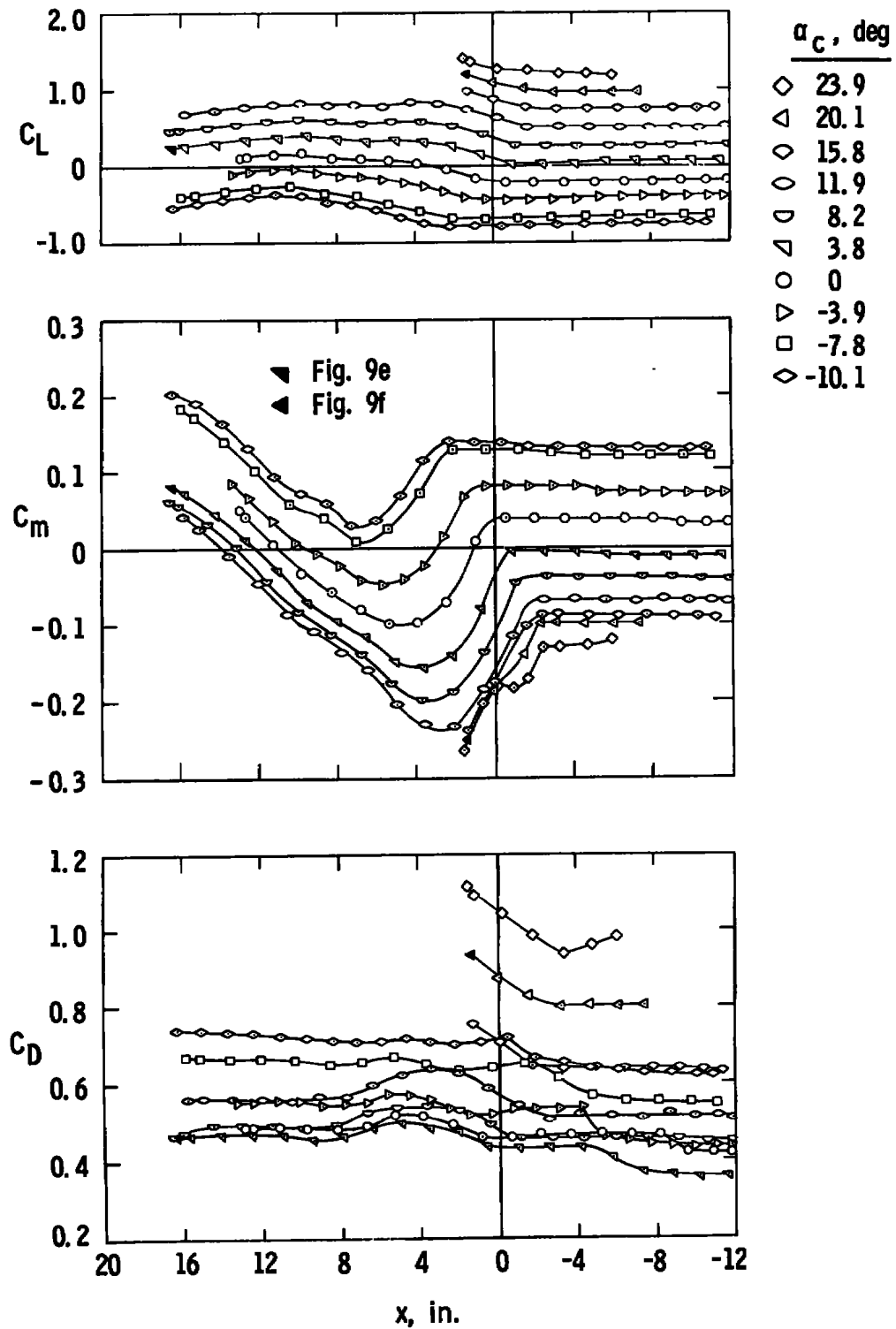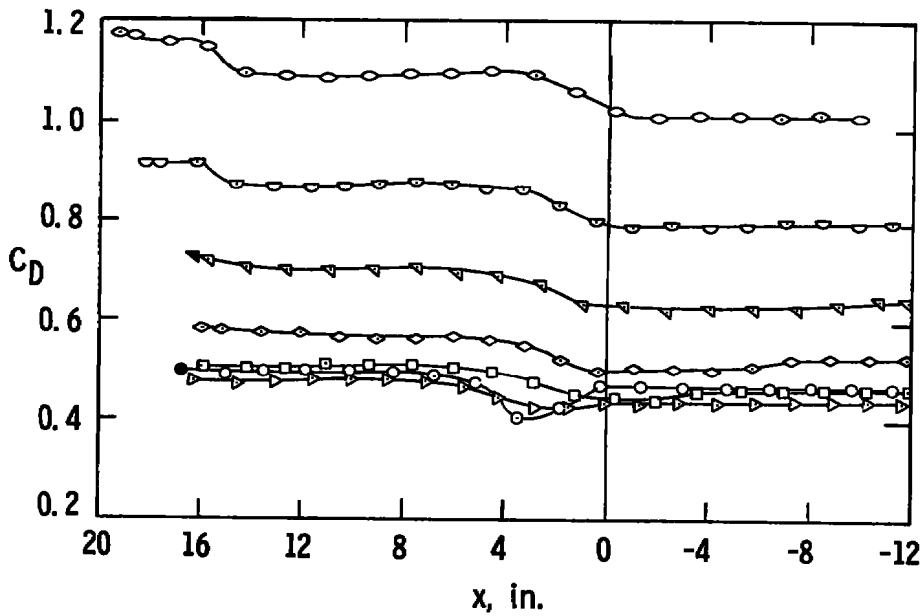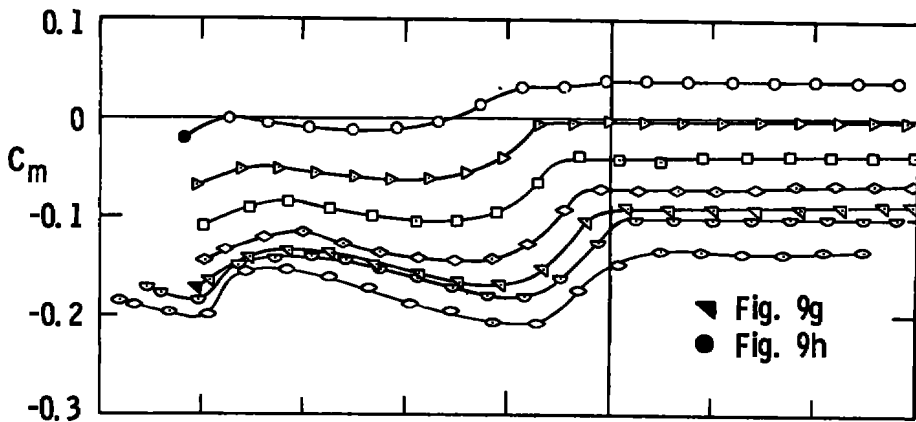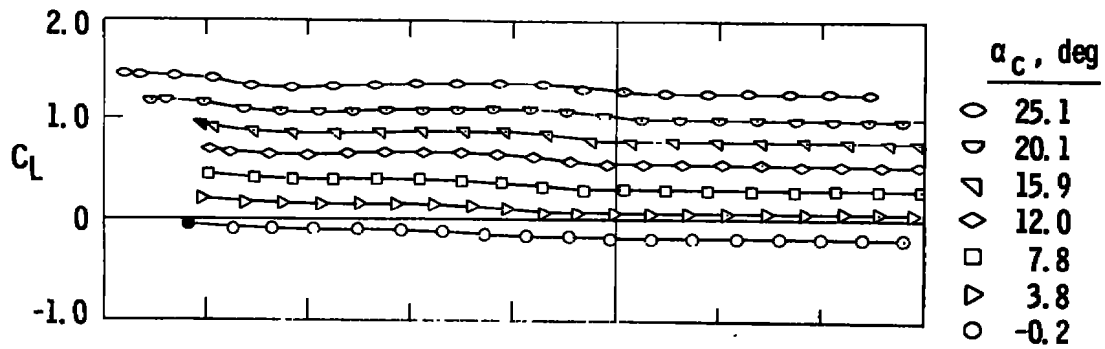
d. z = 14 in., y = 0
Fig. 8 Continued
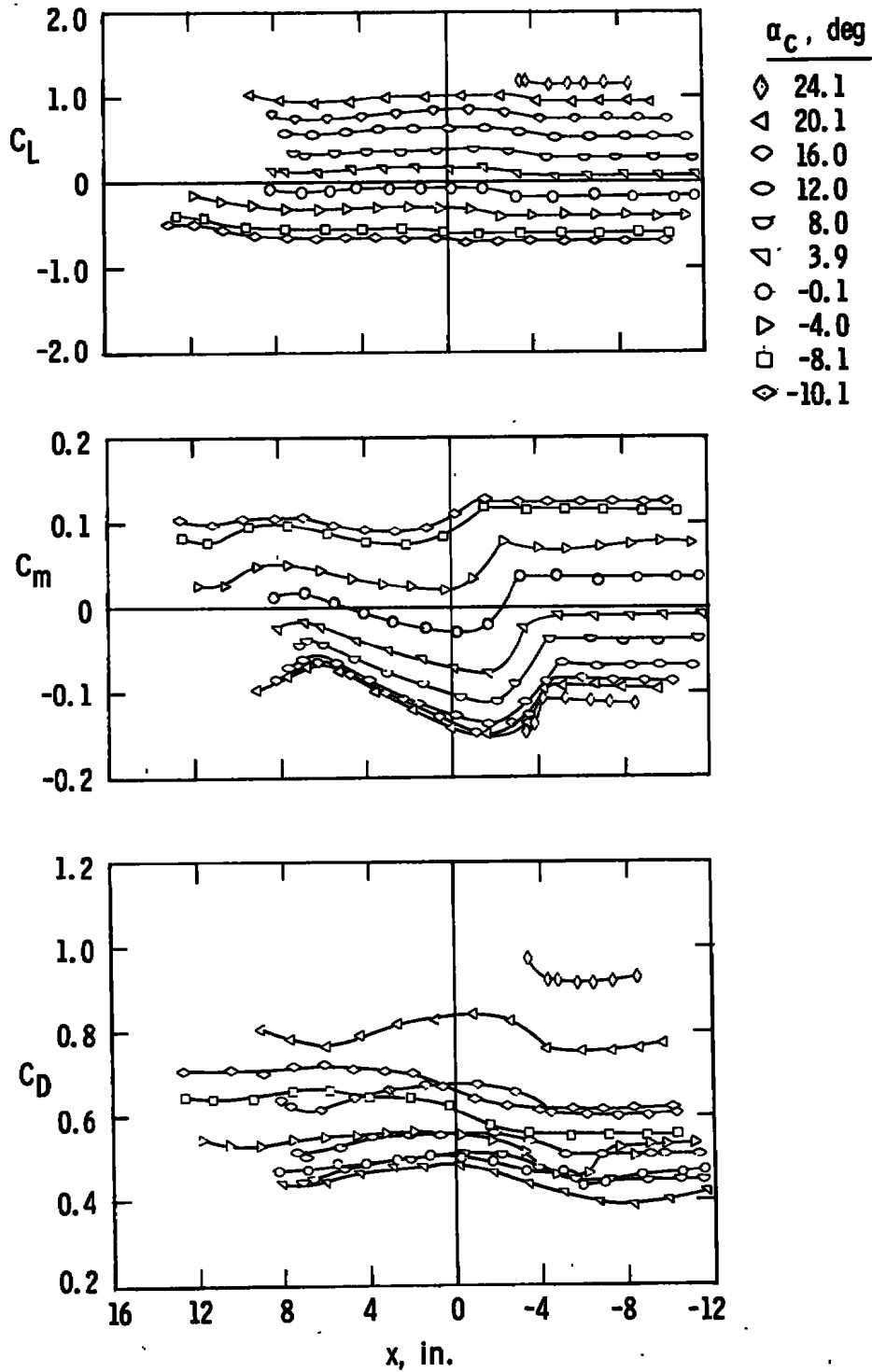
e. z = 10 in., y = 5 in.
Fig. 8 Concluded

31
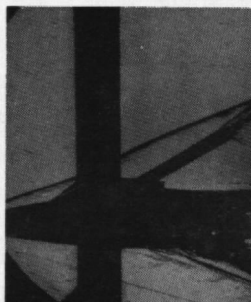
a. $a_c = -0.1$ deg, $y = 0$
   $z = 0$, $x = 0$

b. $a_c = -0.1$ deg, $y = 0$
   $z = 0$, $x = -6.5$ in.
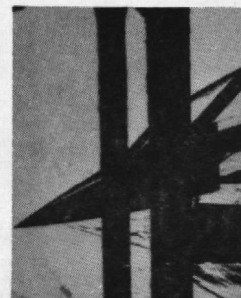
c. $a_c = -15.1$ deg, $y = 0$
   $z = 5$ in., $x = 2.8$ in.

d. $a_c = -7.9$ deg, $y = 0$
   $z = 5$ in., $x = 1.7$ in.
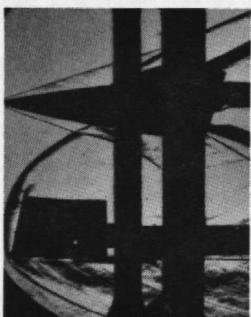
e. $a_c = 3.8$ deg, $y = 0$
   $z = 10$ in., $x = 16.5$ in.
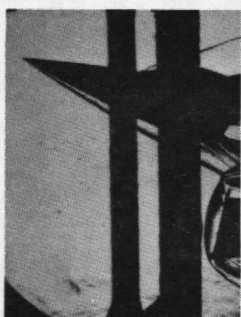
f. $a_c = 20.1$ deg, $y = 0$
   $z = 10$ in., $x = 1.2$ in.

g. $a_c = 15.9$ deg, $y = 0$
   $z = 14$ in., $x = 16.2$ in.

h. $a_c = -0.2$ deg, $y = 0$
   $z = 14$ in., $x = 16.5$ in.

Fig. 9 Schlieren Photographs, Jet Off, $M_\infty = 4$
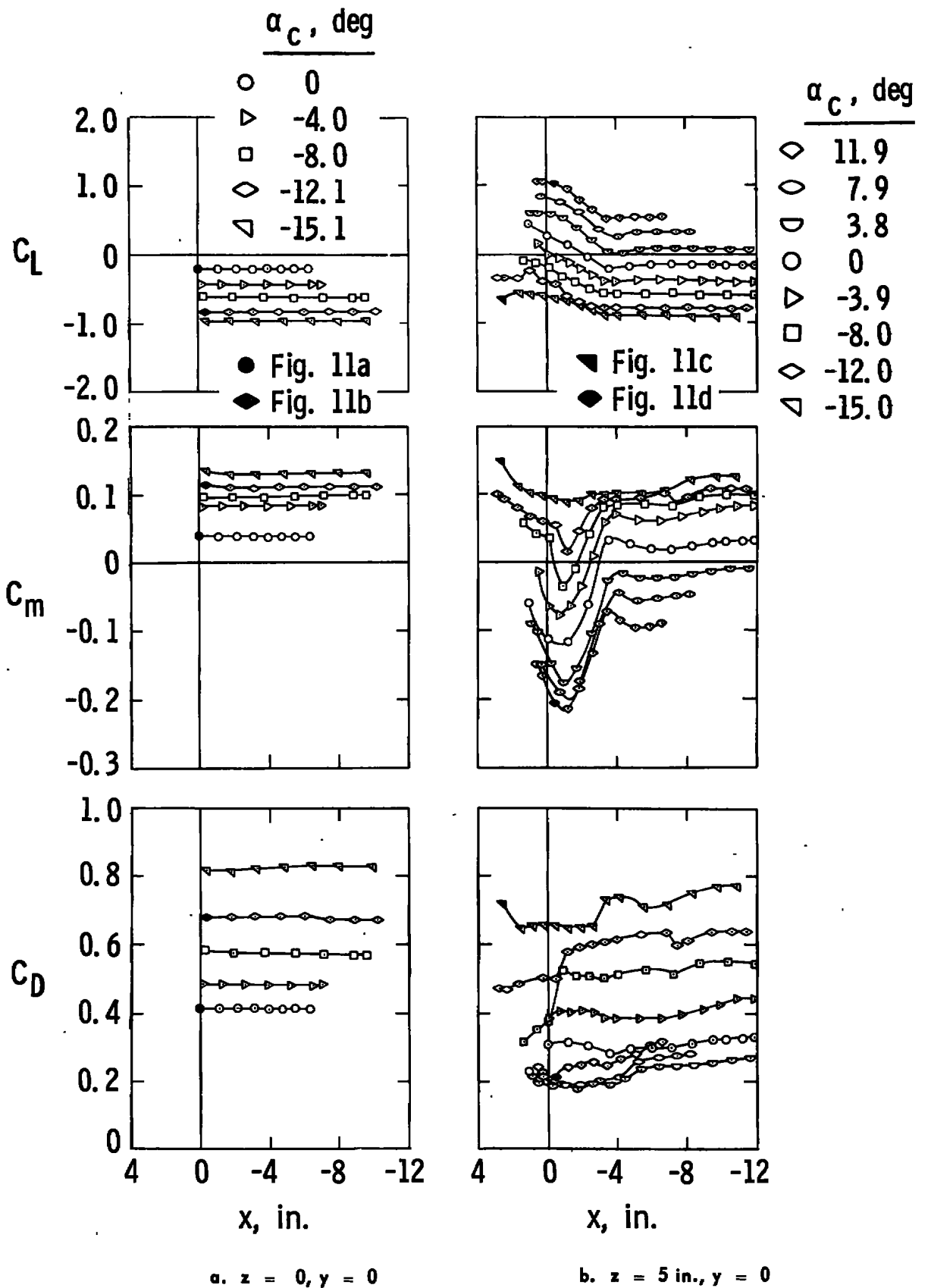
Fig. 10 Lift, Drag, and Pitching-Moment Characteristics of the Capsule, Jet Off, $M_\infty = 5$
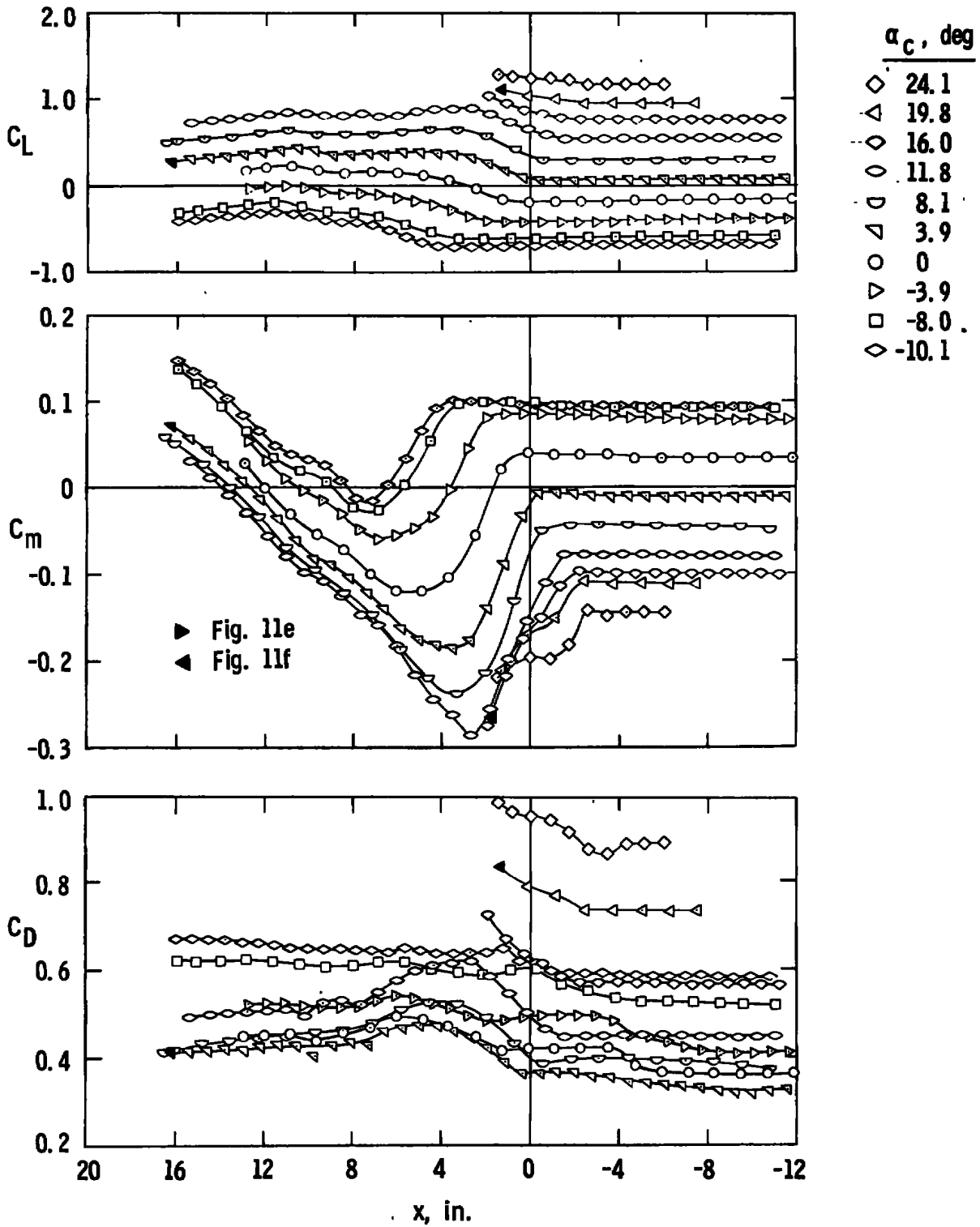
c. z = 10 in., y = 0
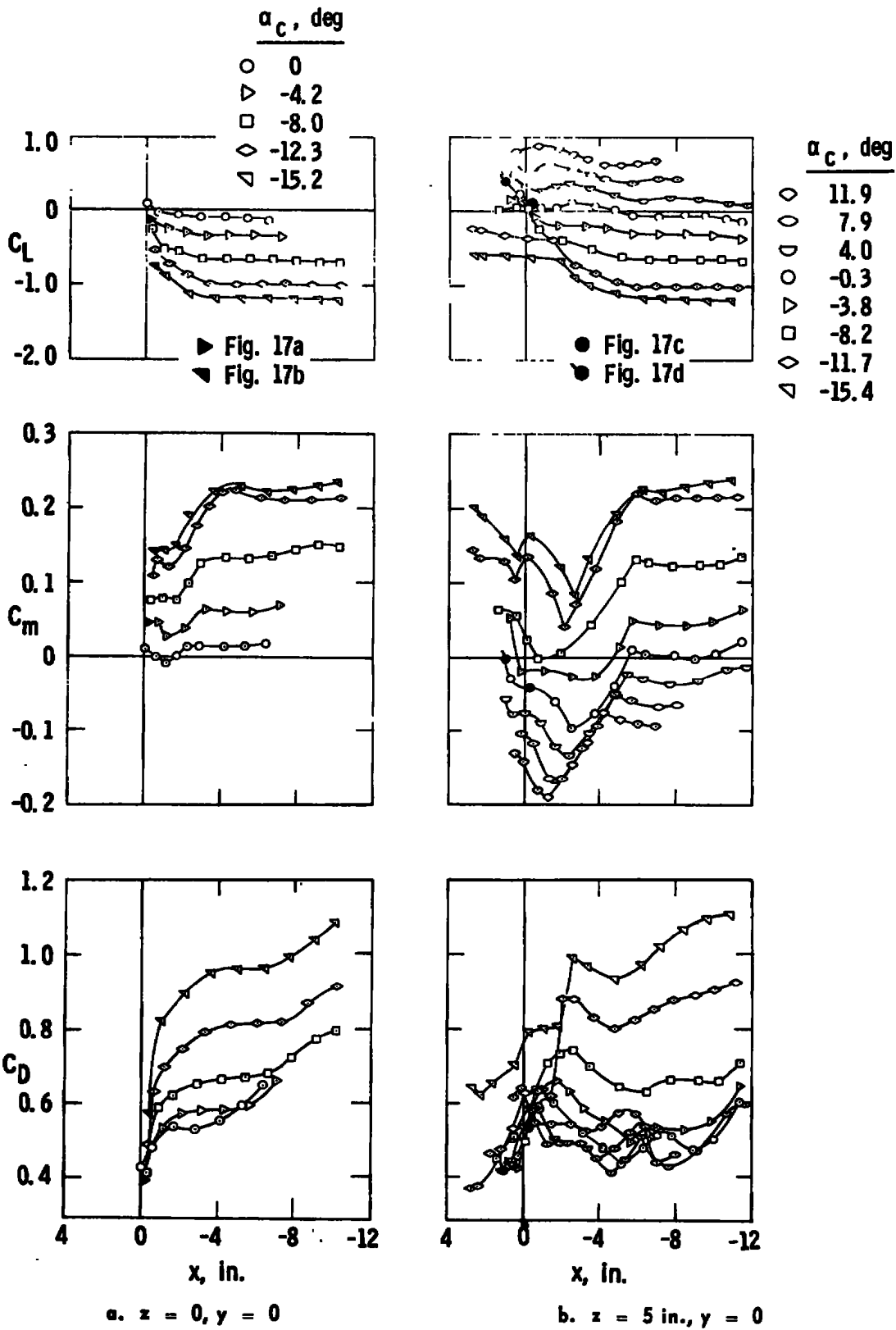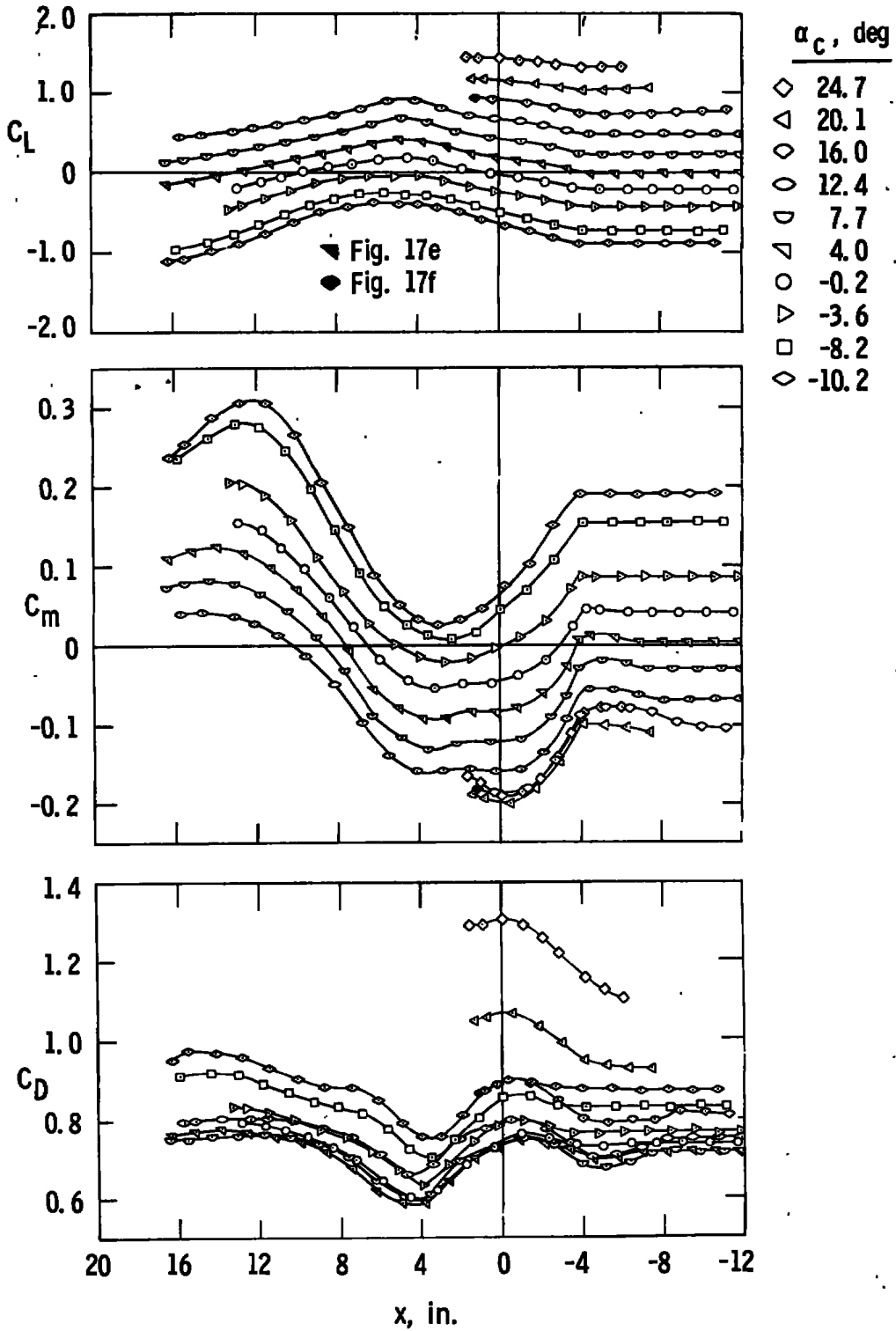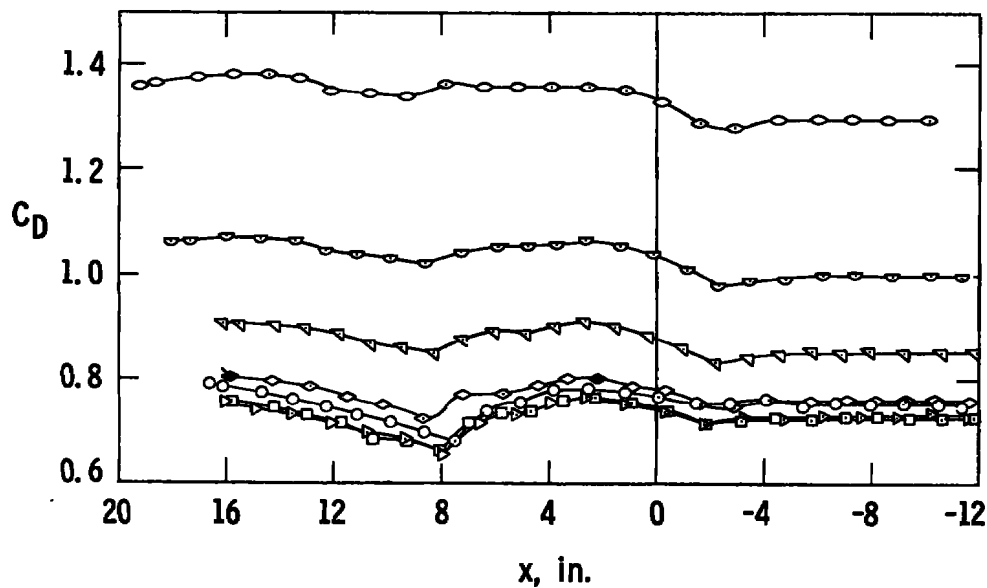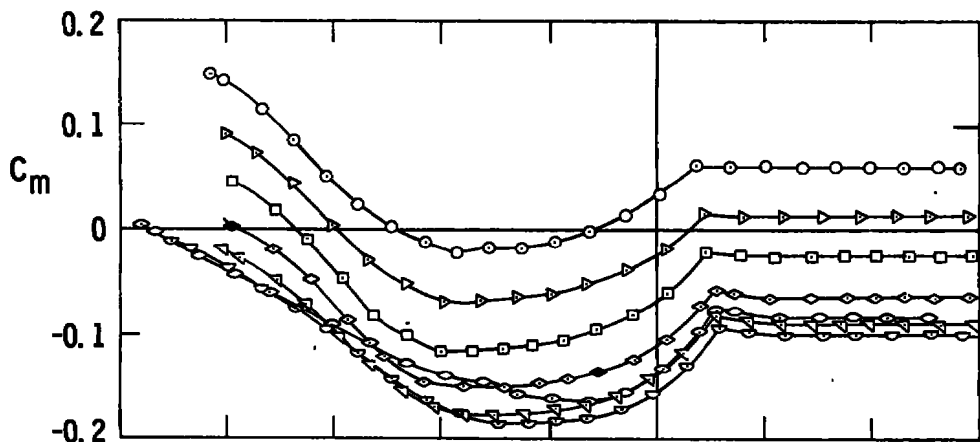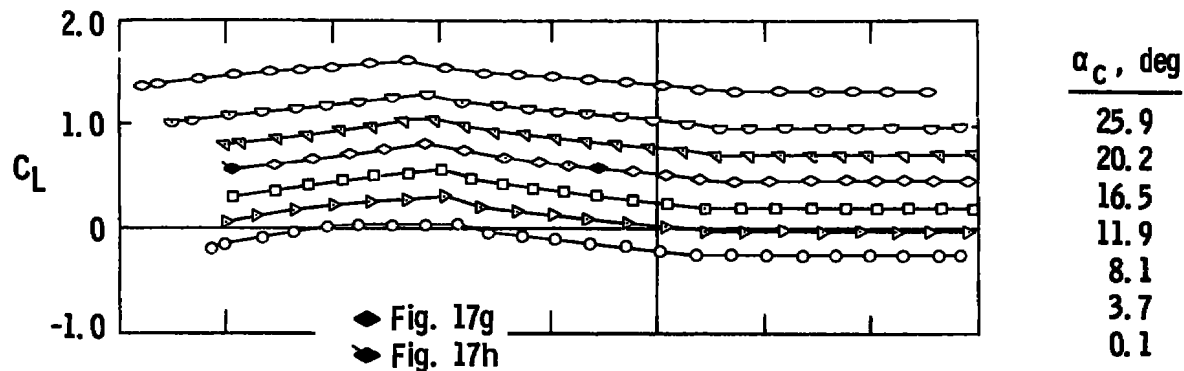Fig. 10 Continued
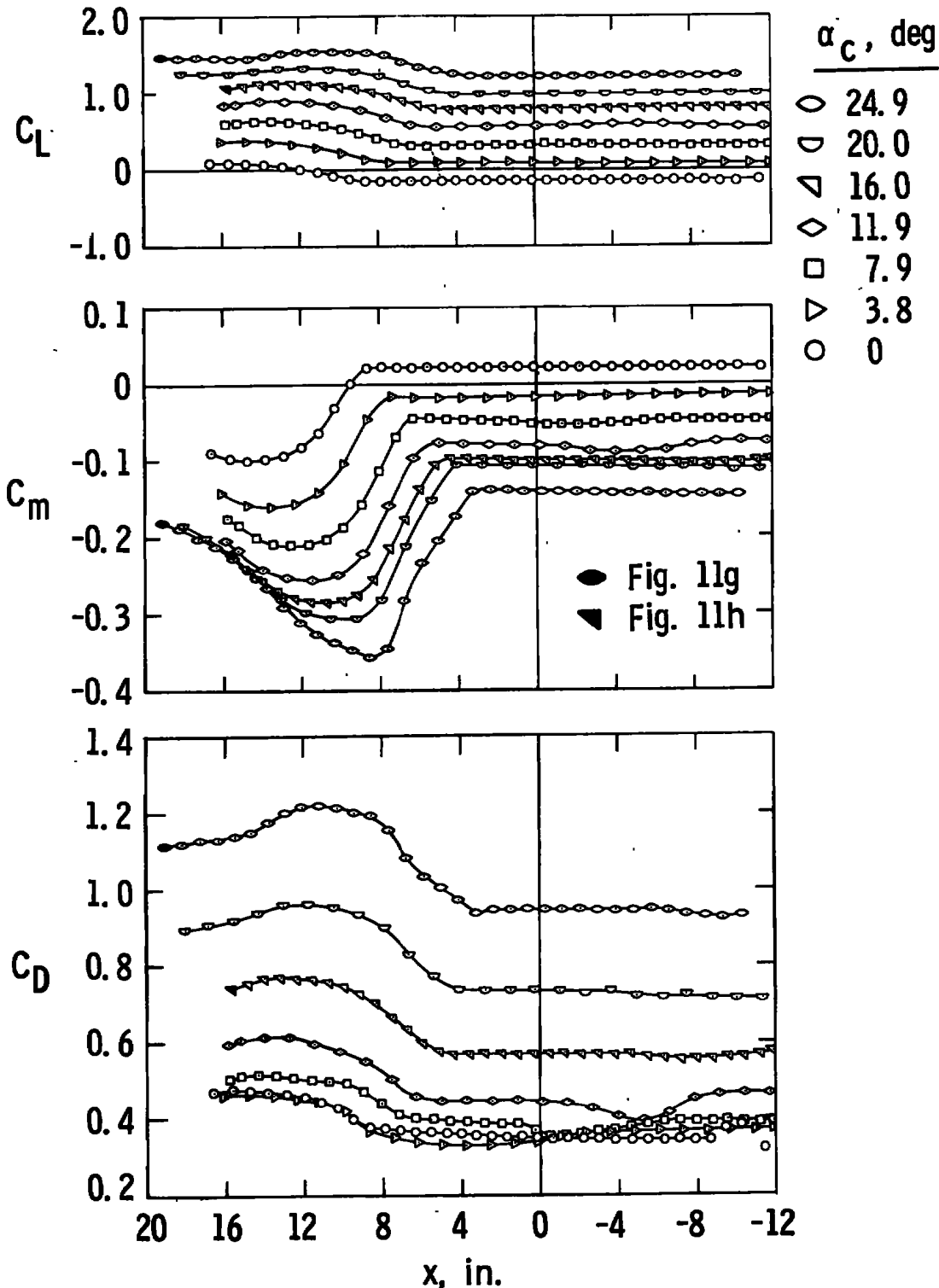
d. z = 14 in., y = 0
Fig. 10 Continued
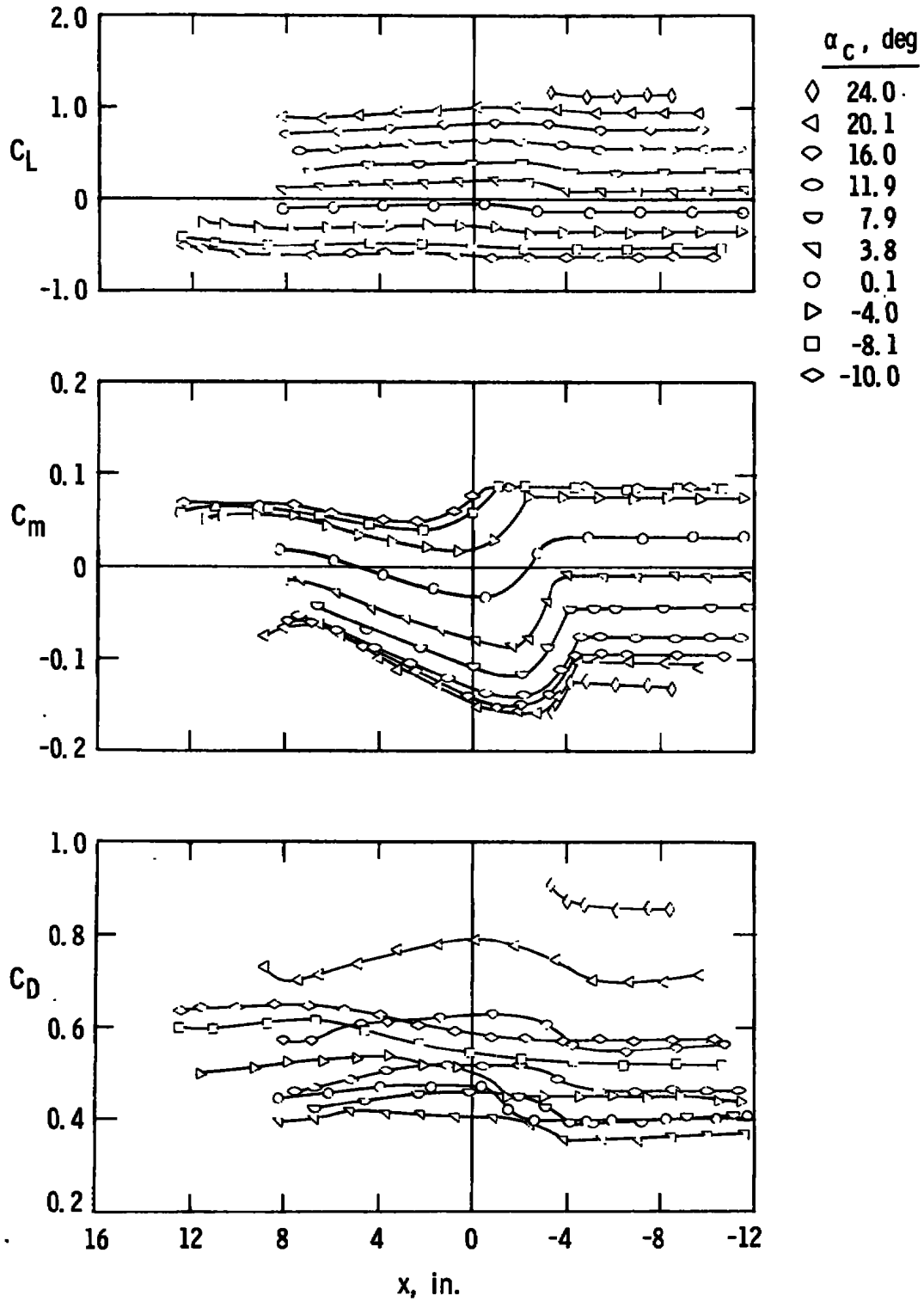
e. z = 10 in., y = 6 in.
Fig. 10 Concluded

a. $\alpha_c = 0$, $y = 0$
 $z = 0$, $x = 0$

b. $\alpha_c = -12.1$ deg, $y = 0$
   $z = 0$, $x = -0.5$ in.
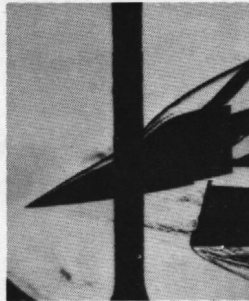
c. $\alpha_c = -15.0$ deg, $y = 0$
   $z = 5$ in., $x = 2.7$ in.
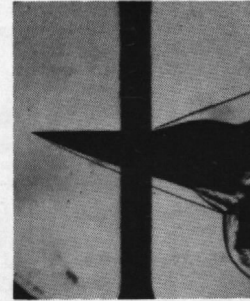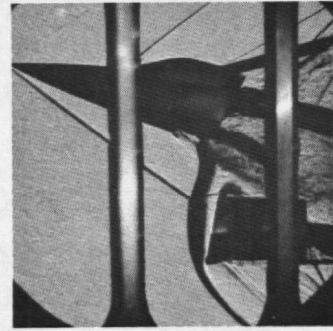
d. $\alpha_c = 11.9$ deg, $y = 0$
   $z = 5$ in., $x = 0.6$ in.
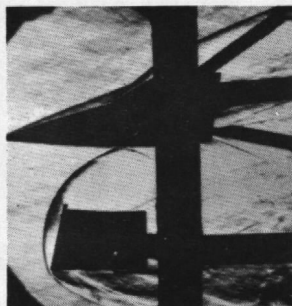
e. $\alpha_c = -3.9$ deg, $y = 0$
   $z = 10$ in., $x = 13.0$ in.
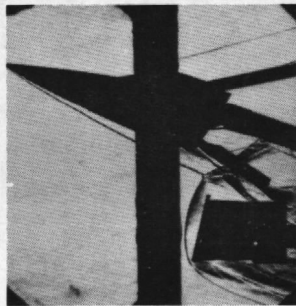
f. $\alpha_c = 19.8$ deg, $y = 0$
   $z = 10$ in., $x = 1.2$ in.
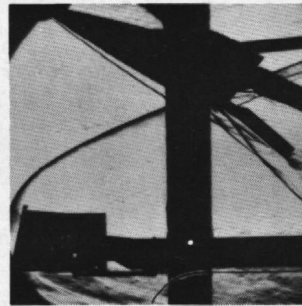
g. $\alpha_c = 24.9$ deg, $y = 0$
   $z = 14$ in., $x = 19.0$ in.
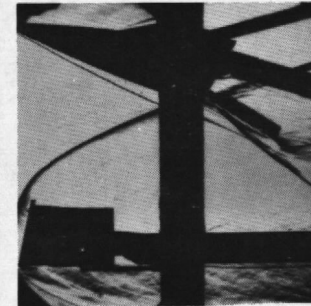
h. $\alpha_c = 16.0$ deg, $y = 0$
   $z = 14$ in., $x = 15.8$ in.

Fig. 11 Schlieren Photographs, Jet Off, $M_\infty = 5$

a. z = 3 in., y = 0

b. z = 4 in., y = 0
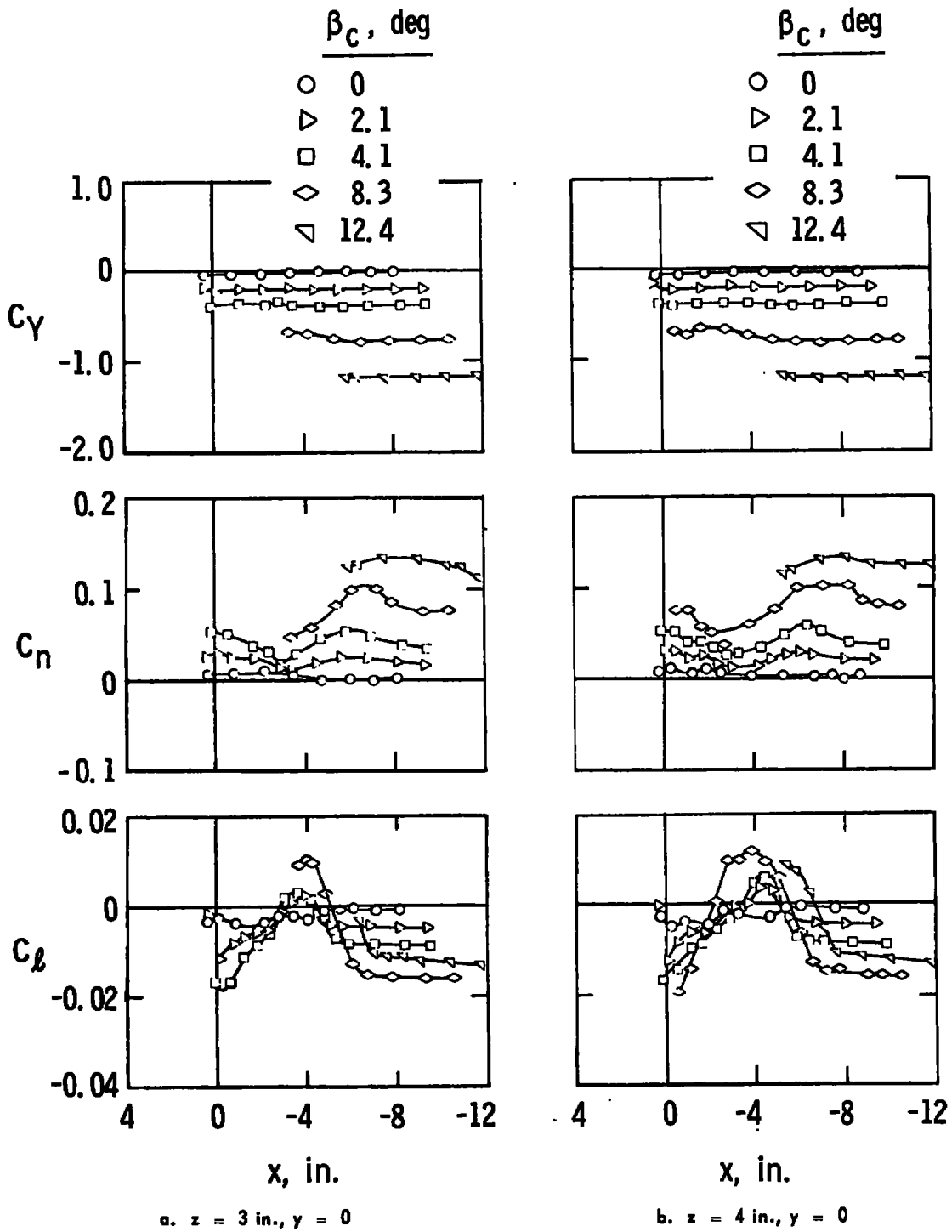
Fig. 12 Side-Force, Yawing-Moment, and Rolling-Moment Characteristics of the Capsule, Jet Off, $M_\infty = 2$
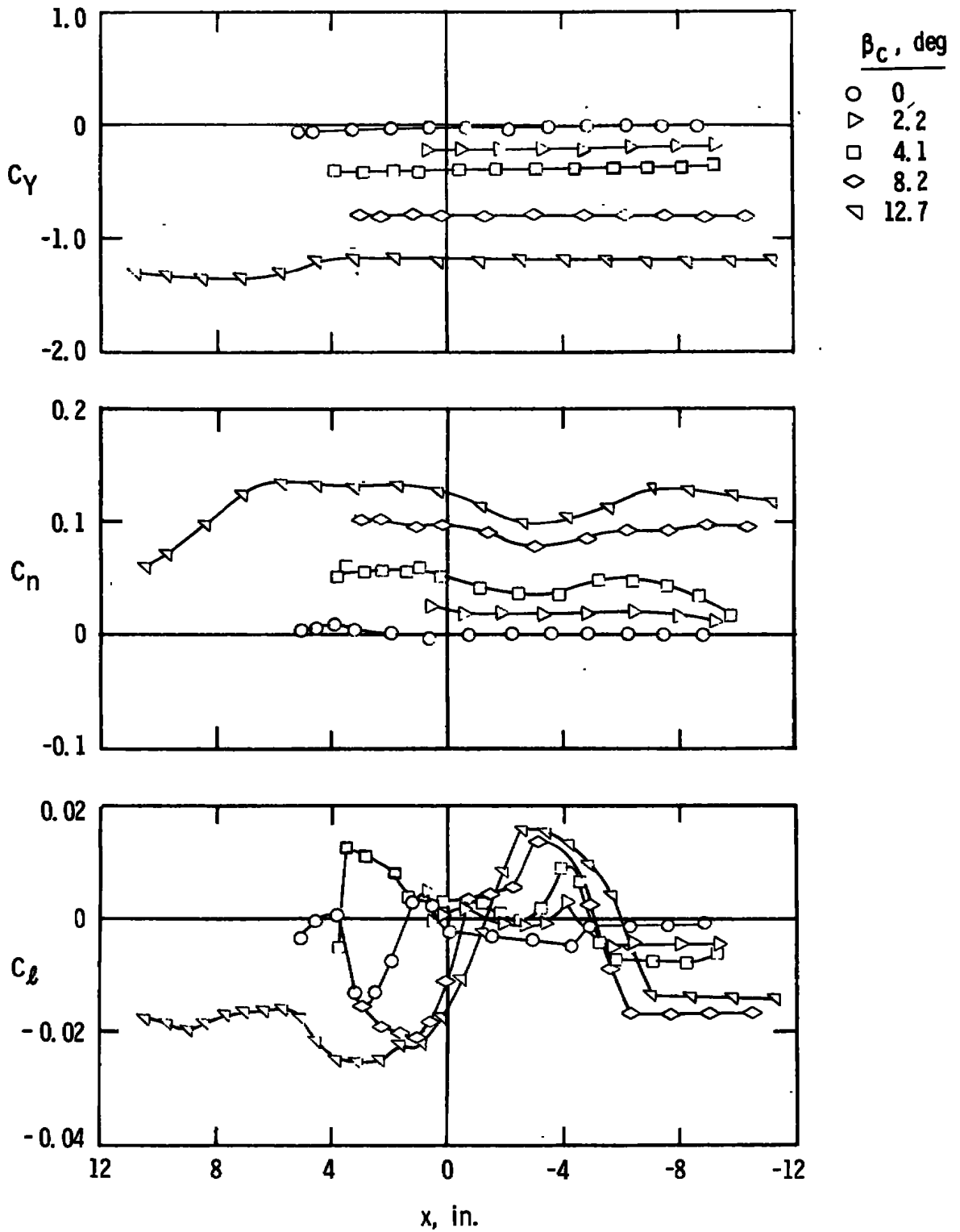
c. z = 8 in., y = 0
Fig. 12 Continued
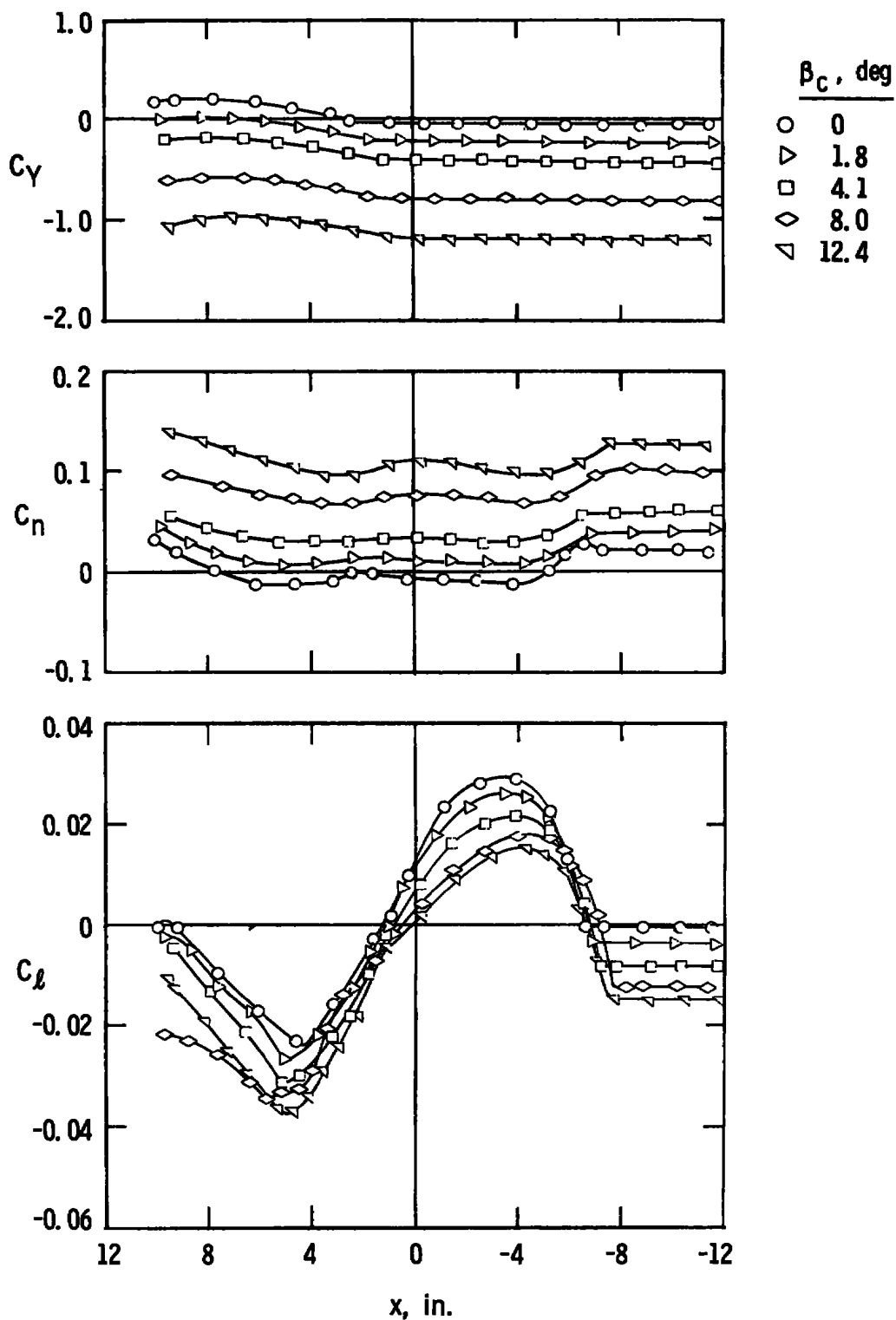
d. z = 8 in., y = –5 in.
Fig. 12 Concluded
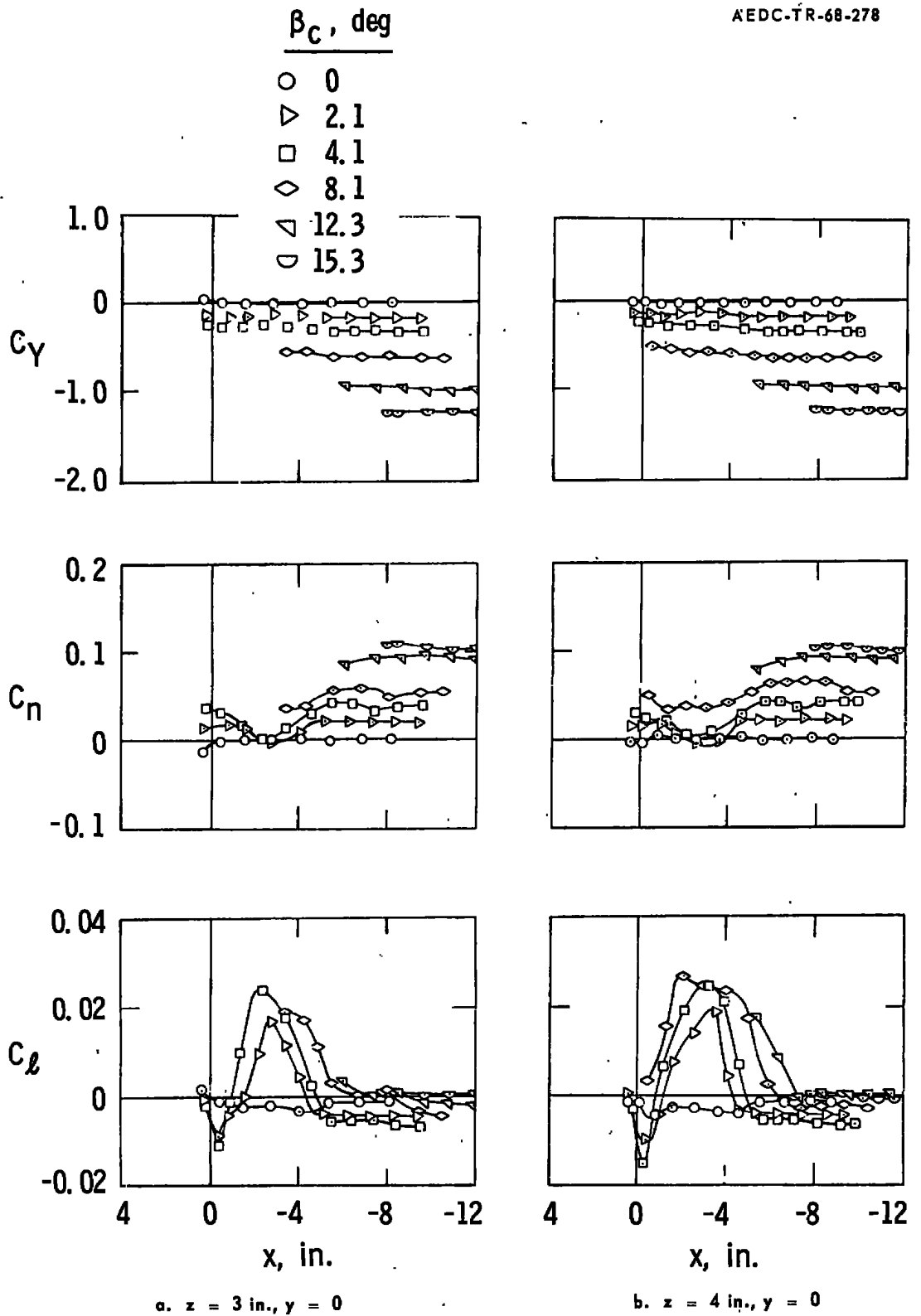
Fig. 13 Side-Force, Yawing-Moment, and Rolling-Moment Characteristics of the Capsule, Jet Off, $M_\infty = 3$
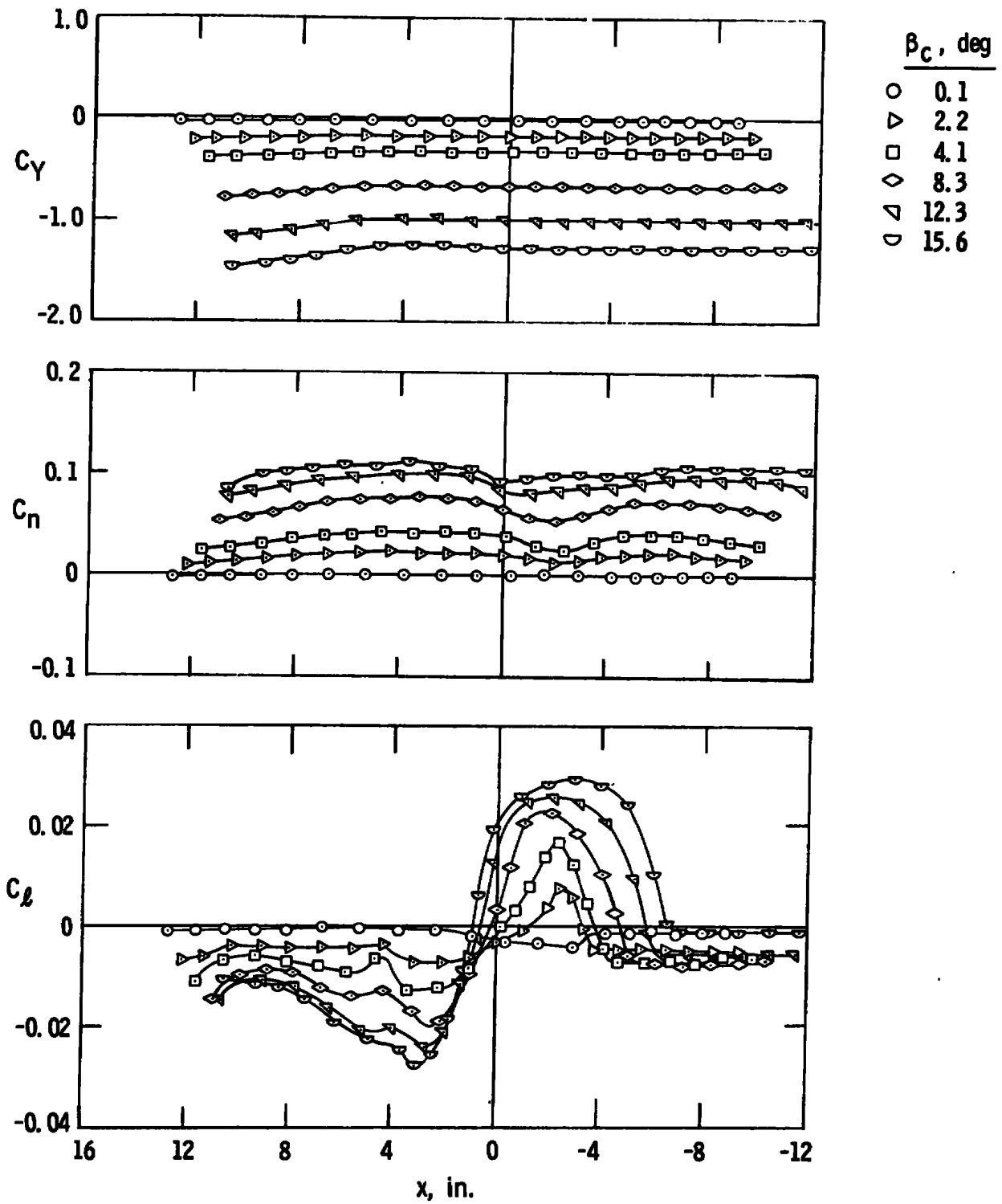
c. z = 8 in., y = 0
Fig. 13 Continued
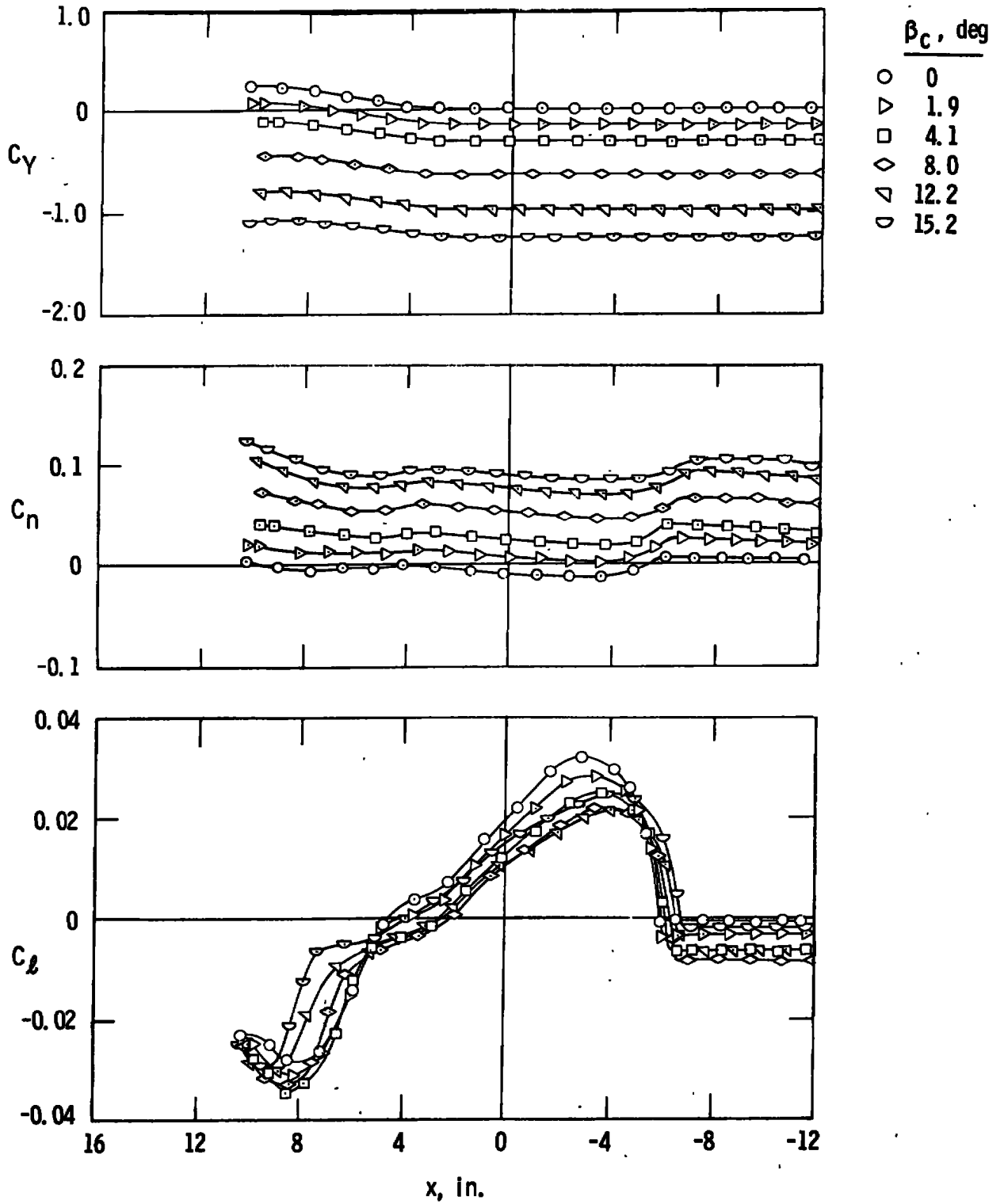
d. $z = 8$ in., $y = -5$ in.

Fig. 13 Concluded

Fig. 14 Side-Force, Yawing-Moment, and Rolling-Moment Characteristics of the Capsule,
Jet Off, $M_\infty = 4$

c. z = 8 in., y = 0
Fig. 14 Continued

d. z = 8 in., y = −5 in.
Fig. 14 Concluded

a. z = 3 in., y = 0   b. z = 4 in., y = 0

Fig. 15 Side-Force, Yawing-Moment, and Rolling-Moment Characteristics of the Capsule,
Jet Off, M_∞ = 5

c. z = 8 in., y = 0
Fig. 15 Continued

d. z = 8 in., y = −5 in.
Fig. 15 Concluded

Fig. 16 Lift, Drag, and Pitching-Moment Characteristics of the Capsule, Jet On,
$M_\infty = 2$, $p_c/p_\infty = 131$

c. z = 10 in., y = 0
Fig. 16 Continued

d. $z = 14$ in., $y = 0$
Fig. 16 Continued
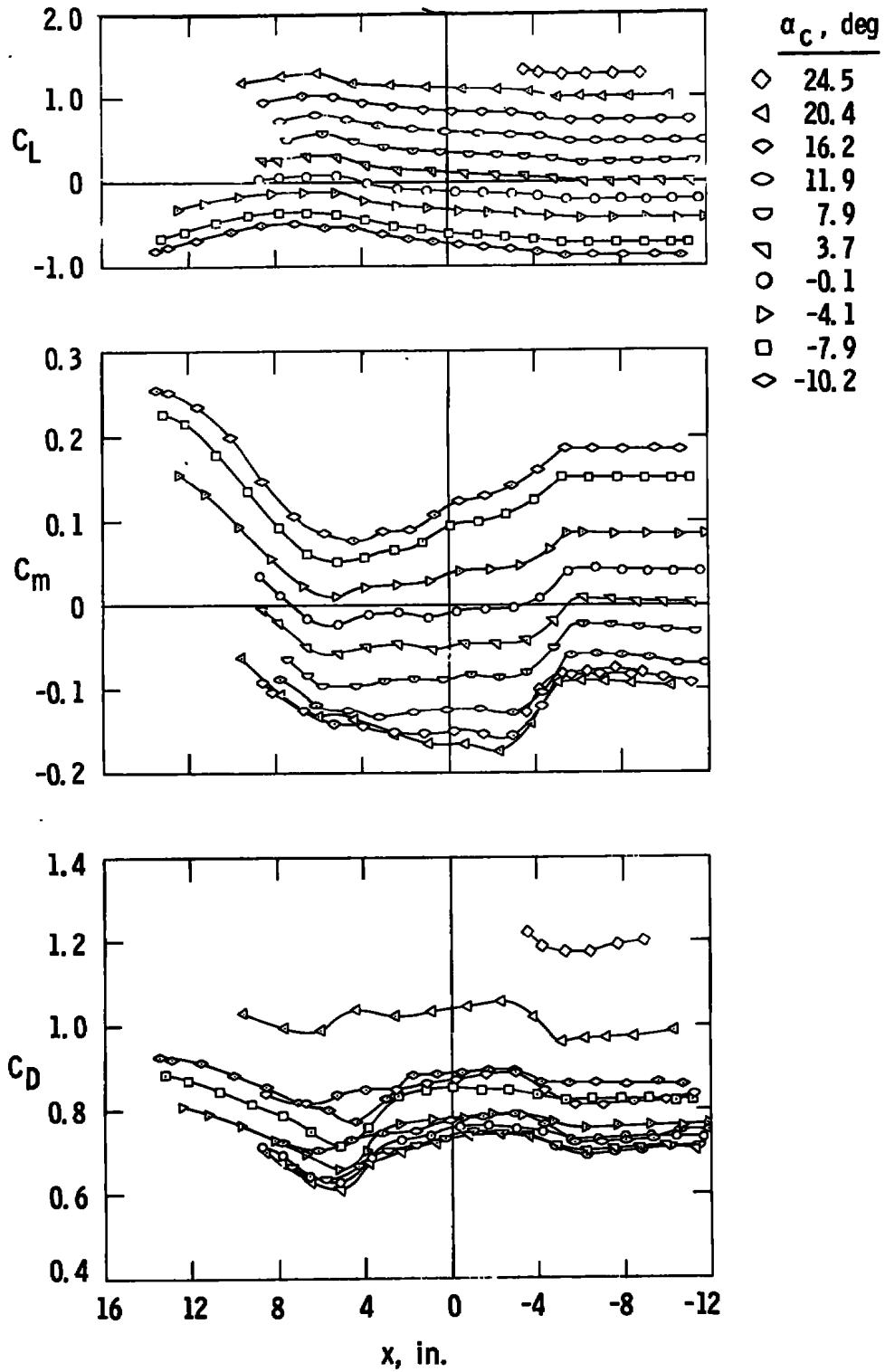
e. z = 10 in., y = 5 in.
Fig. 16 Concluded

53
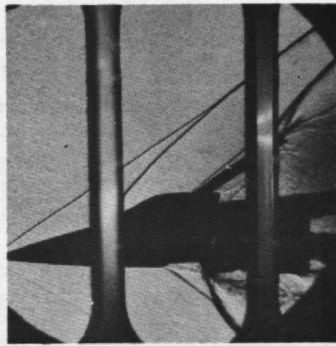
a. α_c = −4.2 deg, y = 0
z = 0, x = −0.3 in.

b. α_c = −15.2 deg, y = 0
z = 0, x = −0.5 in.
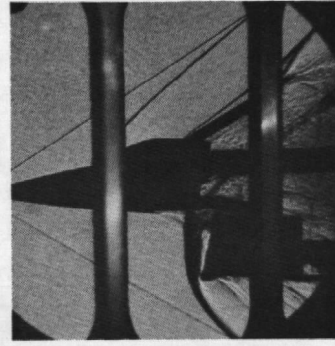
c. α_c = −0.3 deg, y = 0
z = 5 in., x = −0.3 in
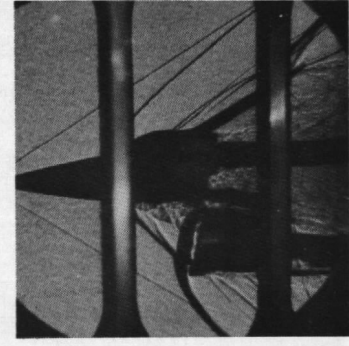
d. α_c = −0.3 deg, y = 0
z = 5 in., x = 1.0 in.
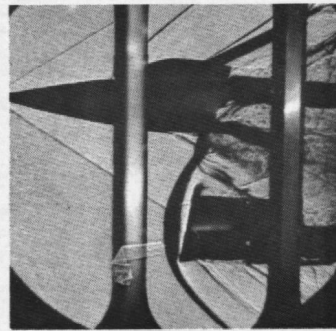
e. α_c = 4.0 deg, y = 0
z = 10 in., x = 2.5 in.

f. α_c = 16.0 deg, y = 0
z = 10 in., x = 1.5 in.
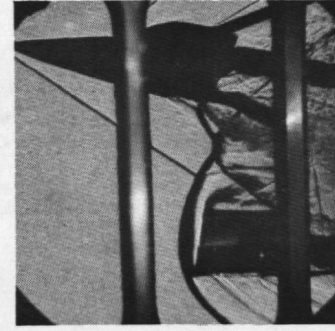
g. α_c = 11.9 deg, y = 0
z = 14 in., x = 2.5 in.

h. α_c = 11.9 deg, y = 0
z = 14 in., x = 15.8 in.

Fig. 17 Schlieren Photographs, Jet On, M_∞ = 2, p_c/p_∞ = 131
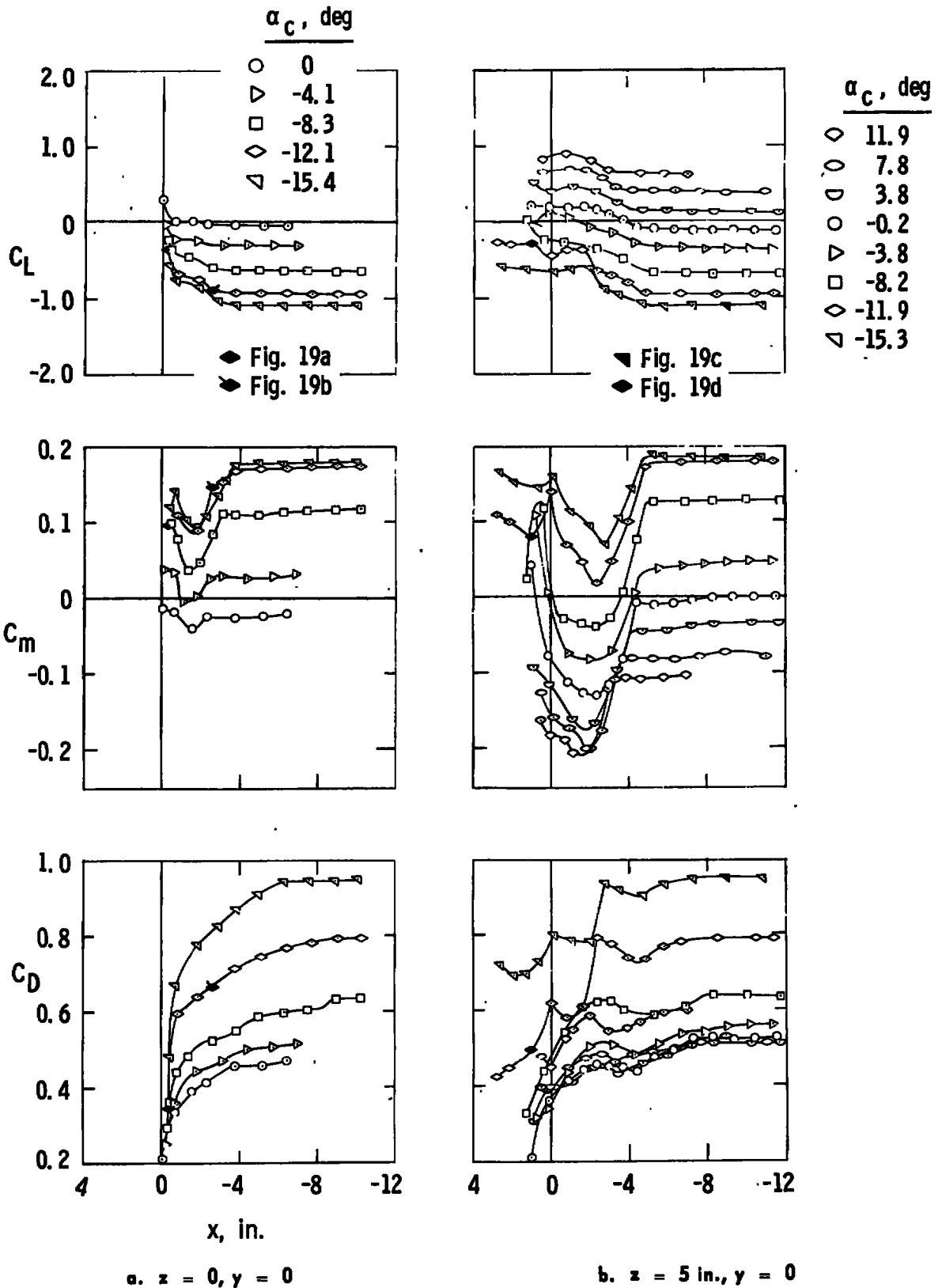
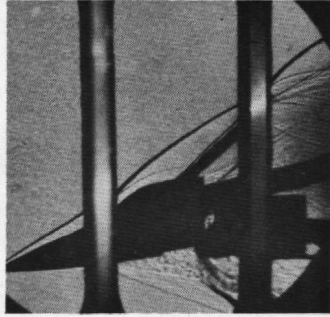Fig. 18 Lift, Drag, and Pitching-Moment Characteristics of the Capsule, Jet On, $M_\infty = 3$, $p_c/p_\infty = 451$
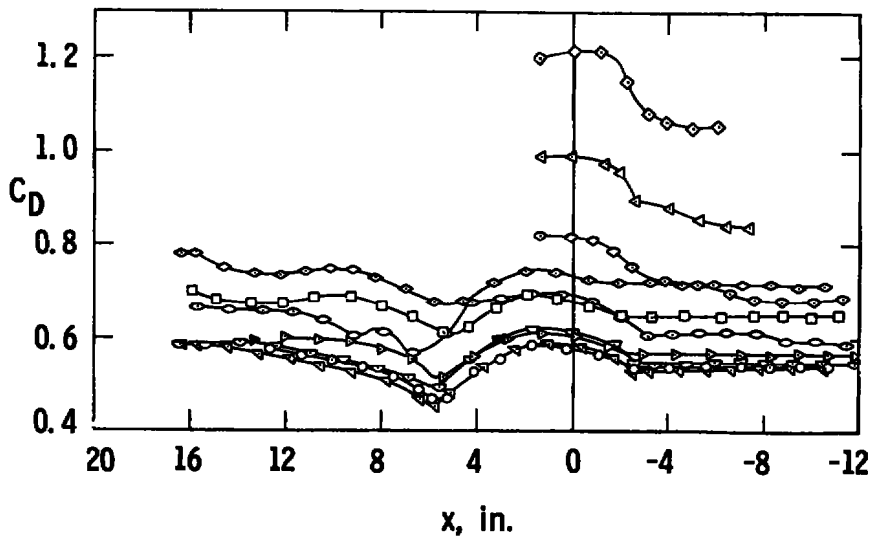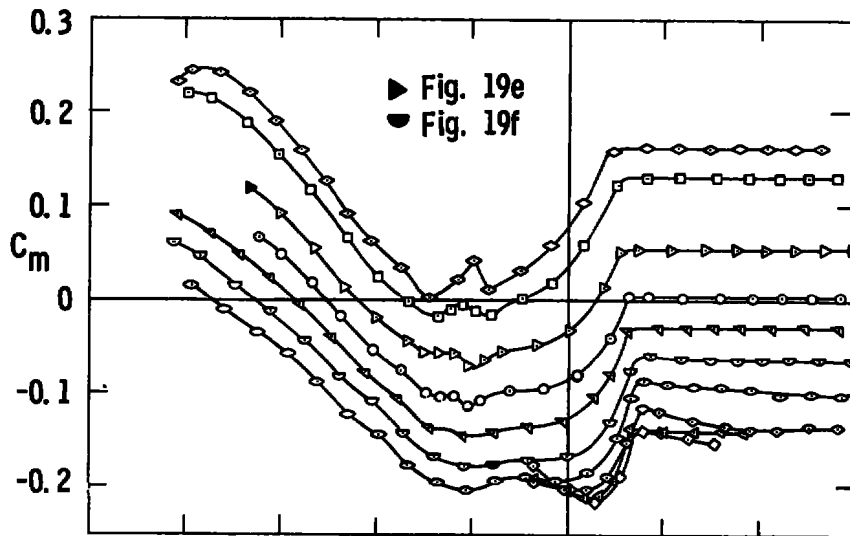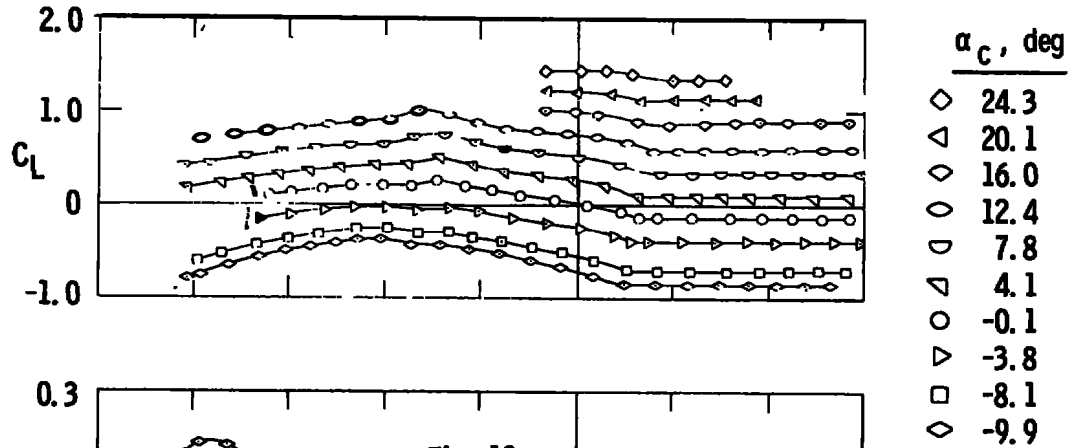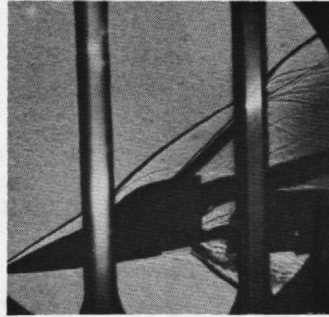
c. z = 10 in., y = 0
Fig. 18 Continued
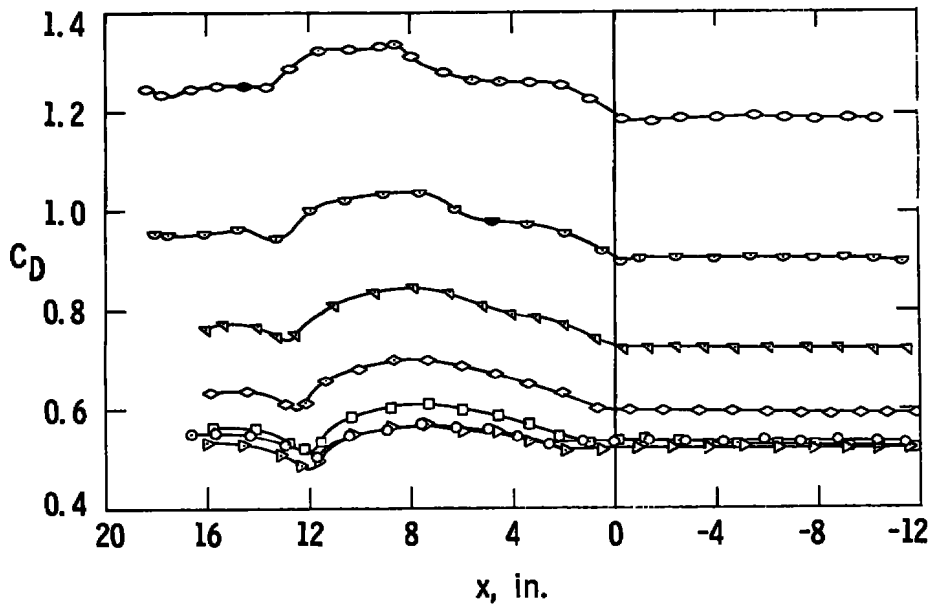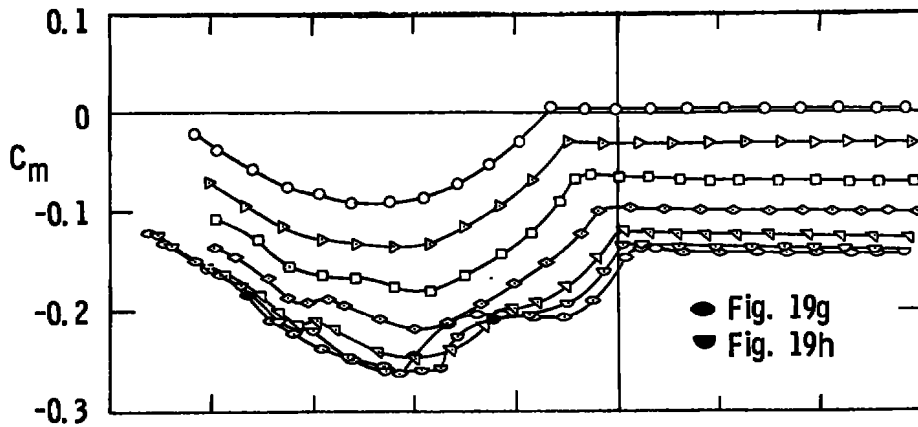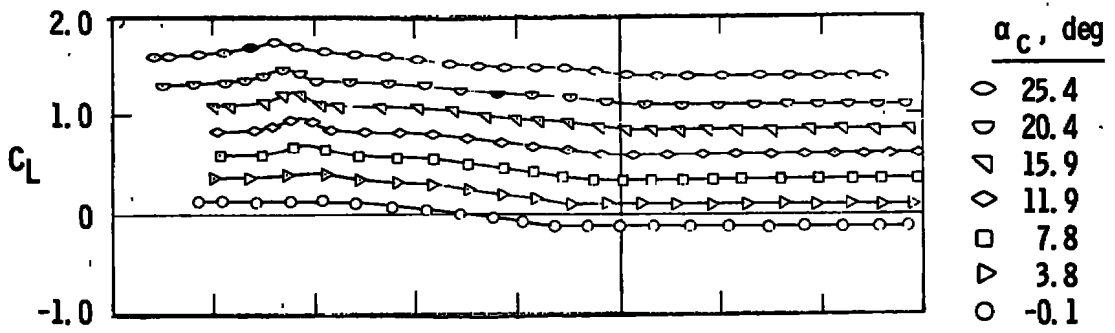
d. z = 14 in., y = 0
Fig. 18 Continued
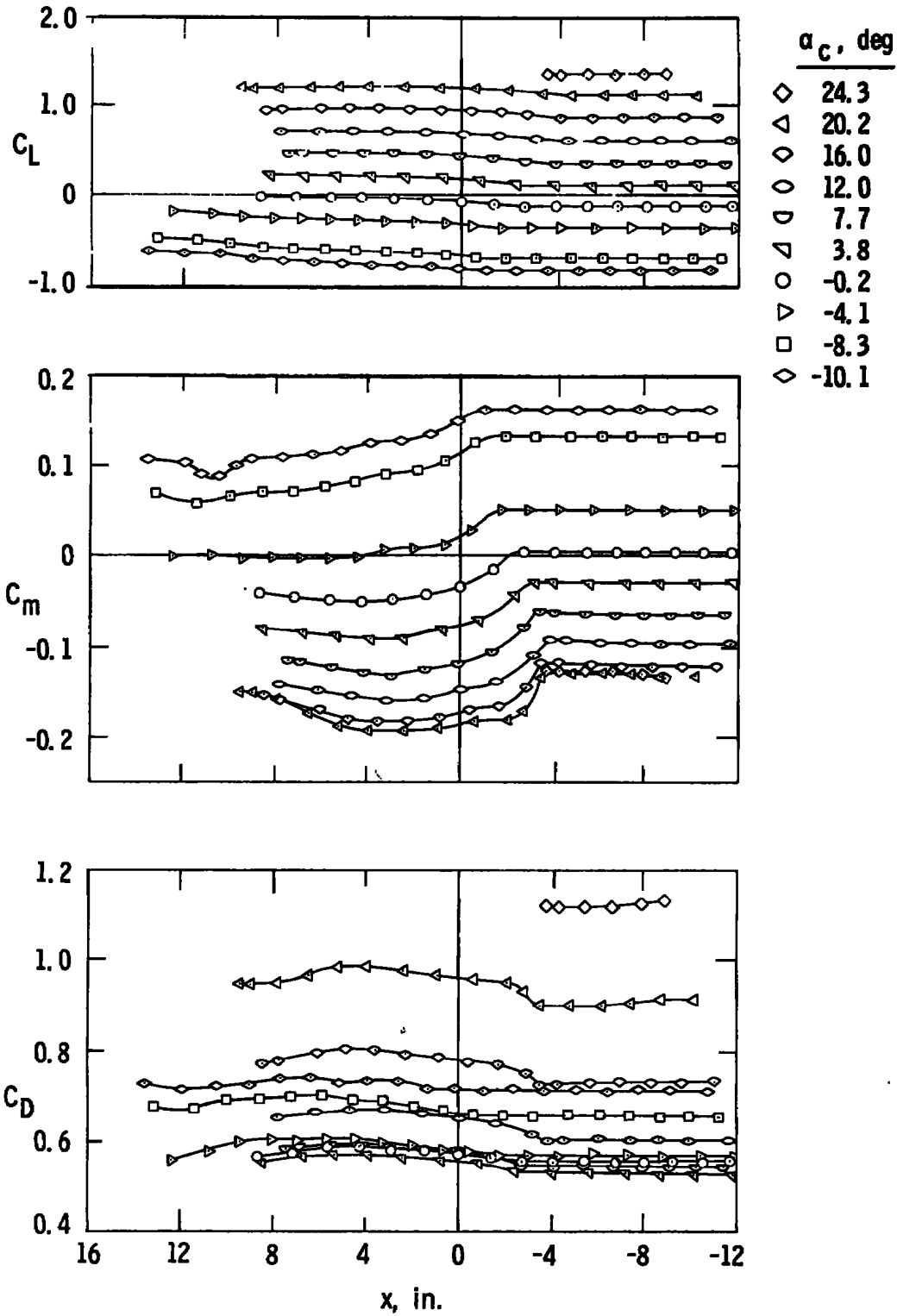
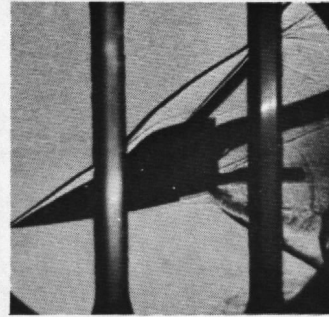e. z = 10 in., y = 5 in.
Fig. 18 Concluded

a. $\alpha_c = -12.1$ deg, $y = 0$
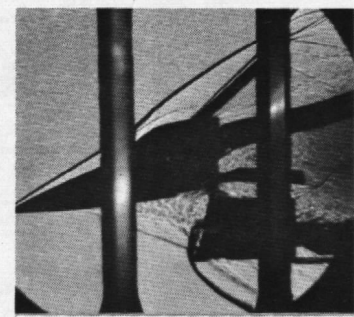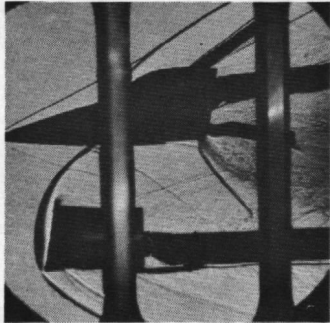$z = 0$, $x = -0.3$ in.

b. $\alpha_c = -12.1$ deg, $y = 0$
$z = 0$, $x = -2.5$ in.

c. $\alpha_c = -15.3$ deg, $y = 0$
$z = 5$ in., $x = -9.5$ in.

d. $\alpha_c = -11.9$ deg, $y = 0$
$z = 5$ in., $x = 1.5$ in.

e. $\alpha_c = -3.8$ deg, $y = 0$
$z = 10$ in., $x = 13.0$ in.
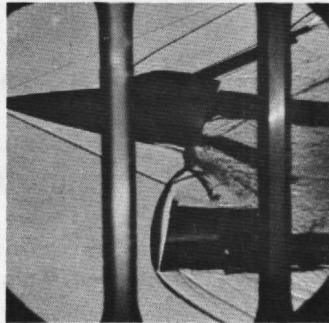
f. $\alpha_c = 7.8$ deg, $y = 0$
$z = 10$ in., $x = 3.5$ in.
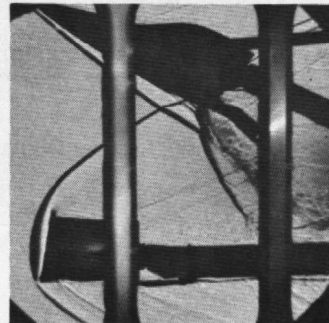
g. $\alpha_c = 25.4$ deg, $y = 0$
$z = 14$ in., $x = 15.0$ in.
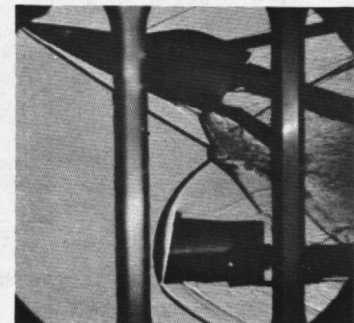
h. $\alpha_c = 20.4$ deg, $y = 0$
$z = 14$ in., $x = 5.0$ in.

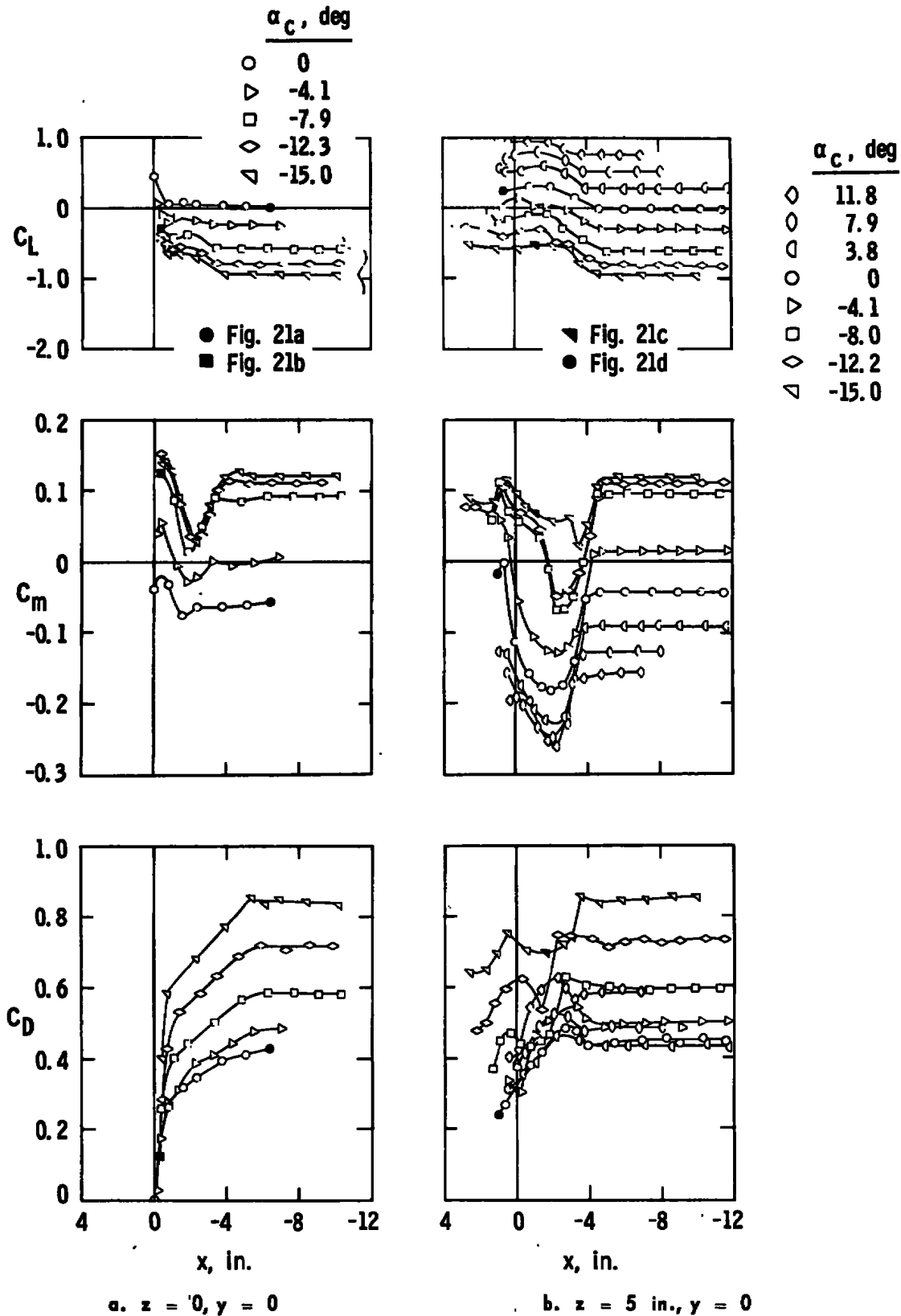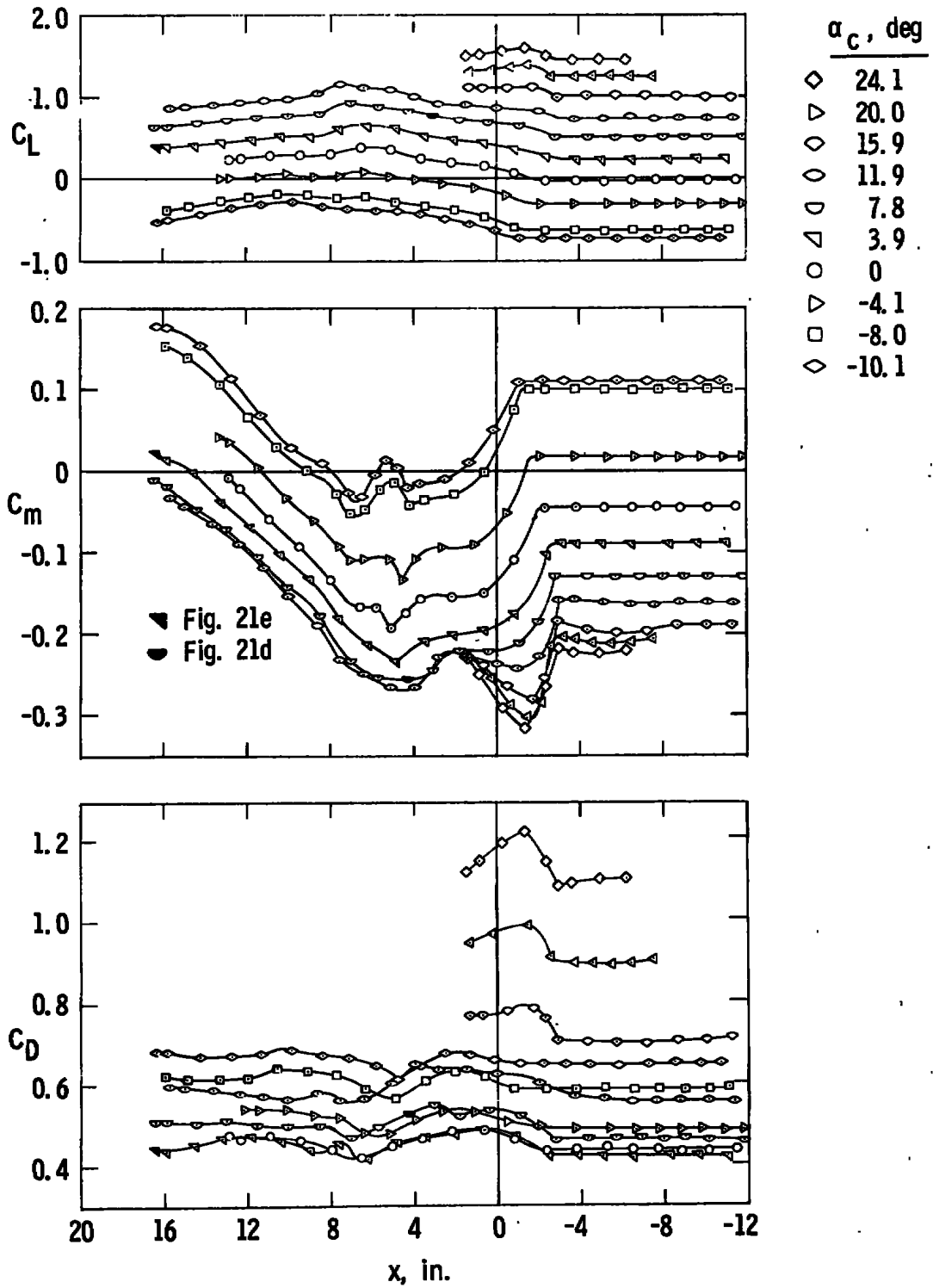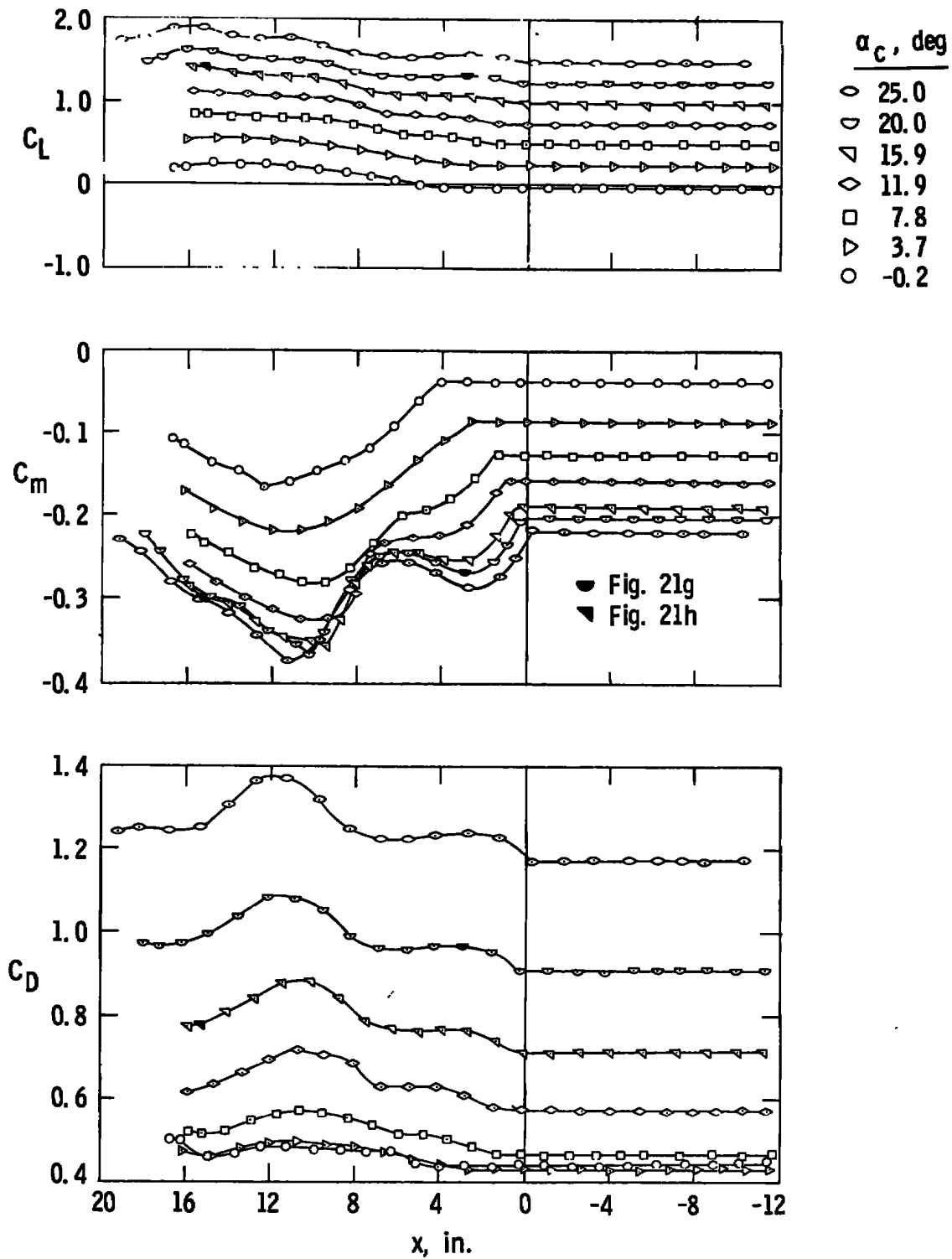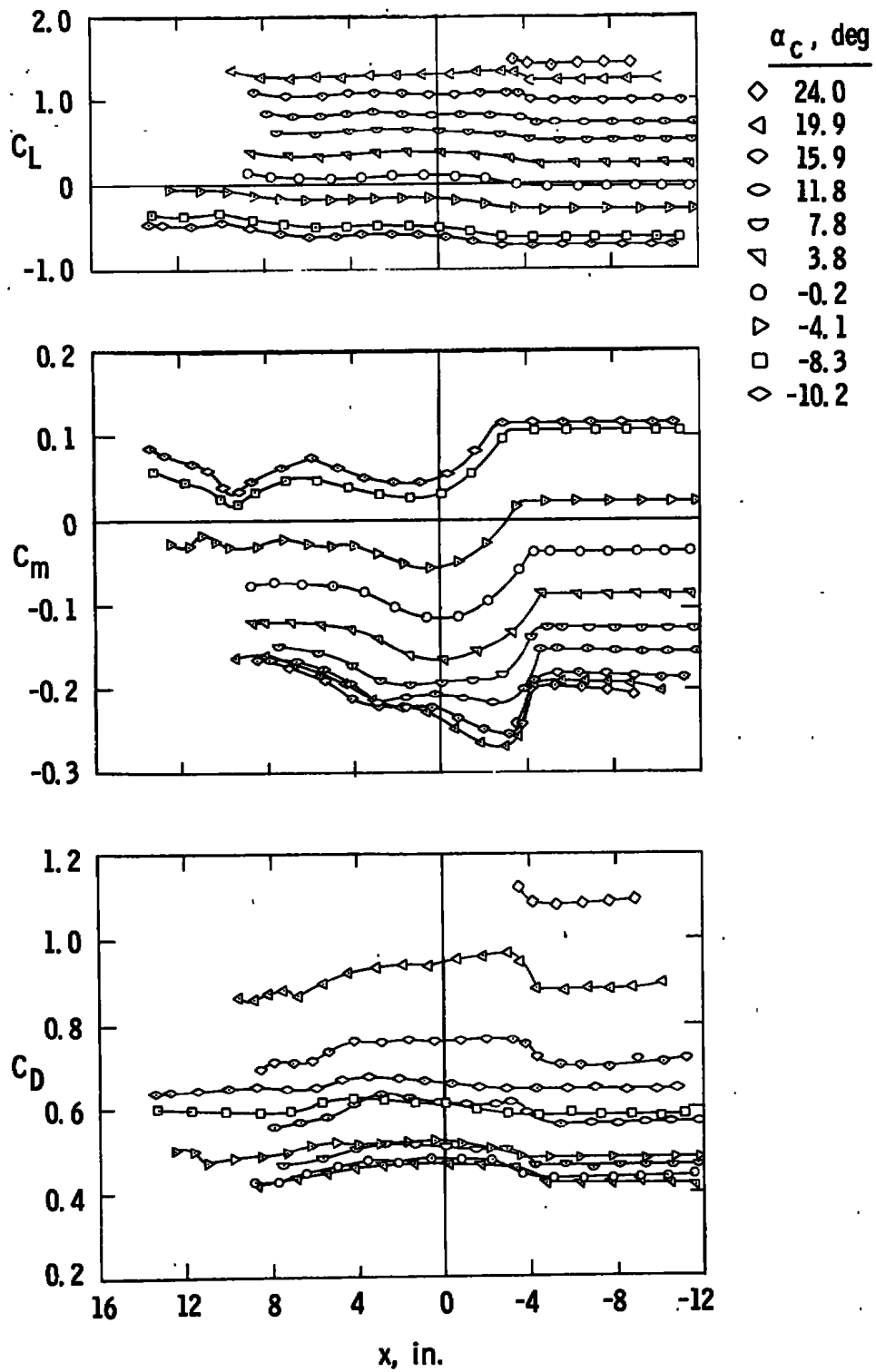Fig. 19 Schlieren Photographs, Jet On, $M_\infty = 3$, $p_c/p_\infty = 451$

Fig. 20 Lift, Drag, and Pitching-Moment Characteristics of the Capsule, Jet On, M_∞ = 4, p_c/p_∞ = 1303
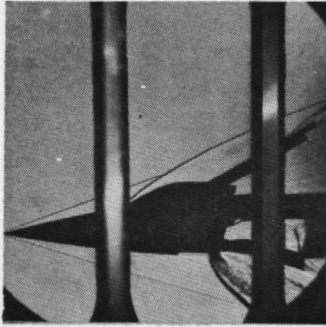
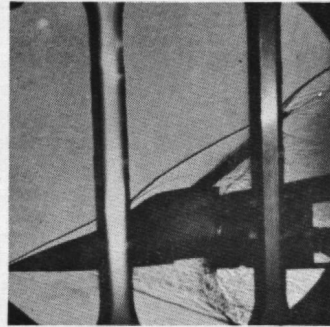c. $z = 10$ in., $y = 0$
Fig. 20 Continued

d. z = 14 in., y = 0
Fig. 20 Continued

e. $z = 10$ in., $y = 5$ in.
Fig. 20 Concluded

a. $\alpha_c = 0$, y = 0
z = 0, x = −6.5 in.

b. $\alpha_c = -7.9$ deg, y = 0
z = 0, x = −0.5 in.

c. $\alpha_c = -15.0$ deg, y = 0
z = 5 in., x = −1.7 in.

d. $\alpha_c = 0$, y = 0
z = 5 in., x = 0.5 in.

e. $\alpha_c = 3.9$ deg, y = 0
z = 10 in., x = 16.3 in.

f. $\alpha_c = 7.8$ deg, y = 0
z = 10 in., x = 4.5 in.

g. $\alpha_c = 20.0$ deg, y = 0
z = 14 in., x = 3.0 in.

h. $\alpha_c = 15.9$ deg, y = 0
z = 14 in., x = 15.5 in.

Fig. 21 Schlieren Photographs, Jet On, $M_\infty = 4$, $p_c/p_\infty = 1303$
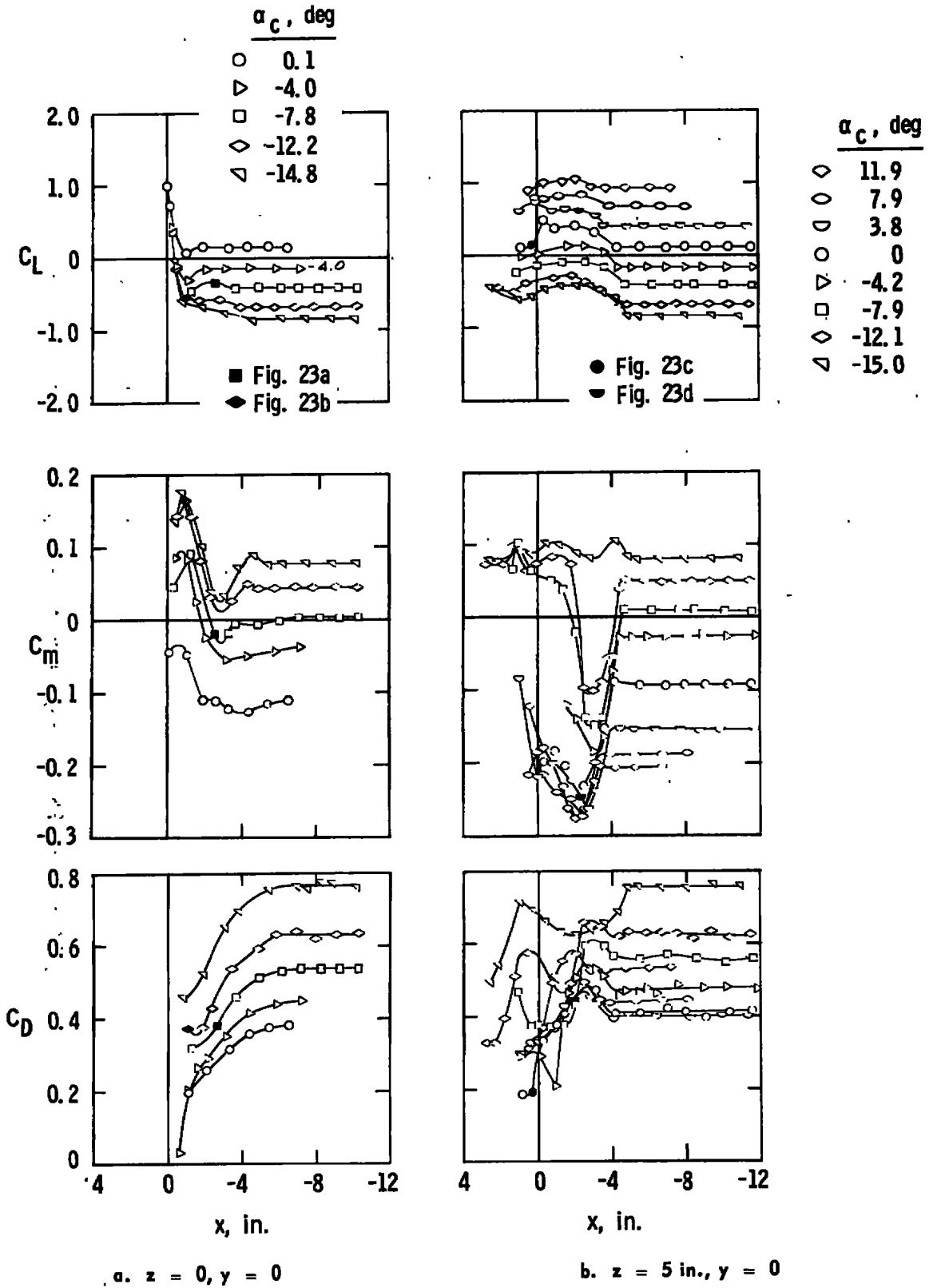
Fig. 22 Lift, Drag, and Pitching-Moment Characteristics of the Capsule, Jet On, M_∞ = 5, p_c/p_∞ = 4204

65

c. $z = 10$ in., $y = 0$
Fig. 22 Continued

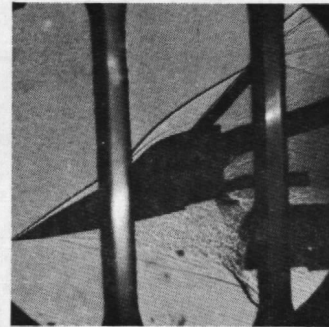d. $z = 14$ in., $y = 0$
Fig. 22 Continued

α_C, deg
◇ 23.9
◁ 20.0
◇ 15.9
○ 11.8
▽ 7.8
▽ 3.7
○ -0.2
▷ -4.1
□ -8.3
◇ -10.2

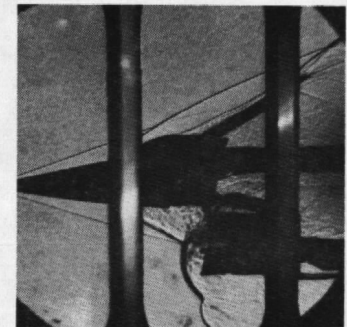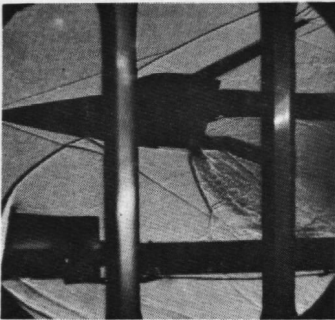e. z = 10 in., y = 5 in.
Fig. 22 Concluded
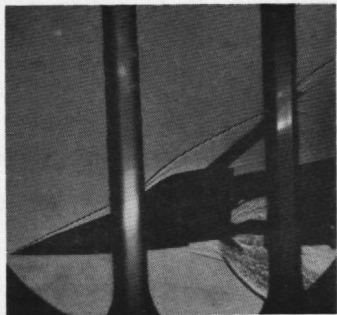
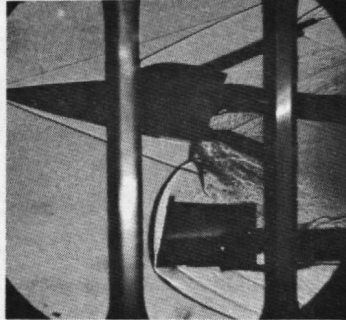a. $\alpha_c = -7.8$ deg, $y = 0$
$z = 0$, $x = -3.0$ in.
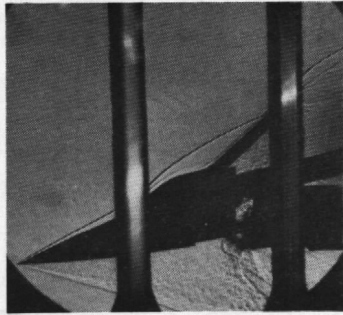
b. $\alpha_c = -12.2$ deg, $y = 0$
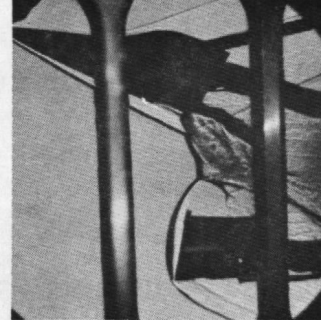$z = 0$, $x = -1.0$ in.
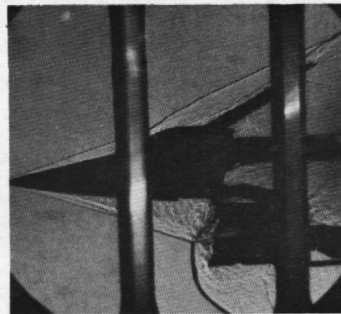
c. $\alpha_c = 0$, $y = 0$
$z = 5$ in., $x = 0.7$ in.
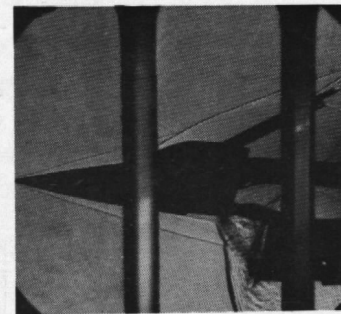
d. $\alpha_c = 3.8$ deg, $y = 0$
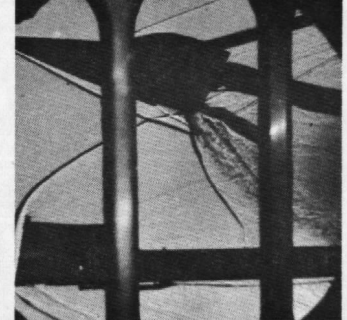$z = 5$ in., $x = -2.0$ in.
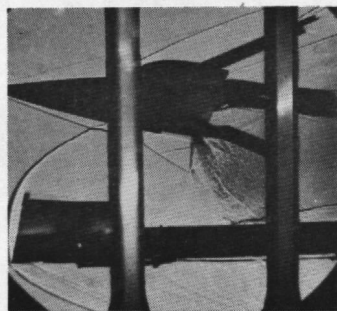
e. $\alpha_c = 7.8$ deg, $y = 0$
$z = 10$ in., $x = 15.5$ in.
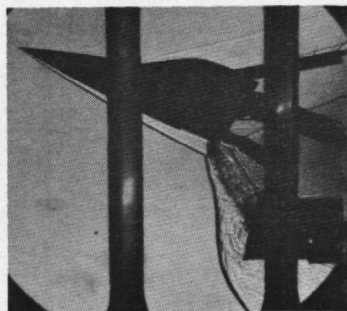
f. $\alpha_c = 19.9$ deg, $y = 0$
$z = 10$ in., $x = -0.5$ in.
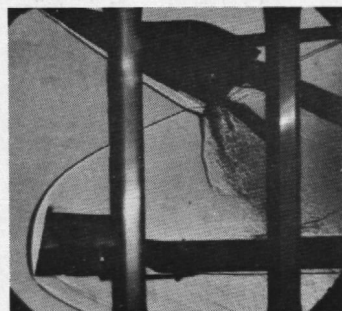
g. $\alpha_c = 25.0$ deg, $y = 0$
$z = 14$ in., $x = 16.5$ in.
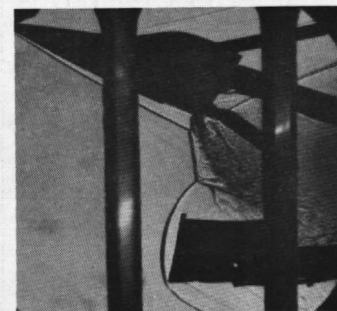
h. $\alpha_c = 20.0$ deg, $y = 0$
$z = 14$ in., $x = 4.5$ in.

Fig. 23 Schlieren Photographs, Jet On, $M_\infty = 5$, $p_c/p_\infty = 4204$
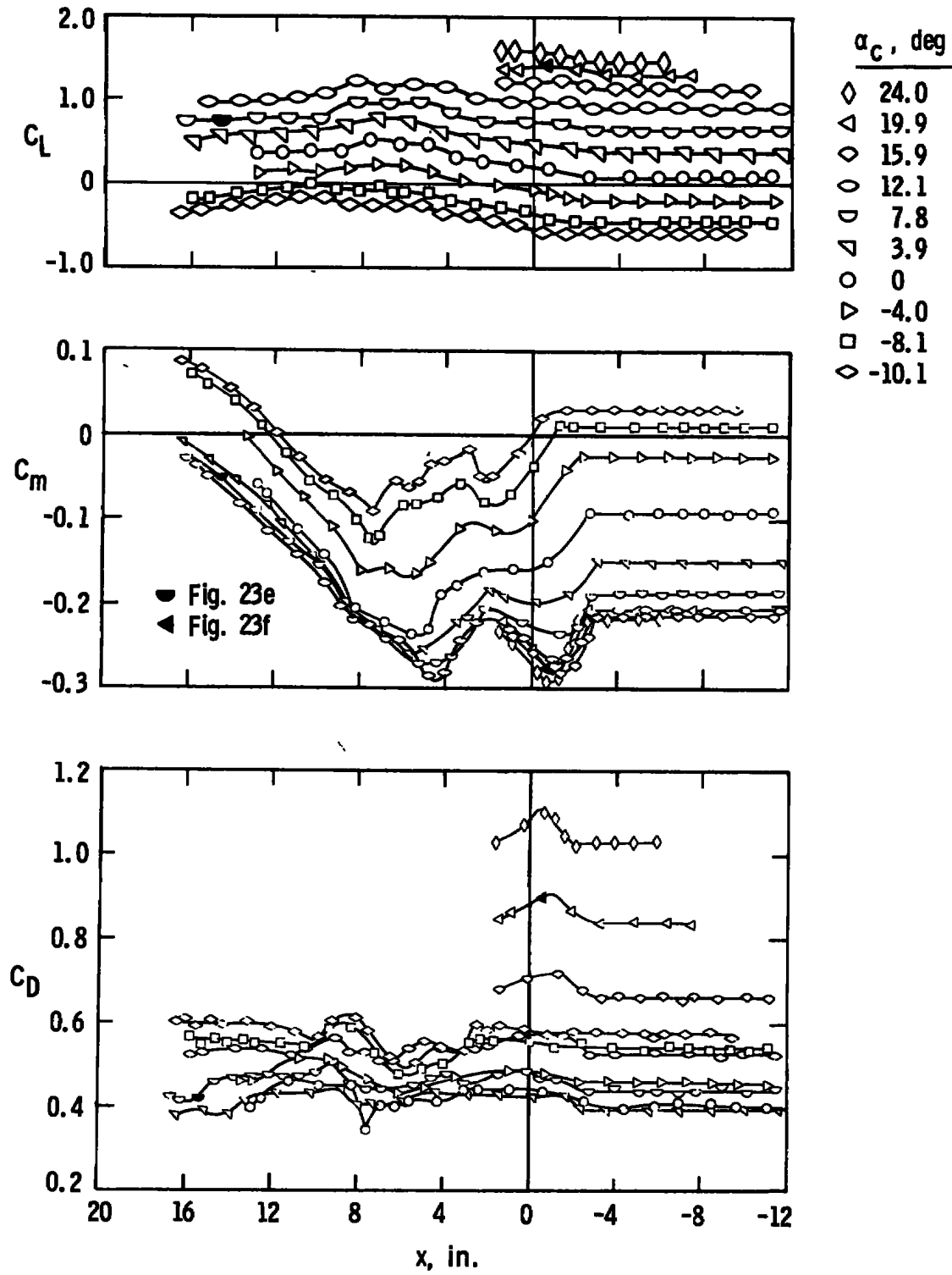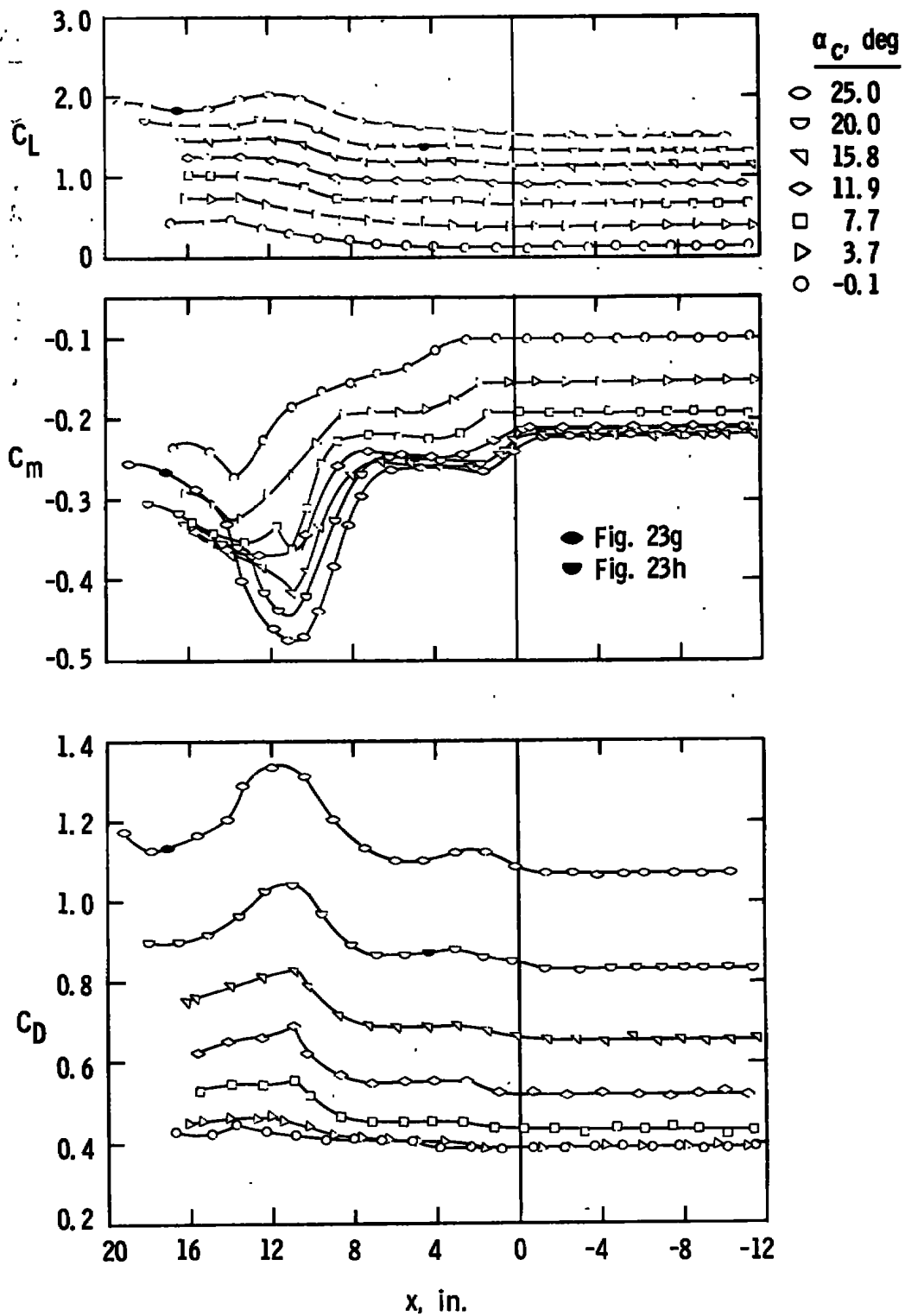
a. z = 3 in., y = 0

b. z = 4 in., y = 0
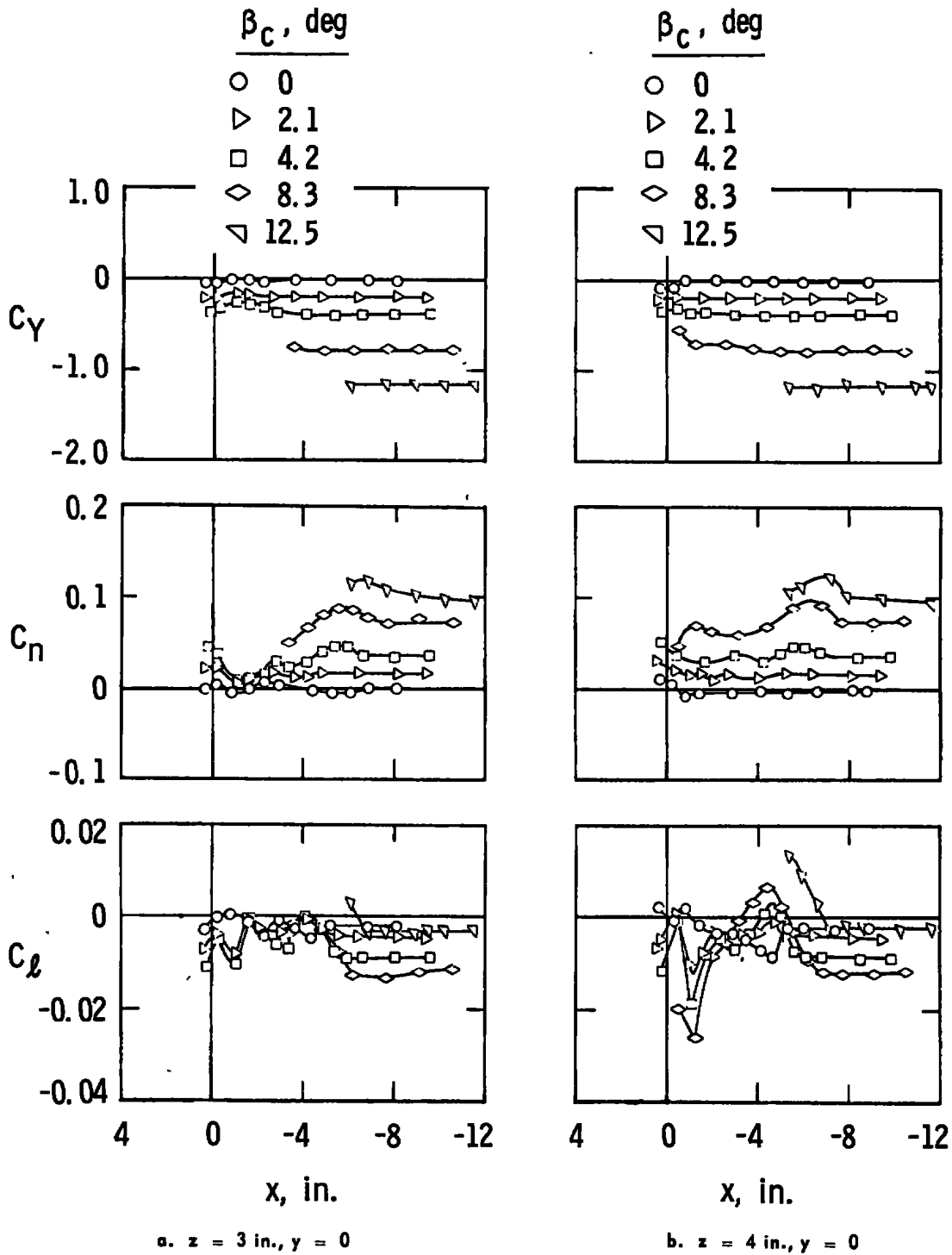
Fig. 24 Side-Force, Yawing-Moment, and Rolling-Moment Characteristics of the Capsule, Jet On, M_∞ = 2, p_c/p_∞ = 131

70
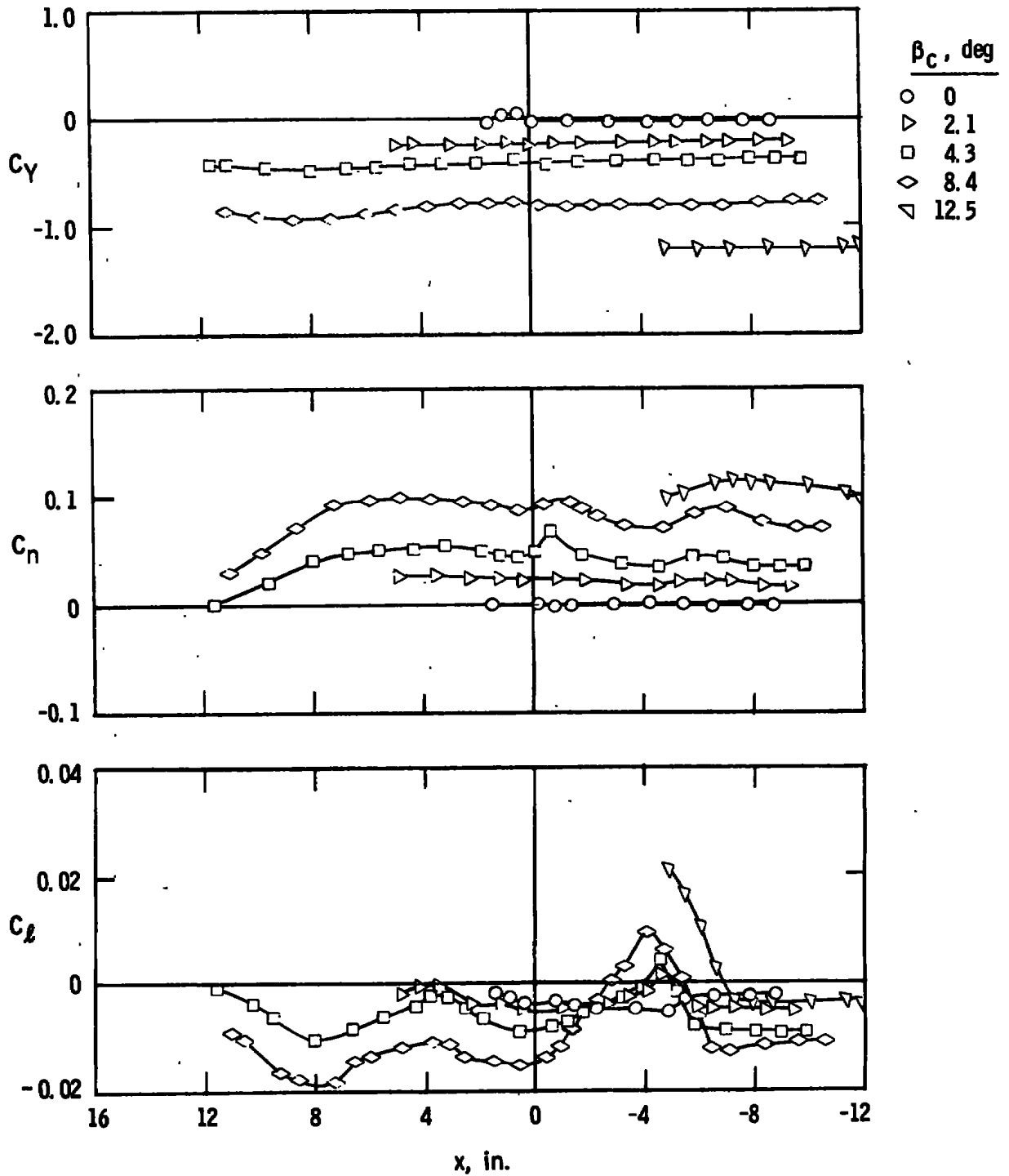
c. $z = 8$ in., $y = 0$
Fig. 24 Concluded
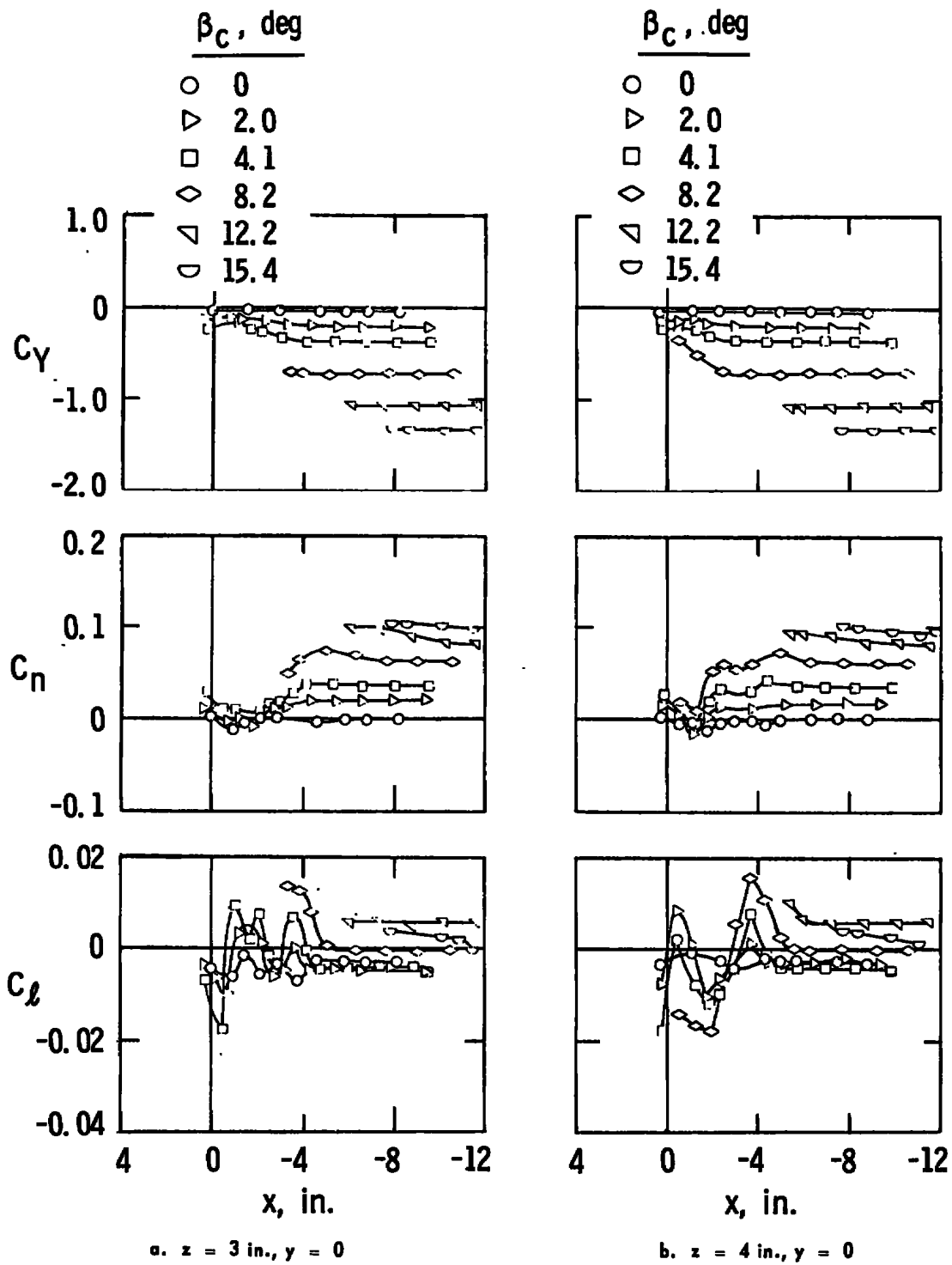
Fig. 25 Side-Force, Yawing-Moment, and Rolling-Moment Characteristics of the Capsule, $M_\infty = 3$, $p_c/p_\infty = 451$
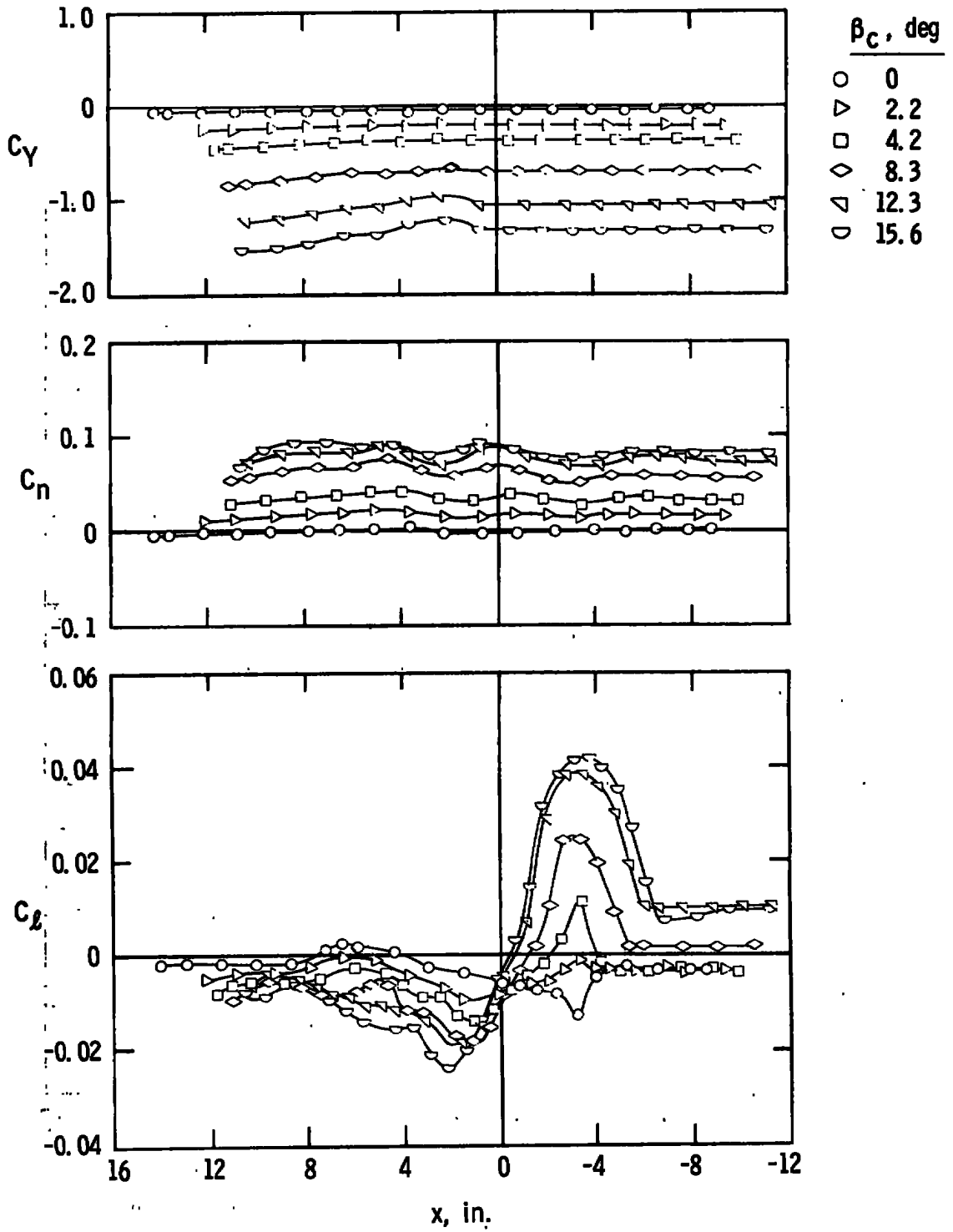
c. z = 8 in., y = 0
Fig. 25. Continued
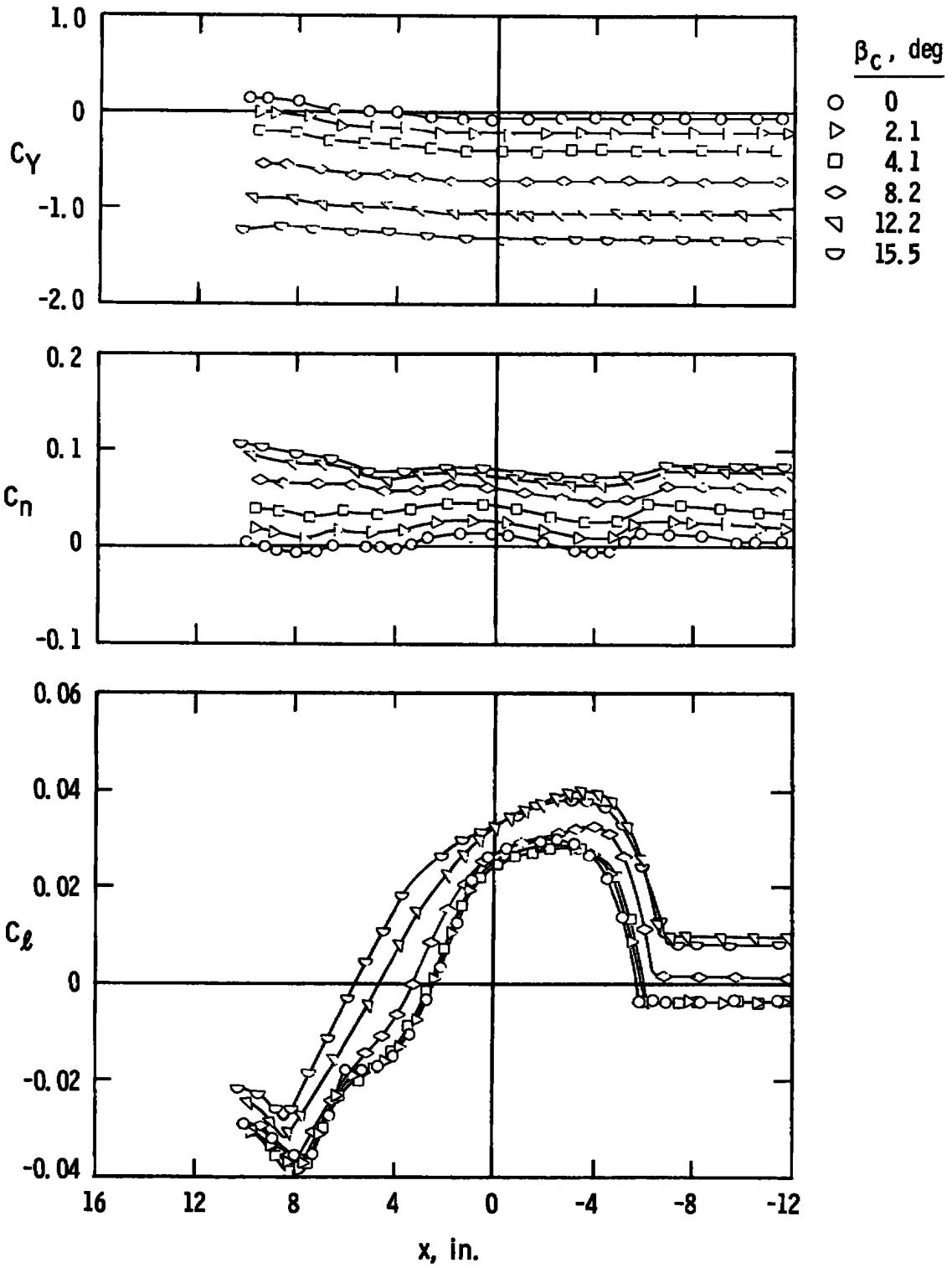
d. z = 8 in., y = –5 in.
Fig. 25 Concluded
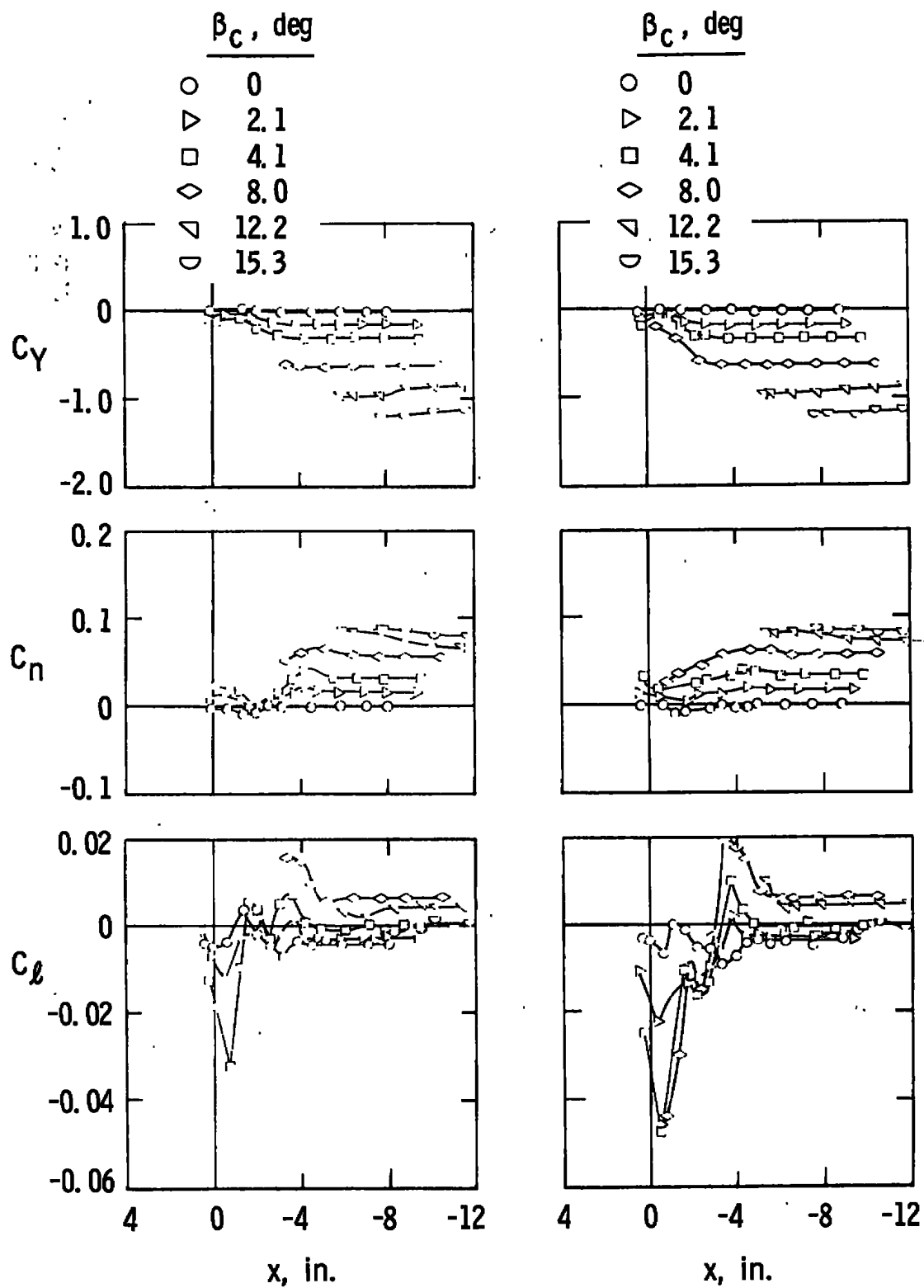
Fig. 26 Side-Force, Yawing-Moment, and Rolling-Moment Characteristics of the Capsule,
Jet On, M_∞ = 4, p_c/p_∞ = 1303

a. z = 3 in., y = 0

b. z = 4 in., y = 0
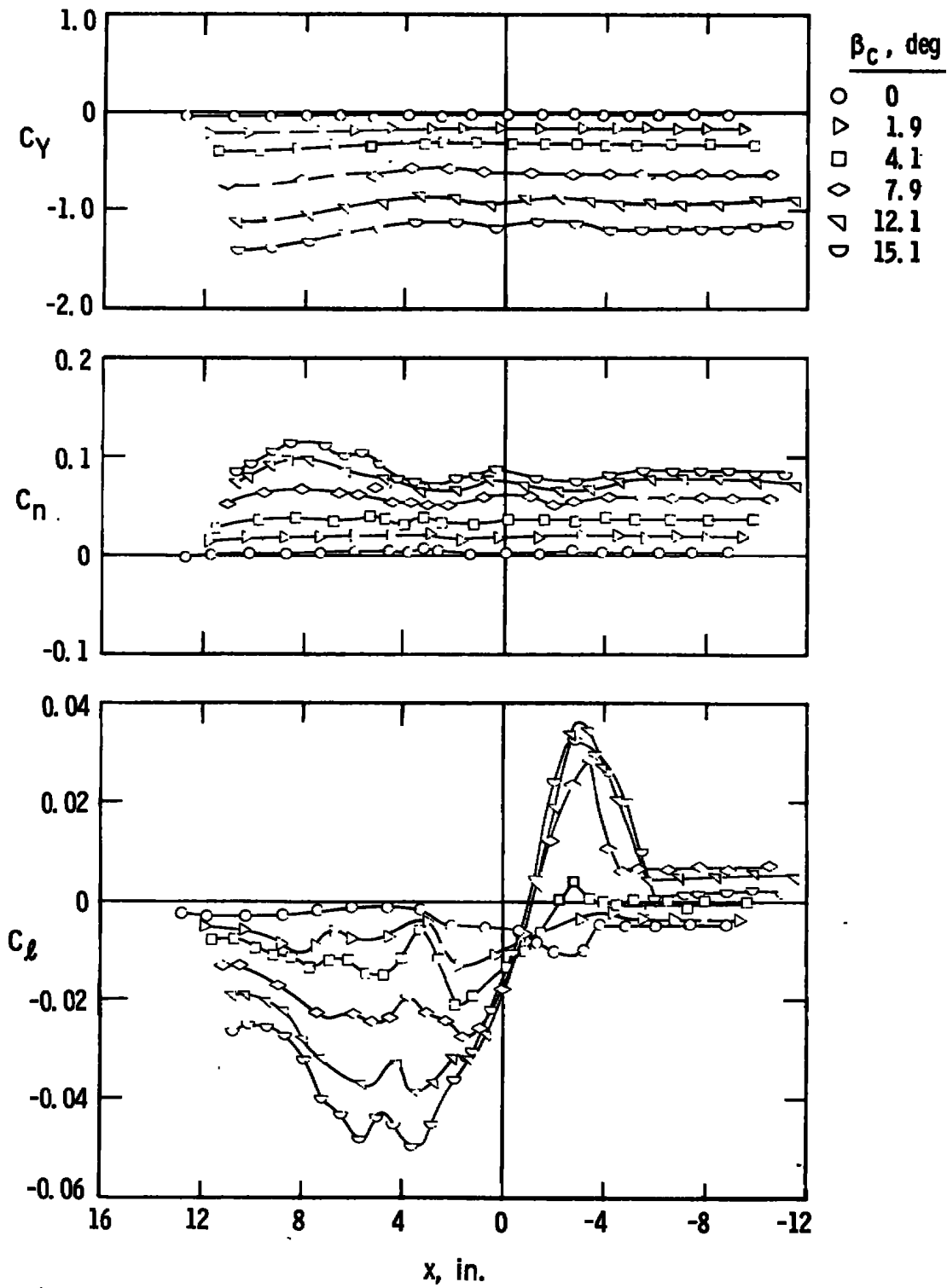
c. z = 8 in., y = 0
Fig. 26 Continued
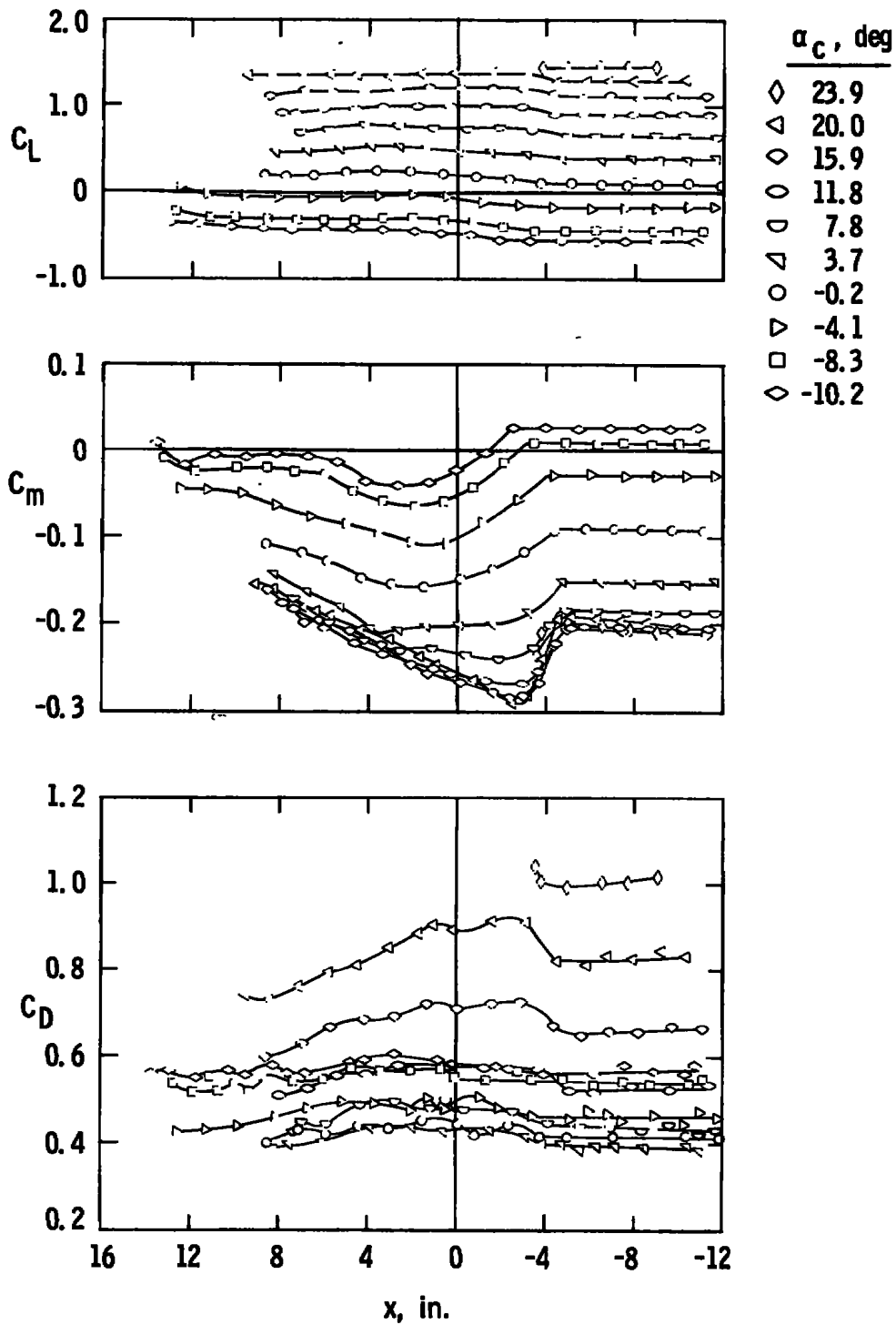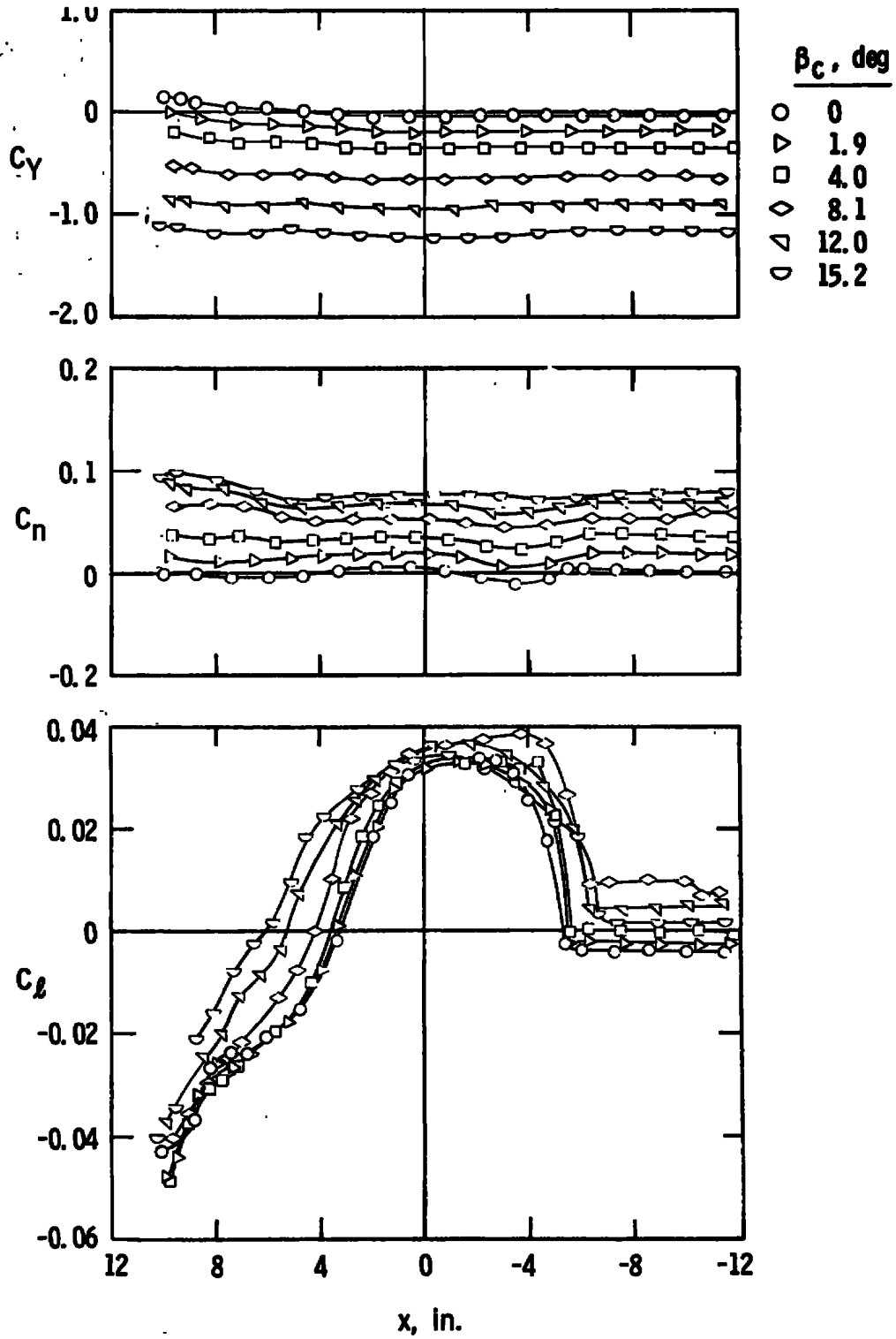
d. z = 8 in., y = –5 in.
Fig. 26 Concluded
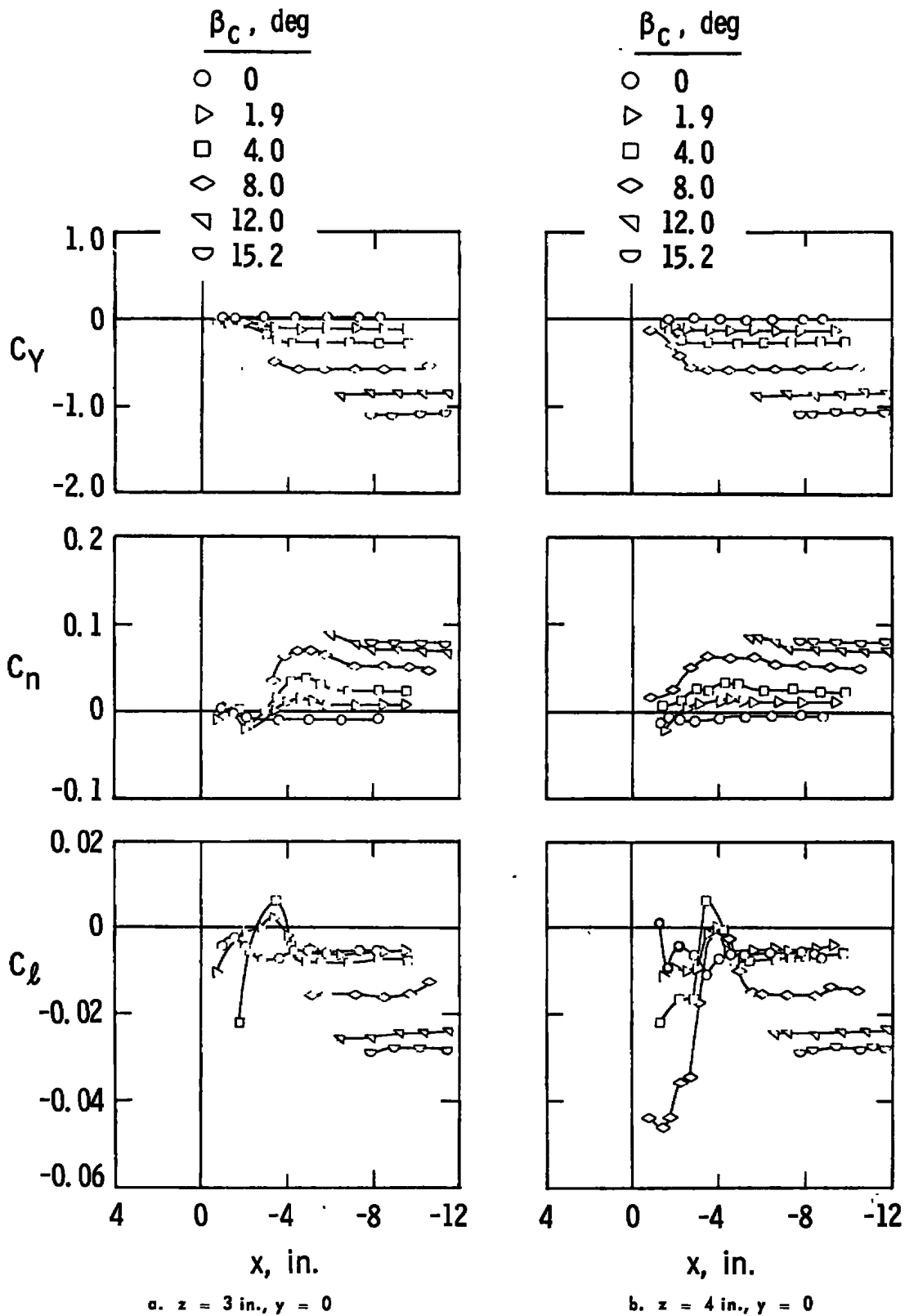
Fig. 27 Side-Force, Yawing-Moment, and Rolling-Moment Characteristics of the Capsule,
Jet On, $M_\infty = 5$, $p_c/p_\infty = 4204$
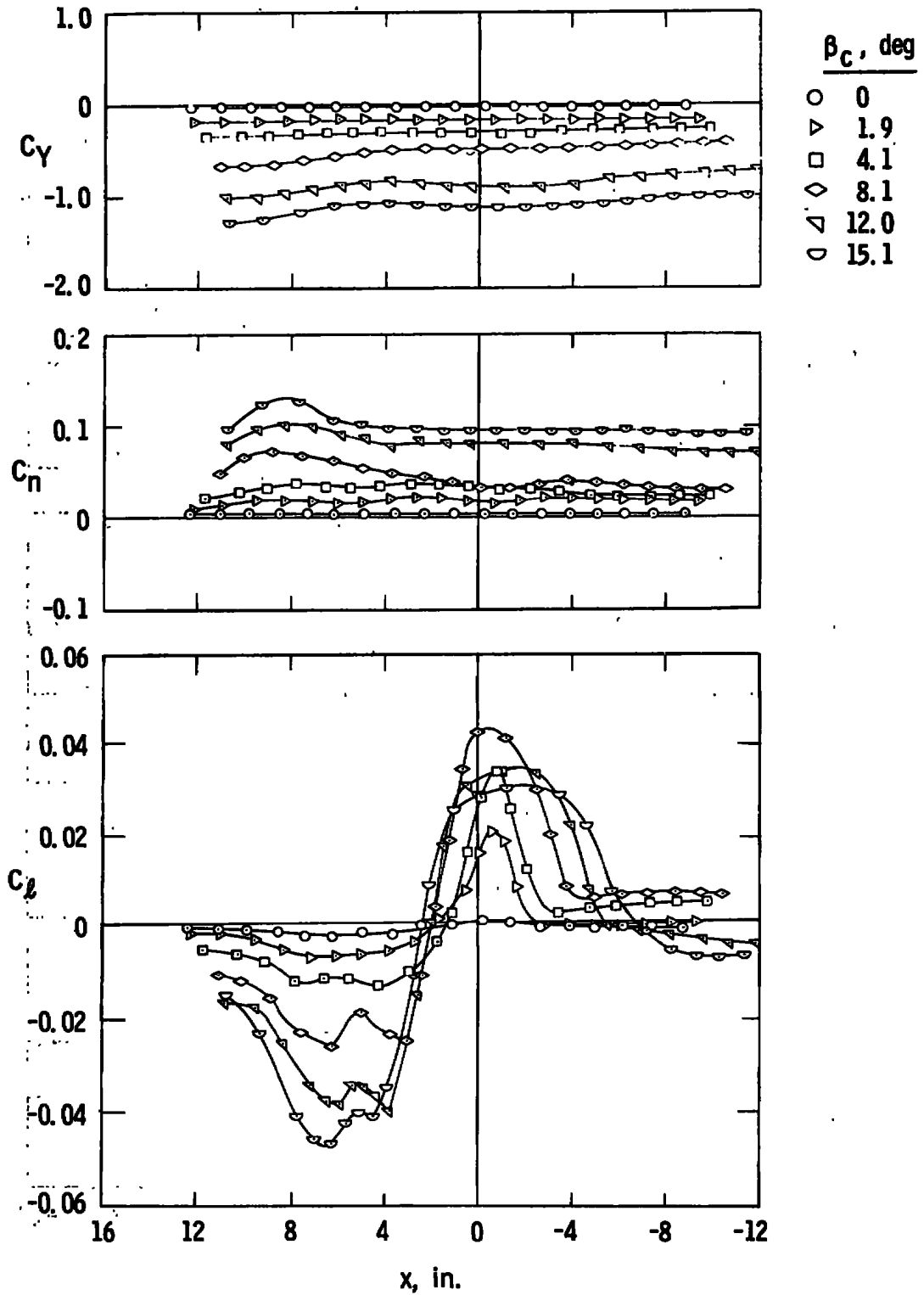
c. z = 8 in., y = 0
Fig. 27 Continued
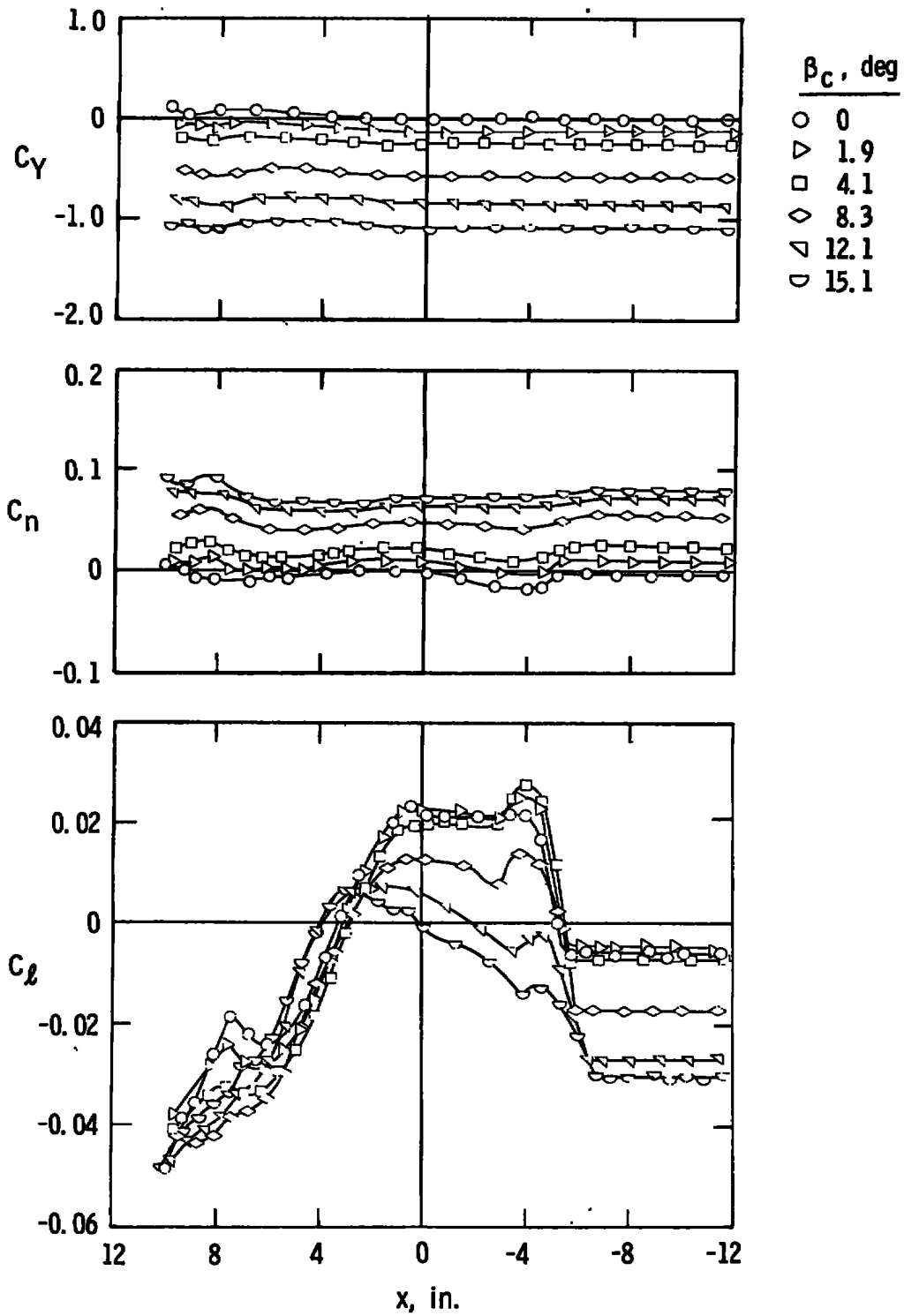
d. z = 8 in., y = 5 in.
Fig. 27 Concluded

TABLE I
TEST CONDITIONS

Nominal M_∞	Calibrated M_∞	p_0, psia	T_0, °R	p_∞, psia	$Re_\infty \times 10^{-6}$, in.$^{-1}$	Pressure Altitude, ft $\times 10^{-3}$	p_c/p_∞
2	1.99	33.6	560	4.365	0.680	30	0, 131
3	3.00	48.9	560	1.330	0.600	55	0, 451
4	4.00	71.0	580	0.468	0.485	76	0, 1303
5	5.02	85.0	620	0.157	0.325	100	0, 4204

TABLE II
MODEL ATTITUDES TESTED

α_c, deg	β_c, deg	x, in.	z, in. *	y, in.
-15	0	$-12 \lessgtr x \lessgtr 18$	0, 1, 2, 3, 4, 5, 6	0
-12			0, 1, 2, 3, 4, 5, 6	
-10			10	
- 8			0, 1, 2, 3, 4, 5, 6, 10	
- 4			0, 1, 2, 3, 4, 5, 6, 10	
0			0, 1, 2, 3, 4, 5, 6, 10, 14	
2			1	
4			2, 3, 4, 5, 6, 10, 14	
6			3	
8			4, 5, 6, 10, 14	
12			5, 6, 10, 14	
14			6	
16			10, 14	
20			10, 14	
24			10	
25			14	0
-15			5	5
-12			5	
-10			10	
- 8			5, 10	
- 4			5, 10	
0			5, 10, 14	
4			5, 10, 14	
8			5, 10, 14	
12			5, 10, 14	
16			5, 10, 14	
20			10, 14	
24			10	
25	0		14	5
0	0		3, 4, 6, 8	0
	2			
	4			
	8			
	12			
	15			0
	0			-5
	2			
	4			
	8			
	12			
0	15	$-12 \lessgtr x \lessgtr 18$	3, 4, 6, 8	-5

*Tests at the values of z underlined were made with the door
on the front face of the fuselage open for sting clearance.

DOCUMENT CONTROL DATA - R & D

(Security classification of title, body of abstract and indexing annotation must be entered when the overall report is classified)

1. ORIGINATING ACTIVITY *(Corporate author)*	2a. REPORT SECURITY CLASSIFICATION
Arnold Engineering Development Center ARO, Inc., Operating Contractor Arnold Air Force Station, Tennessee 37389	UNCLASSIFIED
	2b. GROUP N/A

3. REPORT TITLE

FORCE TESTS ON A SEPARABLE-NOSE CREW ESCAPE CAPSULE IN PROXIMITY TO THE PARENT FUSELAGE WITH COLD FLOW ROCKET PLUME SIMULATION AT MACH NUMBERS 2 THROUGH 5

4. DESCRIPTIVE NOTES *(Type of report and inclusive dates)*

Final Report   October 30, 1967 to September 18, 1968

5. AUTHOR(S) *(First name, middle initial, last name)*

Jerry H. Jones and L. J. Pfaff, ARO, Inc.

6. REPORT DATE	7a. TOTAL NO. OF PAGES	7b. NO. OF REFS
February 1969	90	3

8a. CONTRACT OR GRANT NO.	9a. ORIGINATOR'S REPORT NUMBER(S)
F40600-69-C-0001	
b. PROJECT NO. 421A	AEDC-TR-68-278
c. Program Element 64706F	9b. OTHER REPORT NO(S) *(Any other numbers that may be assigned this report)*
d.	N/A

10. DISTRIBUTION STATEMENT This document is subject to special export controls and each transmittal to foreign governments or foreign nationals may be made only with prior approval of Air Force Flight Dynamics Laboratory (FDFR), Wright-Patterson AFB, Ohio 45433.

11. SUPPLEMENTARY NOTES	12. SPONSORING MILITARY ACTIVITY
Available in DDC.	Air Force Flight Dynamics Laboratory (FDFR), Wright-Patterson AFB, Ohio 45433

13. ABSTRACT

Static force tests were conducted on a separable-nose crew escape capsule in the presence of the forward section of the airplane fuselage. The capsule escape rocket jet plume was simulated with air heated to a total temperature of approximately 100°F. Data were obtained at Mach numbers from 2 through 5 at capsule angles of attack from -15 to 25 deg and angles of sideslip from 0 to 15 deg for various positions of the capsule relative to the fuselage section. All testing was conducted at a fuselage angle of attack and angle of sideslip of zero. Reynolds number, based on a model length of 18.1 in., ranged from 5.7×10^6 to 12.3×10^6. Results are presented showing the effects of the fuselage section on the aerodynamic characteristics of the capsule, with and without simulation of the escape rocket exhaust plume.

This document is subject to special export controls and each transmittal to foreign governments or foreign nationals may be made only with prior approval of Air Force Flight Dynamics Laboratory (FDFR), Wright-Patterson AFB, Ohio 45433.

DD FORM 1473
I NOV 65

14. KEY WORDS	LINK A		LINK B		LINK C	
	ROLE	WT	ROLE	WT	ROLE	WT
force tests						
escape capsules, aircraft						
supersonic flow						

AFSC
Arnold AFS Tenn